

**TECHNICAL UNIVERSITY OF CRETE**  
**SCHOOL OF MINERAL RESOURCES ENGINEERING**  
**MSc. "PETROLEUM ENGINEERING"**

---



Master Thesis

**SENSITIVITY ANALYSIS OF AN ARTIFICIAL  
LIFT SYSTEM**

**Konstantinopoulos Miltiadis**

Scientific Advisor: Dr. Gaganis Vasileios

Examination Committee

Dr. Gaganis Vasileios (Supervisor)

Prof. Varotsis Nikolaos

Prof. Kalogerakis Nikolaos

Chania, 2018



# Table of Contents

Abstract .....	iv
Acknowledgments .....	v
List of Figures.....	vi
List of Tables.....	viii
1. Well Deliverability .....	1
1.1 Introduction.....	1
1.2 Well Deliverability .....	1
1.3 Nodal Analysis .....	2
1.4 Reservoir Deliverability/Inflow Performance.....	3
1.4.1 Undersaturated Reservoirs .....	4
1.4.2 IPR for Gas Reservoirs (Inflow).....	6
1.4.3 IPR for Two-Phase Reservoirs.....	6
1.4.4 Factors Affecting IPR Curve .....	7
1.5 Tubing/Vertical Lift Performance .....	9
1.5.1 Bottom-hole Pressure.....	9
1.5.2 Calculation of Pressure Drop in Tubing.....	10
1.5.3 Multiphase Flow .....	12
2. Artificial Lift Methods.....	15
2.1 The Need for Artificial Lift .....	15
2.2 A Review in Artificial Lift Systems.....	15
2.3 Gas Lift.....	16
2.3.1 Gas Lift Design .....	18
2.3.2 The Effect of Operational Parameters.....	19
2.3.3 Unloading Process .....	21
2.3.4 Gas Lift Equipment .....	22
3. Model Input Data .....	24
3.1 PVT Data .....	24
3.2 Well Data .....	24
3.2.1 Mechanical Properties of the tubing.....	25
3.2.2 Geothermal Gradient .....	26
3.3 Reservoir Data .....	26
3.4 Gas Lift Data .....	26

3.5 PROSPER Default Values.....	26
3.6 PVT Data Pre-Processing .....	26
3.7 Production without Gas Lift.....	29
4. Methodology .....	30
4.1 Section 1: Design Methodology.....	30
4.1.1 Section 1: Sizing of the Tubing and Gas Lift Design.....	30
4.1.2 Simulation Methodology .....	30
4.2 Section 2: Verification of the Design and Sensitivity Analysis.....	31
4.2.1 Parameters Affecting the Inflow Performance .....	31
4.2.2 Parameters Affecting the Tubing Performance.....	32
4.3 Section 3: Unloading Process .....	32
5. Results and Discussion.....	33
5.1 Design and Optimization of Gas Lift System .....	33
5.1.1 Base Case - Tubing OD 4.5" .....	33
5.1.2 Tubing OD 3.5" .....	38
5.1.3 Tubing OD 5.5" .....	39
5.2 Sensitivity Analysis.....	40
5.2.1 Parameters Affecting the Inflow Performance .....	41
5.2.2 Parameters Affecting the Tubing Performance.....	44
5.2.3 Effect of VLP Correlations.....	50
5.2.4 Effect of PVT correlation .....	50
5.3 Unloading Process .....	51
6. Conclusions.....	53
6.1 Design of the Gas Lift System .....	53
6.2 Sensitivity Analysis.....	53
6.3 Unloading Process .....	54
7. References .....	55
8. Appendix.....	56
A.1 Optimization of Gas Lift for Different Wellhead Pressures and Water Cuts.....	56
A.2 Sensitivity for different Wellhead Pressures and Injection Flow Rates for 0% Water Cut .....	59
A.3 Sensitivity for different Wellhead Pressures and Injection Flow Rates for 20% Water Cut .....	62
A.4 Sensitivity for different Wellhead Pressures and Injection Flow Rates for 40% Water Cut .....	66

A.5 Sensitivity for different Wellhead Pressures and Injection Flow Rates for 60% Water Cut .....	69
A.6 Sensitivity for different Wellhead Pressures and Injection Flow Rates for 80% Water Cut .....	73
A.7 Sensitivity for Gas to Liquid Ratio of 4.5" Tubing OD.....	76
A-8 Sensitivity of Gas to Liquid Ratio for 3.5" Tubing OD .....	80

## **Abstract**

The objective of this study is to design a gas lift system for the maximization of the oil production and the verification of this design against various sensitivity analysis scenarios. The injection depth has been set to the maximum possible, i.e. equal to the depth of the casing, to maximize the efficiency of the gas lift operation. The maximum producible flow rate that the well can produce for the given/available reservoir and tubing data using a gas lift system has been computed and that maximum flow rate has been the basis for the design. As variations in the production rate are anticipated by using different tubing ODs, two different sizes of tubing have been considered in this study. All design parameters such as injection depth, gas injection rate, casing pressure and injection pressures have been calculated as well.

Apart from the design, verification of the design has also been performed against the variation of several parameters that might change over the life time of the well and those parameters that may include some sort of uncertainty in measurement/calculation. To include the whole range of scenarios the system a sensitivity analysis has been performed by using nodal analysis. This way the system is divided into three subsystems by means of a node at the bottom-hole. By superimposing the suitable IPR and VLP curves the maximum possible production specific to that sensitivity can be read from the intersection point whereas the injection gas rate, casing pressure and injection pressures can be read from the corresponding sensitivity curves for the gas flow in the annulus.

Moreover, unloading the annulus and production tubing with the drilling fluid has also been analyzed for casing pressure operated (IPO) and tubing pressure operated (PPO) unloading valves. All analyses have been run by means of the PROSPER and PIPESIM software.

## **Acknowledgments**

I would like to express my sincere gratitude to my supervisor Dr. Vasileios Gaganis for his guidance during my master's thesis. Also, I would like to acknowledge Prof Nikolaos Varotsis and Prof Nikolaos Kalogerakis for accepting being members of my thesis examination committee.

Foremost, I would like to say a very big thank to my friend Ravi Kumar Janam for his assistance and guidance during the period of my thesis. Ravi helped me by making me understand the essentials behind the Petroleum Engineering in general. Without his presence my thesis would not reached such a high level.

Also, I would like to thank my friend Dorina Mouloupoulou for her support and help. Finally, I want to thank my family. Without their help I would not have been able to complete this study.

## List of Figures

Figure 1.1: Total loss in production system<sup>1</sup>.

Figure 1.2: IPR curve for an undersaturated reservoir<sup>2</sup>.

Figure 1.3: IPR curve for undersaturated and saturated reservoir<sup>1</sup>.

Figure 1.4: Effect of oil viscosity on IPR curve<sup>1</sup>.

Figure 1.5: Effect of reservoir depletion on IPR curve<sup>1</sup>.

Figure 1.6: Effect of perforations density on IPR curve<sup>1</sup>.

Figure 1.7: Skin removal effect in IPR curve<sup>1</sup>.

Figure 1.8: Flow regime in Vertical flow<sup>3</sup>.

Figure 2.1: The most popular types of artificial lift<sup>1</sup>.

Figure 2.2: Gas Lift well schematic<sup>4</sup>.

Figure 2.3: Production pressure curves for different GLR<sup>5</sup>.

Figure 2.4: Pressure gradient versus depth for continuous gas lift system<sup>6</sup>.

Figure 2.5: Well unloading sequence<sup>7</sup>.

Figure 3.1: Deviation survey of the well.

Figure 3.2: Completion Diagram.

Figure 3.3: PVT matching.

Figure 3.4: Bo comparison.

Figure 3.5: GOR comparison.

Figure 3.6: Oil density comparison.

Figure 3.7: Oil viscosity comparison

Figure 3.8: Production without gas lift-WHP=250 psia.

Figure 5.1: Intersection points of the VLP curves for different injection rates with the reservoir IPR.

Figure 5.2: Operational Parameters as the injected gas rate is increased for wellhead pressure of 250 psia and 0% water cut.

Figure 5.3: Gas lift optimization-OD 4.5" and 0% water cut.

Figure 5.4: Gas lift optimization-OD 4.5" and 20% water cut.

Figure 5.5: Gas lift optimization-OD 4.5" and 40% water cut.

Figure 5.6: Gas lift optimization-OD 4.5" and 60% water cut.

Figure 5.7: Gas lift optimization-OD 4.5" and 80% water cut

Figure 5.8: Gas lift optimization-OD 3.5" and 0% water cut.

Figure 5.9: Gas lift optimization-OD 5.5" and 0% water cut.

Figure 5.10: Effect of reservoir pressure on inflow performance.

Figure 5.11: Effect of water cut on inflow performance.

Figure 5.12: Effect of productivity index on inflow performance.

Figure 5.13: Different VLP curves for a range of WHP of 250 to 650 psia, 0% water cut and with formation GLR.

Figure 5.14: The effect of water cut for a WHP=450 psia and gas injection rate=9 MMscfd.

Figure 5.15: Effect of GLR for constant liquid rate of 4000 stb/d and 4.5" OD.

Figure 5.16: Effect of tubing diameter on VLP.

Figure 5.17: Effect of overall heat transfer coefficient on VLP-WHP=250psia.

Figure 5.18: Effect of overall heat transfer coefficient on VLP-WHP=250 psia.

## List of Tables

Table 3.1: PVT properties of the fluid

Table 3.2: Geothermal gradient of the well.

Table 4.1: ID and wall thickness data<sup>8</sup>.

Table 5.1: Operational Parameters as the injected gas rate is increased for wellhead pressure of 250 psia and 0% water cut.

Table 5.2: Gas lift optimization-OD 4.5" and 0% water cut

Table 5.3: Gas lift optimization-OD 3.5" and 0% water cut.

Table 5.4: Gas lift optimization-OD 5.5" and 0% water cut.

Table 5.5: Effect of viscosity,  $k * h$  product and Bo on PI.

Table 5.6: The effect of tubing roughness on VLP.

Table 5.7: Comparison of VLP correlations.

Table 5.8: Deviation (%) of PROSPER EOS correlations in oil viscosity.

Table 5.9: Deviation (%) of PROSPER EOS correlations in GOR.

Table 5.10: Depth and number of unloading valves for different injection pressures

# 1. Well Deliverability

## 1.1 Introduction

Reservoirs are generally classified into five types based on the critical properties of the reservoir fluid with respect to the pressure and temperature governing in the reservoir.

**Undersaturated Oil Reservoirs:** When the reservoir pressure is above the bubble point pressure, the reservoir will produce a single phase undersaturated oil, unless the pressure falls below this point, during the production life of the field. For undersaturated oil if the pressure falls below the bubble point in the tubing, then gas will evolve out of the liquid phase and the flow is multiphase in the tubing.

**Saturated Oil Reservoirs:** When the pressure falls below the bubble point within the reservoir, it becomes saturated oil reservoir and produces both oil and gas.

**Retrograde gas-condensate reservoirs:** If the reservoir temperature lies between the critical temperature and the cricondentherm of the reservoir fluid, the reservoir is classified as a retrograde gas reservoir. The unique element of this type of reservoir is that when the pressure is decreased on this mixture, instead of expanding (if a gas) or vaporizing (if a liquid) as might be expected, they vaporizing instead of condensing.

**Wet gas reservoirs:** In this type of reservoir the reservoir temperature exceeds the cricondentherm of the hydrocarbon system, so the fluid will always remain in the vapor phase region in the reservoir. As the produced gas flow to the surface the pressure and temperature will decline gas will enter to the two phase region. If in the separator it is not formed liquid, then the fluid can be categorized as wet gas.

**Dry gas reservoirs:** The hydrocarbon mixture exists as a gas in both the reservoir and in surface facilities. The only liquid associated is water<sup>9</sup>.

As far as gas lift is concerned, these types of reservoirs except the undersaturated one, does not need gas lift. When the pressure is always above the bubble point even in the tubing the flow is monophasic in the tubing. Mainly gas lift application is required for undersaturated oils as they have higher density that will cause the huge liquid head and high viscosities that will cause resistance to flow, thus causing huge pressure drops in the tubing.

## 1.2 Well Deliverability

Well productivity/deliverability is defined as the ability of the well to deliver oil and gas to the wellhead thus the deliverability of the well. It consists on two components.

- Well inflow performance (the ability of the reservoir to deliver fluids to the wellbore) – governed by Inflow Performance Relation (IPR)
- Well tubing performance (the ability of the well to deliver fluids from the wellbore to the surface) - governed by Vertical Lift Performance (VLP)

Well deliverability is determined by the combination of both IPR and VLP.

The final design of a production system cannot be separated into inflow performance and tubing system performance and handled separately; since the amount of oil and gas flowing into the well from the reservoir depends on the pressure drop in the tubing system and the pressure drop in the tubing system depends on the flow rate of the fluid. Therefore, the entire production system MUST be analyzed as a SINGLE unit.

Nodal analysis is the technique that is used to analyze the combined effect of both IPR and VLP on the overall deliverability of the well by isolating the two components of the system at the node of our choice.

### 1.3 Nodal Analysis

Nodal analysis is a tool to predict the oil and gas flow rate and the pressure at any node or nodes. Nodal analysis is based on the principle of pressure continuity i.e. only one pressure can exist for the specific system configuration at any node/point and the flow that enters into the node must be equal to the flow rate exiting the node.

Fluid properties change with the location-depending on pressure and temperature in oil and gas production systems. To simulate the fluid flow in a particular system, it is necessary to “break” the system into discrete elements (equipment sections) by nodes. Fluid properties in the elements are then evaluated locally<sup>2</sup>. The components that make up a detailed flowing well system are illustrated Figure 1.1.

At any time, the pressure of the endpoints (static reservoir pressure and separator pressure) are fixed, thus

$$\bar{P}_R - (\text{pressure loss in upstream components}) = P_{node}$$
$$P_{sep} + (\text{pressure loss in downstream components}) = P_{node}$$

In Nodal analysis the pressures at the two endpoints are fixed and the unique flow that enters into the node must be equal to the flow rate exiting the node; and needs to be determined.

Nodal analysis gives the flexibility to divide the system into any number of nodes and analyze the performance at each node. But it is always advisable to have a node at the bottom-hole and isolate the system into two components and check the effect of each component on the total system performance and optimize for economics.

$$P_{node} = P_{FBHP}$$

In order to find this unique flow rate for the specific system configuration a graphical solution is adopted. By plotting Inflow Performance Curve and Outflow Performance on the same plot yields an intersection point between these two curves which determines the achievable flow rate for this system configuration. Furthermore, if these two curves do not intersect; the well is not able to produce and is referred as a “dead well”.

Different IPR curves are generated via sensitivity analysis by changing various reservoir parameters. Similarly by changing various tubing system parameters different VLP curves are produced and therefore the system's deliverability or flow capacity can be optimized<sup>10</sup>.

Therefore, one of the advantages of the system analysis approach is the ability to predict the effect in design variables which is caused by the aforementioned changes. Every component in a producing well (or all wells in a producing system) can be optimized by Nodal analysis in order to economically achieve the objective flow rate. An optimized tubing design can also be found using the Nodal analysis plot<sup>11</sup>.

Sometimes, Nodal analysis is also referred to as Total System Analysis.

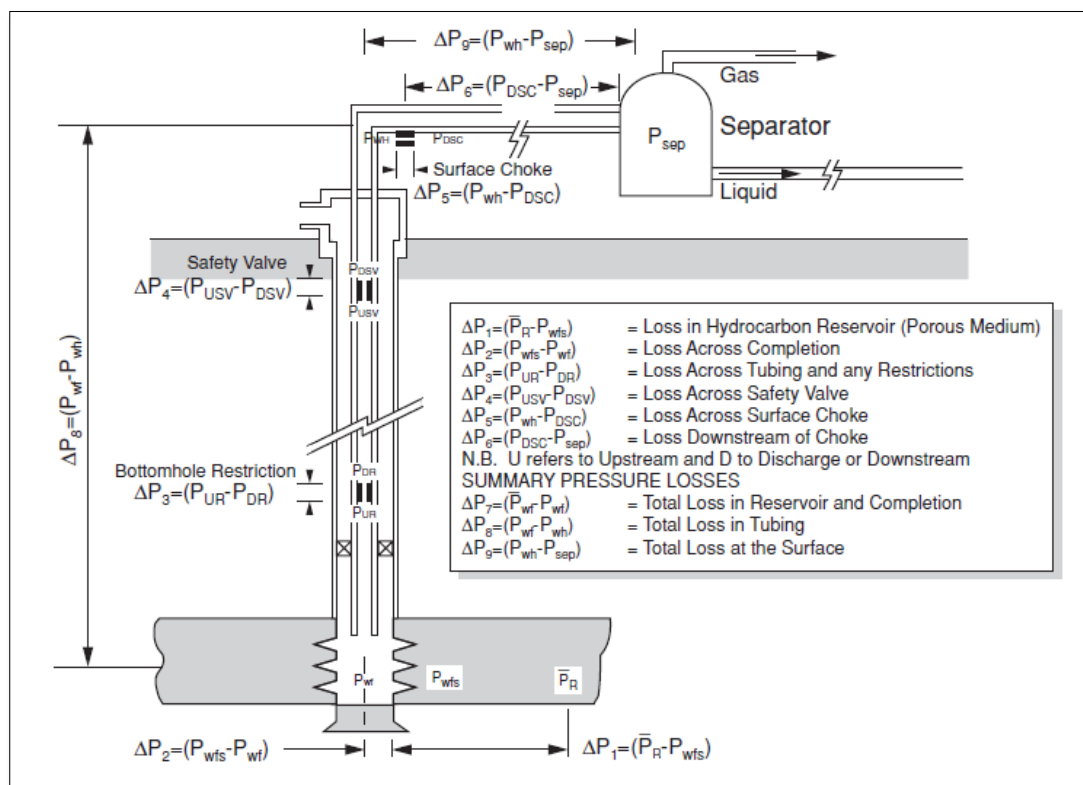


Figure 1.1: Total loss in production system<sup>1</sup>.

### 1.4 Reservoir Deliverability/Inflow Performance

Inflow performance is a relation between the flow in porous media and the pressure drop (bottom-hole pressure). Reservoir deliverability is the oil or gas production rate that can be achieved from the reservoir at a given bottom-hole pressure and is a major factor affecting well deliverability.

Darcy's law gives analytical expressions in a porous media that relates all the reservoir parameters with flow rate and the bottom-hole pressure and pressure drop can be calculated for any given flow regime (for given prevailing conditions).

$$q = -\frac{k * A}{\mu} * \frac{dP}{dL}$$

where,

$k$  = permeability,

$A$  = cross sectional area

$\mu$  = liquid viscosity

$\frac{dP}{dL}$  = pressure gradient

Reservoir deliverability determines the completion design such as size of the tubing, artificial lift and ESP requirements. A thorough understanding of IPR is hence required for accurately predicting well productivity<sup>2</sup>.

In this chapter the focus is mainly on the vertical wells and the flow is assumed to be radial. Darcy's equation can be simplified based on the type of the reservoir (phase of the flowing fluid) and the reservoir pressure regime.

By keeping the constant reservoir data for a time period a relationship between the liquid rate and the bottom-hole pressure can be formulated. This relationship is called Inflow Performance and the plot of liquid producing flow rate versus the bottom-hole pressure is called Inflow Performance Relationship (IPR). IPR is a graphical representation of the relationship between the flowing bottom-hole pressure and the liquid flow rate. The magnitude of the slope of this graph (of IPR curve) is referred as productivity index, PI or J. PI can be derived through mathematical form using reservoir data either it can be estimated through well tests.

#### **1.4.1 Undersaturated Reservoirs**

Reservoir that is producing at the bottom-hole pressure above the bubble point pressure at the reservoir temperature is called an undersaturated reservoir.

For pseudo steady state radial flow Darcy's law simplifies to:

$$q = PI * (\bar{P}_R - P_{wf})$$

where,

$q$  = volumetric flow rate (sbbl/day)

$\bar{P}_R$  = the static reservoir pressure (psia)

$P_{wf}$  = the flowing bottom – hole pressure (psia)

$$\text{and } PI = \frac{k * h}{141.2 * B_o * \mu_o * (\ln \frac{r_e}{r_w} - 0.75 + S)} \quad (\text{sbbl/day/psia})$$

where,

$h$  = pay thickness (ft)

$k$  = permeability (mD)

$B_o$  = oil formation volume factor

$S$  = skin factor

$r_e$  = external radius of the reservoir (in)

$r_w$  = radius of the well (in)

Productivity index reflects the ability of the reservoir to deliver fluid to the wellbore. The productivity index for an undersaturated reservoir in general is measured by well tests. PI is useful for comparing wells because it combines into a single value all the relevant rock, fluid and geometrical properties to describe (relative) inflow performance<sup>1</sup>.

For a reservoir producing under steady state conditions above the bubble point pressure the reservoir parameters such as  $k$ ,  $h$ ,  $B_o$ ,  $S$ ,  $r_e$ ,  $r_w$  and  $\mu_o$  are constant and the pressure drops steadily with the flow rate. The above equation represents a straight line between flow rate and the bottom-hole pressure with a slope of  $-PI$  as illustrated in Figure 1.2.

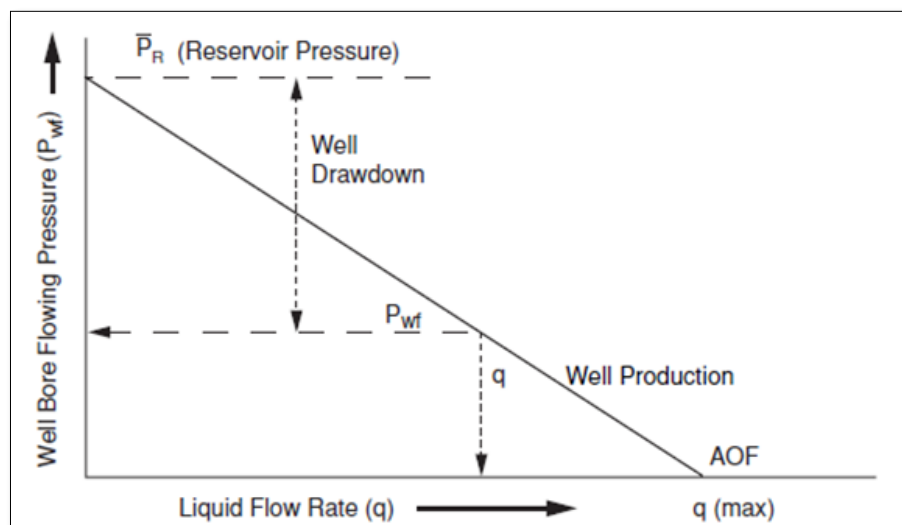


Figure 1.2: IPR curve for an undersaturated reservoir<sup>2</sup>.

From the IPR curve it can be noticed that:

- When the flowing bottom-hole is equal to the reservoir's pressure, the flow rate is zero due to the absence of any pressure drawdown.
- When the flowing bottom-hole pressure is equal to zero then the maximum flow rate occurs. These theoretical conditions are called as Absolute Open Flow and referred as AOF. Although, these conditions in practice are not possible to achieve, AOF is a useful definition that has widespread applications in Petroleum Industry i.e. comparing deliverability of wells within a field since it combines PI and reservoir pressure in one number representative of well inflow potential.

For an undersaturated reservoir a single well test is enough to predict the PI value, since one of the points of the straight line is the zero flow rate at the maximum reservoir pressure (initial static reservoir pressure). Once PI is calculated IPR curve for an undersaturated reservoir be generated by calculating the flow rates at any draw-down (or  $P_{wf}$ ). The difference between the flowing bottom-hole pressure and the static reservoir pressure is referred as drawdown.

### 1.4.2 IPR for Gas Reservoirs (Inflow)

The compressible nature of gas results in the IPR no longer being a straight line. However, the extension of this steady state relationship derived from Darcy's Law, using an average value for the properties of the gas between the reservoir and wellbore, leads to:

Due to the compressible nature of gas the IPR curve of the gas reservoirs is not a straight line. For gas reservoirs Darcy's law can be written as follows:

$$q = C(\bar{P}_R^2 - P_{wf}^2)^n$$

where,

$C = \text{constant}$

'n' is a flow coefficient and takes values for 0.5 to 1 depending in the type of flow<sup>1</sup>. For laminar flow  $n=1$ .

### 1.4.3 IPR for Two-Phase Reservoirs

In reality, in most reservoirs the flowing bottom-hole pressure is below the bubble point pressure. When the pressure of the reservoir falls below the bubble point pressure, solution gas escapes from the oil and becomes free gas and therefore the previous assumptions are no longer valid. From well test data it has been observed/indicated that the straight PI is not valid and a downward curving line has been observed. This is due to the reduction in oil relative/effective permeability due to the increase in gas saturation, and hence the PI cannot be illustrated as a straight line (deviates from a straight line relationship). Also, oil viscosity is increasing since its solution gas content is decreasing which result in lower oil production rate for the same drawdown<sup>9</sup>.

Several empirical methods have been developed to predict the non-linear behavior of the IPR for solution gas drive reservoirs. One of the methods used to predict Inflow Performance (under solution gas drive) for saturated reservoir has been proposed by Vogel<sup>12</sup> is as follows:

$$\frac{q}{q_{max}} = 1 - 0.2 * \left(\frac{P_{wf}}{\bar{P}_R}\right) - 0.8 * \left(\frac{P_{wf}}{\bar{P}_R}\right)^2$$

Vogel's key contribution was the introduction of the concept of normalizing the production rate to the AOF value ( $q_{max}$ ) and the bottom hole pressure to the initial static reservoir pressure to express the relationship in dimensionless form. This equation can be used for both undersaturated and saturated reservoirs, where IPR is a straight line above the bubble point and it is curved downwards below the bubble point pressure, as illustrated in Figure 1.3.

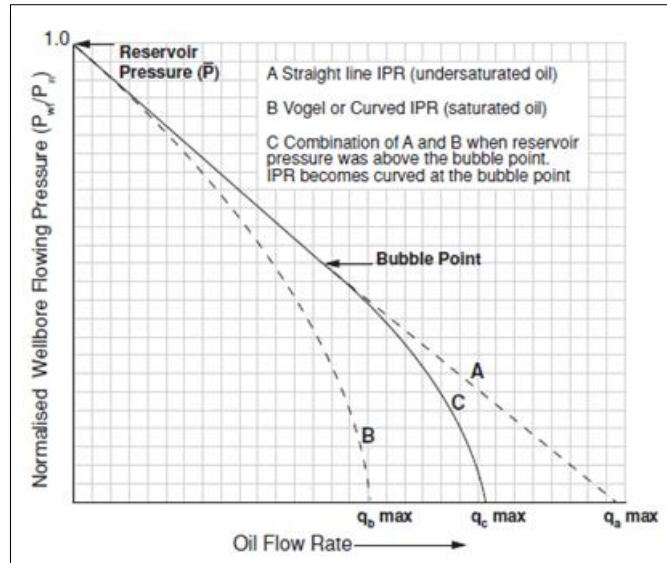


Figure 1.3: IPR curve for undersaturated and saturated reservoir<sup>1</sup>.

#### 1.4.4 Factors Affecting IPR Curve

As it has become obvious, the IPR curve is affected by parameters related to the reservoir. The factors affecting reservoir deliverability are summarized below:

- Reservoir pressure
- Pay zone thickness
- Effective permeability
- Reservoir boundary type and distance
- Wellbore radius
- Reservoir fluid properties
- Near-wellbore conditions
- Completion effects (perforations, well damage)

Examples on factors affecting the IPR curve are summarized in the following section.

#### Effect of Viscosity

It is obvious that the increase viscosity of the fluid adversely affects the drawdown. Figure 1.5 shows the effect of oil viscosity on IPR curve.

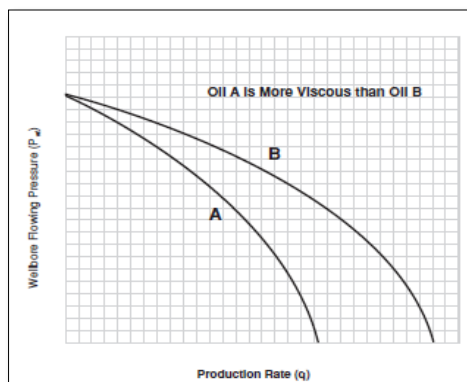


Figure 1.4: Effect of oil viscosity on IPR curve<sup>1</sup>.

## Reservoir Depletion

As the reservoir keeps on producing fluids the static reservoir pressure decreases. As a result gas escapes from the oil which makes oil more viscous making oil flow progressively more difficult. Also it contributes to the increasing gas saturation that adversely affects the relative permeability of oil and hence reducing the overall oil production. This reduction in oil production rate makes the IPR curve deviating from being a straight line and making it to bend downwards. Figure 1.4 shows different IPR curves of a reservoir for various initial static reservoir pressures<sup>4</sup>.

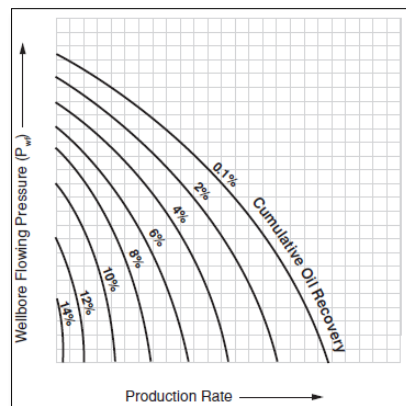


Figure 1.5: Effect of reservoir depletion on IPR curve<sup>1</sup>.

## Perforations Effect

As it can be appreciated from Figure 1.6 that increasing the perforations density improves the inflow from the reservoir and hence larger liquid flow rate for a given bottom-hole pressure. The increase in liquid flow rate for the same drawdown flattens the IPR curve.

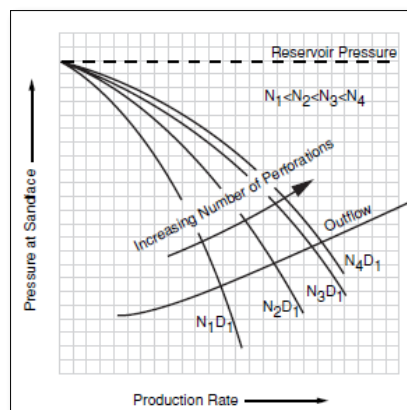


Figure 1.6: Effect of perforations density on IPR curve<sup>1</sup>.

## Skin Effect

Skin is a measure of the resistance to the flow. In Figure 1.7 is demonstrated the effect of skin in the inflow performance. As it was expected, a decrease in the skin factor improves the liquid flow rate from the reservoir to the well and well stimulation, acidization and fracturing are few methods to achieve it.

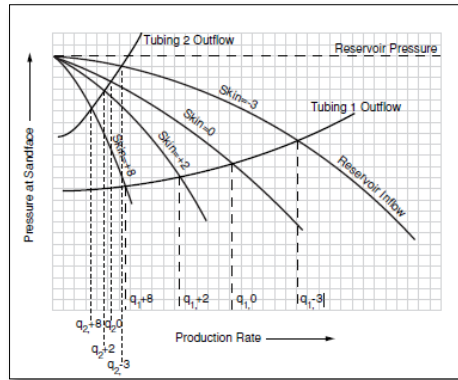


Figure 1.7: Skin removal effect in IPR curve<sup>1</sup>.

## 1.5 Tubing/Vertical Lift Performance

The pressure drop required to lift reservoir fluids from the perforations level to the surface is another main factor affecting the well deliverability. VLP is a relation between the liquid flow rate and the bottom-hole pressure (required). In general, as much as 80% of the total pressure loss in the system is to lift the reservoir fluids to the surface. Hence VLP is an important parameter for the overall Well Deliverability. Well deliverability is the optimum flow rate that is supported by both IPR and VLP for the given reservoir and surface pressure conditions.

Basically VLP is an alternative form of Bernoulli's equation and it is a general energy equation which can be written as follows:

The General Energy Equation describes the conservation of energy and states that the change in energy between two points of a flowing fluid is equal to the work done on the fluid minus energy losses. The contribution of total pressure losses from the perforations level through the 'flowline' to the separator can be attributed in the following components:

$$dP_{tubing} = dP_g + dP_f + dP_k$$

### 1.5.1 Bottom-hole Pressure

The bottom-hole pressure in VLP is generally determined by adding all the pressure losses in tubing to the back pressure at the wellhead. If the flowline from wellhead to separator is short the pressure losses are negligible and separator pressure can be taken as the wellhead pressure. Otherwise back pressure shall be calculated by adding the pressure losses in the upstream flow line of wellhead and the separator pressure.

$$P_{FBHP} = dP_{tubing} + dP_{flowline} + P_{sep}$$

Where  $P_{BHP}$ = bottom-hole pressure (required)

$dP_{tubing}$ = pressure losses in the tubing

$dP_{flowline}$ = pressure losses in the flowline

$P_{sep}$ = the separator pressure

$$P_{FBHP} = P_{sep} + dp_{flowline}$$

The relationship between the flowing bottom-hole pressure and the liquid flow rate is called Tubing Performance Relationship (TPR) or Vertical Lift Performance (VLP). The VLP curve depends on many factors including fluid PVT properties, well depth, tubing size, surface pressure, water cut and GOR. It describes the flow from the bottom-hole of the well to the wellhead.

### **1.5.2 Calculation of Pressure Drop in Tubing**

Oil, gas and water along with possibility of sand carry over past the packers the existence of multiple phases in the production tubing is very common in the industry. Calculation of the pressure drop in the multiphase flow is itself a big course. To understand the basics of multiphase flow it is necessary to understand the single-phase flow first.

#### **1.5.2.1 Hydrostatic Gradient**

This term is also known as elevation term and stands for the changes in potential energy between the bottom-hole and the wellhead depth.

$$dP_g = \rho * g * L * \sin\theta$$

where,

$\rho$  = is the density

$g$  = acceleration due to gravitational forces

$L$  = the length of the pipe

$\theta$  = the angle between horizontal and the directional of flow

#### **1.5.2.2 Frictional Losses**

##### **Single Phase Flow**

In general, liquid is practically incompressible and hence it can be assumed that flow velocity is constant in the pipe. Therefore, the most important parameter for pressures losses along the well for a liquid is the hydrostatic head compare to frictional pressure losses. In contrast, the most important feature of gas flow, compared to the flow of liquids, is the fact that gas is highly compressible. This effect results in increasing velocity as it flows. At the bottom of the well the pressure is higher so the gas occupies less space and hence the flow velocity is less than further down the line. Consequently, gas velocity increases in the direction of flow. Therefore, friction losses will not be constant all along the pipe line because they vary with the square of flow velocity. Therefore, the calculation of flowing pressure losses cannot be done for the total pipe length at once as was the case in the single-phase liquid flow.

Frictional pressure is a function of the fluid characteristics (Newtonian or non-Newtonian fluid viscosities), fluid conditions (velocity and laminar or turbulent flow) and the properties of the tubing (diameter and roughness). It accounts for the irreversible energy losses required to overcome friction losses due to viscous drag. Frictional losses are a function of

fluid's flow rate, flow regime, fluid's viscous properties as well as the roughness, the diameter and the length of the tubing. Frictional pressure losses in vertical or inclined oil wells are usually rather low when compared to the hydrostatic or elevation pressure drop. In wells producing medium to high liquid rates, frictional drops amount to a maximum of 10% of the total pressure drop. This number, of course, increases for extremely high liquid production rates.

The Reynolds Number (Re) is the ratio of the inertial forces to the viscous forces for fluid (density,  $\rho$  and viscosity,  $\mu$ ) flowing in a circular pipe.

$$R_e = \frac{\rho * v^2}{\frac{\mu * v}{D}} \text{ or } \frac{\text{inertial forces}}{\text{viscous forces}}$$

Where,  $v$  is the average fluid velocity.

If the  $R_e < 2100$ , it can be classified as laminar flow. If  $R_e > 4300$  it is turbulent flow. In between is the transition zone.

### **Laminar Flow**

For laminar flow regimes, the Fanning friction factor is inversely proportional to the Reynolds number, or

$$f_F = \frac{16}{N_{RE}}$$

### **Turbulent Flow**

$$dP_f = \frac{2 * f_f * \rho * u^2 * L}{D}$$

where,

$f_f$  = the Fanning friction factor

$u$  = velocity of the fluid

$D$  = Inside diameter of tubing

The Fanning friction factor ( $f_f$ ) can be evaluated based in the relative roughness of the tubing string interior and the Reynolds number is usually determined from Moody's diagram.

#### **1.5.2.3 Losses due to Acceleration**

$$dP_k = \rho * (u_2 - u_1)^2$$

Where,  $u_2$  = Velocity at a downstream point

$u_1$  = Velocity at an upstream point

Kinetic energy losses due to acceleration of the expanding fluid are usually neglected since they are minimal.

For the liquid flow in vertical wells hydrostatic head is the major component in the pressure loss since the fluid has to move against the head and the frictional loss is rate dependent and becomes vital at very high flow rates. In contrast, in gas wells the effect of the hydrostatic head is negligible and the frictional losses are huge.

### **1.5.3 Multiphase Flow**

When a pipeline is occupied by both gas and liquid (oil and water) few sections of the pipe may be occupied by liquid or gas or oil and gas together. So, assuming the constant density of fluid along the length of tubing is not valid in this case. So, to define the densities in every section of the tubing corresponding volumes of both gas and liquid shall be determined.

Multiphase flow is much more complicated than the single-phase flow. The parameters that must be considered in order to calculate accurately the pressure losses in the tubing are the following:

#### **1.5.3.1 Liquid Hold Up/Slip Effects**

When two or more phases are present in a pipe, they tend to flow at different in-situ velocities. These in-situ velocities depend on the density and the viscosity of each phase. Typically, the less dense phase is travelling faster. This causes a “slip” effect between the phases. As a consequence, the in-situ volume fractions of each phase (under flowing conditions) will differ from the input volume fractions of the pipe.

When liquid and gas are flow together in a pipe, the velocities differ so that the gas phase always overtakes or slips past the liquid phase. This phenomenon is called gas slippage or slippage and is caused by the following factors:

- Gas due to its compressibility is expanded in the direction of flow causing an increase in the velocity
- The different in density of gas (light phase) and liquid (dense phase) have a result in buoyance forces acting on the gas phase that increase the gas velocity
- Gas moves easier because energy losses in gas phase are lower compare to oil's phase<sup>4</sup>

Liquid hold up is a consequence of slip effect,  $H_L$ , and it is defined as the fraction of an element of pipe which is occupied by liquid at same instant.

$$\text{Where, } H_L = \frac{\text{Volume of liquid in a pipe section}}{\text{Volume of a pipe element}} \text{ and } H_G = \frac{\text{Volume of gas in a pipe section}}{\text{Volume of a pipe element}}$$

#### **1.5.3.2 Superficial Velocity and In situ velocity**

The superficial velocity of each phase is defined as the volumetric flow rate of each phase divided by the cross-sectional area of the pipe.

$$V_{SL} = \frac{q_L}{A_p} \text{ and } V_{SG} = \frac{q_G}{A_p}$$

The in-situ (or actual) velocity can be defined as the volumetric flow rate of each phase divided by the cross-sectional area that is occupied by the phase.

$$V_L = \frac{q_L}{A_L} \text{ and } V_G = \frac{q_G}{A_G}$$

Where,  $A_L$  and  $A_G$  are the actual areas of the pipe occupied by that liquid and phases respectively. Hence,  $A_L + A_G = A_p$

### **1.5.3.3 Flow Patterns (Flow Regimes)**

Another important feature of multiphase flow is the distribution of each phase in the so-called flow patterns. Flow patterns are visually observed and cataloged in laboratory conditions. Each flow pattern corresponds to a particular spatial distribution of the phases. As flow conditions are changed (like gas or liquid flow rates), flow patterns change from one configuration to another. The distribution of the flow patterns for different flow conditions is known as a flow pattern map i.e. graphical representations of the ranges of occurrence for each pattern.

The different flow regimes though, can be classified into the following categories: They occur in the given sequence if gas flow rate is continuously increased for a constant liquid flow rate and shown in Figure 1.8.

**Bubble Flow:** The gas phase is distributed in discrete bubbles within a liquid continuum

**Slug Flow:** When the concentration of bubbles in bubble flow becomes high, bubble coalescence occurs and, progressively, the bubble diameter approaches that of the tube. Once this approach, the slug -flow (or plug -flow) regime is entered with the characteristics bullet shaped bubbles

**Churn Flow:** As the gas flow is increased the velocity of these bubbles increases and ultimately, a breakdown of these bubbles occurs leading to an unstable regime in which there is, a wide bore tubes, an oscillatory motion of the liquid upwards and downwards in the tube, thus the name of churned flow is applied. For narrow-bore tubes the oscillations may not occur and a smoother transition between the slug flow and annular flow may be observed.

**Annular Flow:** The liquid flows on the wall of the tube as a film and the gas phase flows in the center. Usually, some liquid phase is entrained as small droplets in the gas core.

**Mist Flow/Wispy Annular Flow:** As the liquid flow rate is increased the droplet concentration in the gas core of annular flow increases and, ultimately, droplet coalescence occurs leading to large lumps or streaks as wispy liquid occurring in the gas core. This regime is characteristics of high mass velocity flows<sup>3</sup>.

To find the pressure distribution along the production tubing or flowline, the pipe is divided into small segments. Fluid properties and pressure gradients are calculated at average conditions of pressure, temperature, and pipe inclination angle within each of these pipe segments.

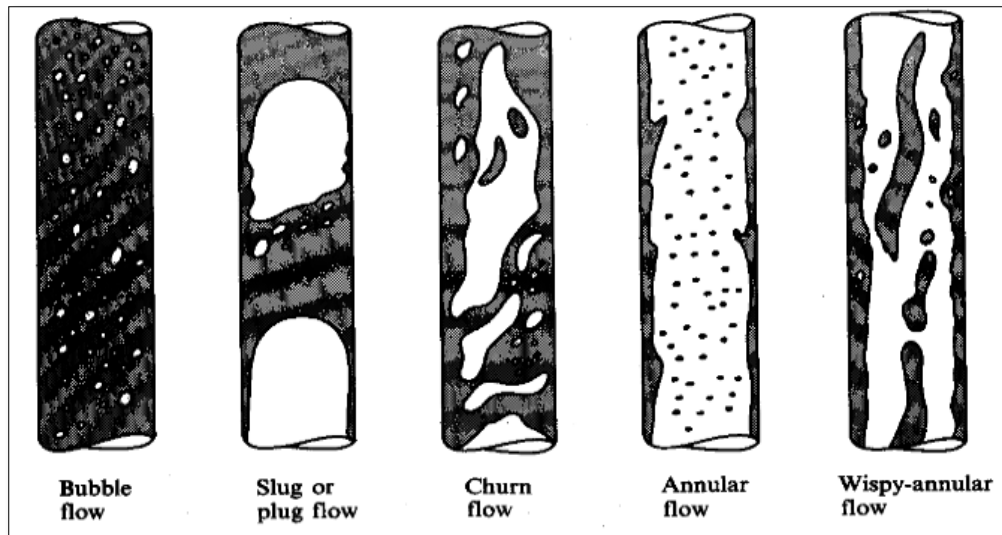


Figure 1.8: Flow regime in Vertical flow<sup>3</sup>.

#### **1.5.3.4 Multiphase Flow Correlations**

Multiphase flow correlations are used to predict the liquid holdup and frictional pressure gradient. Depending on the particular correlation, flow regimes are identified and specialized holdup and friction gradient calculations are applied for each flow regime. The density difference between gas and either water and oil is far greater than the density difference between oil and water. The multi-phase flow correlations lump oil and water together as liquid and calculations are based on liquid/gas interactions. Such flow correlations are more accurately described as two-phase methods. The calculation errors resulting from lumping the water and oil together have been found to be insignificant for the majority of oil well pressure calculations. The primary purpose of a flow correlation is to estimate the liquid holdup (and hence the flowing mixture density) and the frictional pressure gradient.

All these correlations are empirical in nature and were fitted to available flow loop data for the small sizes of pipelines and inclination angles. They are best suited to be used for the similar flow conditions such as angle of inclination, GOR and average pressures. Therefore, care should be exercised in section of the right VLP correlation specific to the application.

## **2. Artificial Lift Methods**

### **2.1 The Need for Artificial Lift**

Most oil wells in the early stages of their lives flow naturally to the surface with their natural energy. A well to be able to produce on natural flow, means that the pressure at the bottom of the well is sufficient enough to overcome the total pressure losses from the flow path to the wellhead/separator. If this criterion is not met the production will cease and the well will be dead.

The fluid production from the well results in a reduction of the reservoir pressure and also the increase in the fraction of water being produced together with a corresponding decrease in the produced gas fraction. All these factors may lead the well either to stop flowing or not be able to produce fluids at economical rates. In such cases artificial lifting methods are installed so the required bottom-hole flowing pressure can be maintained.

Maintaining the required flowing bottom-hole pressure is the basis of the design of any artificial lift installation; if a predetermined drawdown in pressure can be achieved, the well will produce the desired fluids. Artificial lift adds energy to the well fluid which, when added to the available energy provided “for free” by the reservoir itself, allows the well to flow at a (hopefully economic) desired rate<sup>1</sup>.

### **2.2 A Review in Artificial Lift Systems**

The most popular forms of artificial lift are illustrated in Figure 2.1. They are:

**Rod Pumps:** A downhole plunger is moved up and down by a rod connected to an engine at the surface. The plunger movement displaces produced fluid into the tubing via a pump consisting of suitably arranged travelling and standing valves mounted within a pump barrel.

**Hydraulic Pumps** use a high pressure power fluid to:

- Drive a downhole turbine or positive displacement pump or
- Flow through a venturi or jet, creating a low pressure area which produces an increased drawdown and inflow from the reservoir

**Electric Submersible Pump (ESP)** employs a downhole centrifugal pump driven by a three phase, electric motor supplied with electric power via a cable run from the surface penetrates the wellhead and is strapped to the outside of the tubing.

**Progressing Cavity Pump (PCP)** employs a helical, metal rotor rotating inside an elastomeric, double helical stator. The rotating action is supplied by downhole electric motor or by rotating rods<sup>1</sup>.

**Gas Lift** is a procedure to inject gas at some downhole point to lighten the column and in turn reduce the bottom-hole pressure.

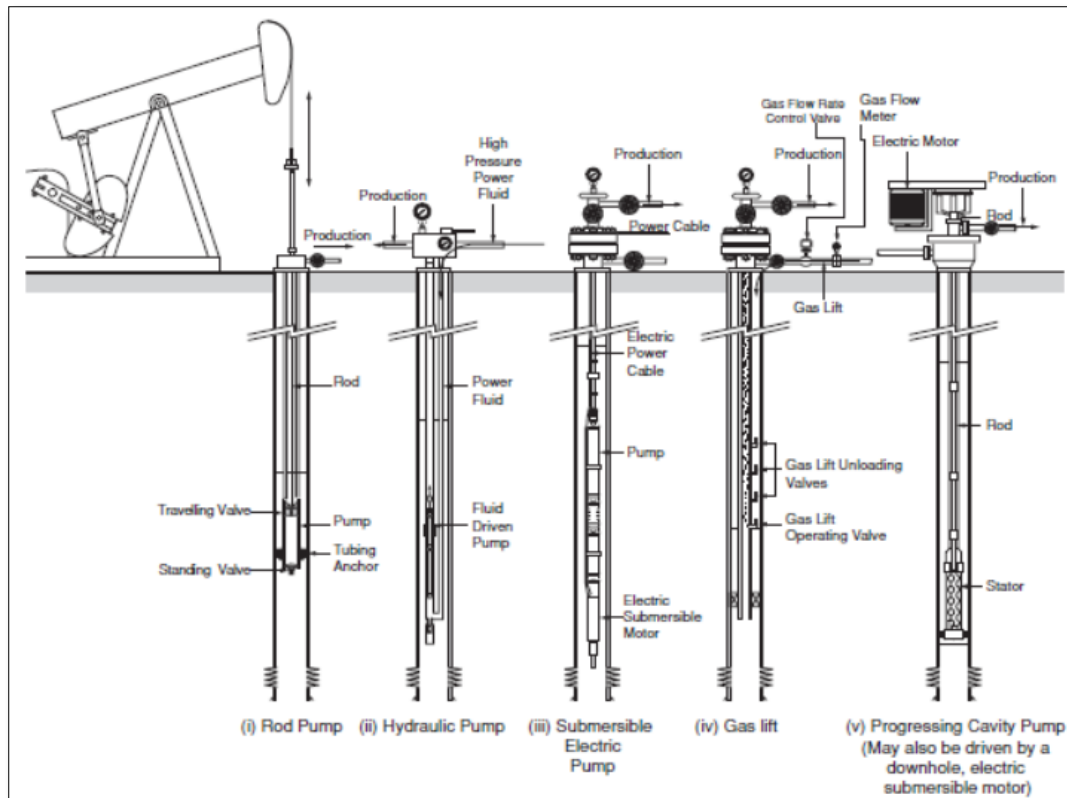


Figure 2.1: The most popular types of artificial lift<sup>1</sup>.

### 2.3 Gas Lift

Gas lift method involves the supply/injection of compressed gas at some downhole point in the tubing to aerate or lighten the fluid column, so as to reduce the average density of the fluid and the flow resistance of the ascending flow column. The increased gas/liquid ratio from the valve to the surface results in the reduction of the hydrostatic pressure gradient into the tubing, which is the major factor of the pressure drop in vertical multiphase flow. By this way the average flowing density is decreased and eventually the pressure at the bottom of the well is decreased creating a drawdown and consequently the flow from the well.

For the liquid flow in vertical wells hydrostatic head is the major component in the pressure loss since the fluid has to move against the head and the frictional loss is rate dependent and becomes vital at very high flow rates. The injected gas also improves the liquid flow rate by the energy of expansion which pushes the oil to the surface.

The lifting of fluid can be accomplished by either continuous or intermittent gas injection. In continuous gas lift the flowing bottom-hole pressure will remain constant for a particular set of conditions and is considered as a steady state flow operation. In intermittent gas lift, the reservoir fluid is produced intermittently by displacing liquid slugs with high pressure injection gas. At intermittent lift the flowing bottom-hole pressure will vary with the particular operation time of one cycle in production. Economics enter the design of any lift installation. Intermittent lift is applicable to low productivity wells with low reservoir pressure.

This study is focus on continuous gas lift method. In continuous flow gas lift a continuous volume of compressed gas is introduced into the annulus to tubing at a fixed rate, through a gas lift valve at a fixed depth. Continuous gas lift method is usually applied in wells which have high bottom-hole pressure relative to their depths or/and with high productivity index. In this way the bottom-hole pressure is reduced. A schematic drawing of a well placed on continuous flow gas lift is given in Figure 2.2<sup>4</sup>.

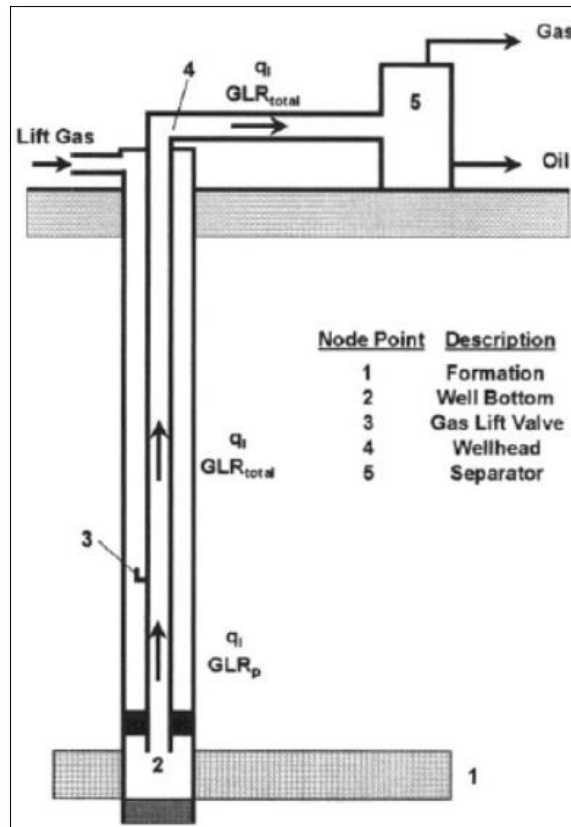


Figure 2.2: Gas Lift well schematic<sup>4</sup>.

The operation of a continuous gas lift well is very similar to that of a naturally flowing well with the difference that the GLR changes above the point of injection to the surface. The depth that the operating valve is located is dependent on the available surface injection pressure at the compressor. The more pressure available the deepest the injection point. Furthermore, the deepest the injection point the most efficient the method is.

The well can be divided in two sections where the flowing multiphase mixtures gas content is different. Assuming the point of injection at the bottom-hole, the inflow and outflow performance at the bottom hole of the well can be expressed as<sup>10</sup>.

Inflow:

$$\bar{P}_R - \Delta P_{res} = P_{BHP}$$

Outflow:

$$P_{sep} + \Delta P_{flowline} + \Delta P_{(tubing\ above\ the\ valve)} + \Delta P_{(tubing\ below\ valve)} = P_{BHP}$$

The inflow performance is independent of the injected GLR, but the pressure drop in the flowline changes notably as the GLR is increased. The pressure drop at the tubing below the point of injection is estimated using multiphase flow correlations or pressure traverse curve with the formation GLR ratio, while above the valve using the total GLR. The total GLR is calculated from the summation of the lift and produced gas rate divided by the liquid rate. Gas injection requirements can be found as follows:

$$GLR_{inj} = GLR_{TOTAL} - GLR_{formation}$$

The effect of the GLR, keeping the well head pressure, the liquid rate and the tubing diameter constant, is shown at Figure 2.3. As GLR is increased, there is a limit where above which the pressure difference in the well will begin to increase, because the reduction in the hydrostatic pressure will be offset by the increase in the friction pressure. At this point, where the friction losses in the tubing counterbalance the hydrostatic head/component term, the maximum GLR is obtained and eventually the gas injection rate is optimized. This point is referred at the “technical optimum gas injection rate” and at which consequently the well liquid production is maximized<sup>6</sup>.

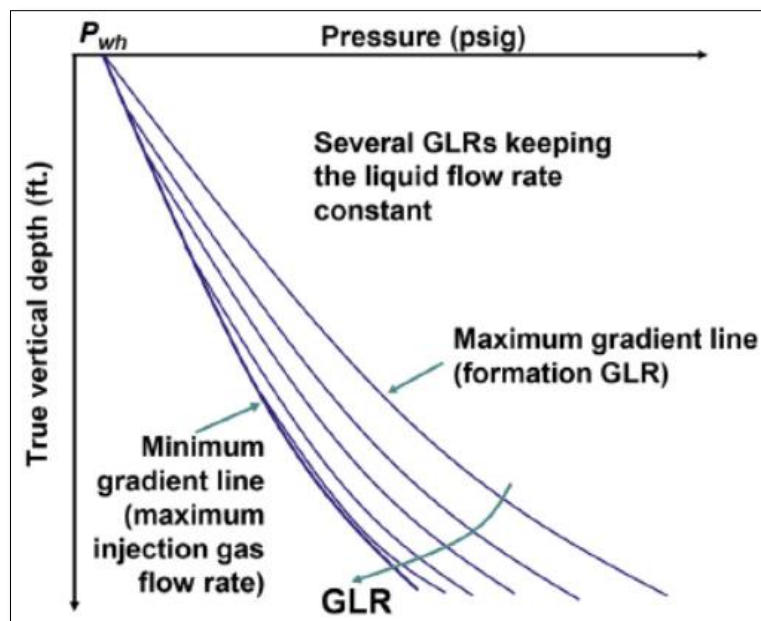


Figure 2.3: Production pressure curves for different GLR<sup>5</sup>.

### 2.3.1 Gas Lift Design

The design of a gas lift completion thus consists of two separate distinct parts. One is unloading of the completion fluid for the well startup and the second is to find the gas lift parameters for continuous operation such as the optimum depth of the operating valve, which is the final point of injection once the well has been unloaded, gas injection rate, maximum casing pressure and surface injection pressure at the compressor<sup>5</sup>.

Therefore the aim/objective is to find out the optimum GLR at the deepest injection depth. The purpose of finding the maximum GLR is to find the minimum pressure drop in tubing in order to maximize the production rate specific to the current conditions. The advantage of

gaining the optimum GLR must be utilized the whole tubing. Having said that/ By considering the principal it becomes obvious that the injection must be the deepest possible/deepest most point in the tubing.

The depth of injection is affected mainly from the available surface injection pressure at the compressor. Hence, sufficient injection pressure is supposed to be installed at the surface. A schematic of the pressure gradient versus depth for gas lift operation is shown in Figure 2.4.

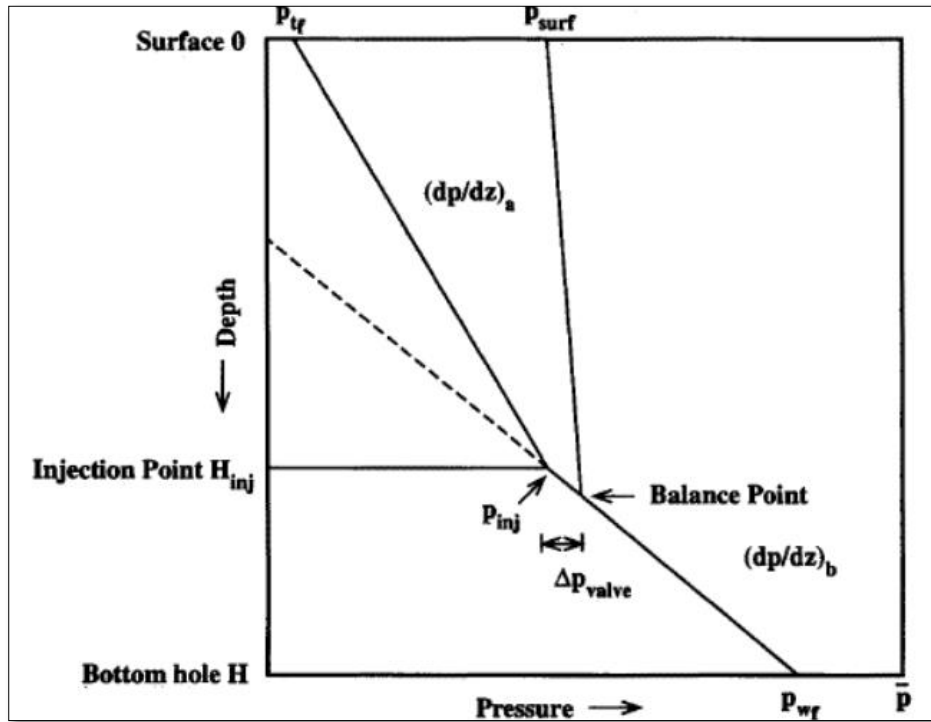


Figure 2.4: Pressure gradient versus depth for continuous gas lift system<sup>6</sup>.

### 2.3.2 The Effect of Operational Parameters

Following are the main/basic operational parameters/conditions that needed to be optimized and set for various production conditions through the life of the well are:

- Pressure of the wellhead
- Surface injection pressure
- Gas injection flow rate- the GLR injected
- Injection Depth
- Tubing Size

Few parameters can be adjusted from the surface as required in a day to day basis (also liquid rate) and summarized in the following section. And other parameters such as tubing size and injection depth shall be calculated and installed for once to be constant all through the life of the well.

### **2.3.2.1 Effect of Wellhead Pressure**

The pressure drop in tubing is depended on wellhead pressure. Since the solution node for IPR and VLP curve is the bottom-hole the calculated or required bottom-hole pressure at the bottom-hole is crucial/important for the overall tubing performance. In case of shortage of the required bottom-hole pressure of the tubing an option to reach the required bottom-hole pressure is by reducing the wellhead pressure.

$$P_{BHP} = P_{wh} + dP_{total(in\ tubing)}$$

To reduce the bottom-hole pressure the wellhead pressure must also be reduce, but the real optimization of tubing performance is in the optimization of dP itself and not the wellhead pressure. The total pressure losses in tubing can be separated/divided into two parts, one part is the pressure losses due to hydrostatic head and the other part is the pressure losses due to friction.

$$dP_{total(tubing)} = dP_{gravitational} + dP_{frictional}$$

Pressure loss due to friction is depended on the velocity. When the wellhead pressure decreases, the velocity of the fluid also decreases and hence more frictional pressure drop. There is a point that/where when the pressure of wellhead is reduced/reached the frictional losses dominate the gravitational losses and hence the overall pressure reduction that contributes to the minimum wellhead pressure can be found.

### **2.3.2.2 Gas Injection Pressure**

For the existing facilities in the gas lift design injection pressure is the main control/parameter on finding out the injection point.

The gas injection pressure is the main control on the depth of gas injection. Greater injection pressures mean that gas injection into the flow pipe can take place at greater depths, and deeper points of gas injection result in lower gas requirements. Higher injection pressure results in lower gradient and consequently less gas needed to decrease the flow gradient.

The injection pressure in the production tubing must be reduced by an additional 100-50 psi for the pressure drop across the valve. The value of this pressure drop will be supplied by the manufacturer.

### **2.3.2.3 Injection Gas Rate**

The gas injection contributes to increase the GLR in the tubing and hence in the reduction of the pressure drop in the tubing. The maximum gas injection rate corresponds to the optimized GLR. There is a point where the summation of the hydrostatic head losses and the frictional losses in the tubing becomes minimum. At this point the GLR is optimized.

### **2.3.2.4 Tubing Size**

Since continuous flow gas lifting involves flow of a multiphase mixture with varying gas content, the injection gas requirement must reflect the size of the flow pipe. The effect of pipe size on the multiphase pressure drop, however, is not as simple as that of the wellhead

pressure and may vary in different ranges of the flow parameters. A smaller pipe may develop less pressure drop than a bigger one, provided mixture flow rates are low to medium. For higher liquid flow rates, bigger pipes become more and more favorable as the mixture rate increases because friction losses become the governing factor in the total pressure drop<sup>4</sup>.

### ***2.3.3 Unloading Process***

If not designed, the gas compressor cannot provide the desired pressure with the available gas down to the designed depth of gas injection because the static pressure of the fluid in that depth is greater than the pressure of the injected gas; hence a sequence of unloading valves should be placed to unload the well.

During the initial unloading process casing and tubing pressure gradients in the static loaded conditions are equal. The well is stagnant with the completion fluid at specific level depending on the in the wellhead and the casing pressure. All gas lift valves are in the open position from the height of the hydrostatic fluid in tubing and casing annulus. As gas is injected down the casing annulus it displaces the completion fluid through the open gas lift valves into the tubing string and to the separator. As the lift gas continues to display and unload the fluid in the annulus; the pressure in the casing will continue to increase maximizing the artificial lift capability.

When the annulus fluid is unloaded to the first valve depth, the casing pressure will have reached its desired/designed kick-off pressure. This pressure is sufficient to lower the casing fluid below the first mandrel and allow gas injection into the top valve. This injected gas causes a lighter gradient into the tubing allowing the well to unload the kill fluid entering the tubing string from the lower valves, as the well continues to unload.

Once the annular fluid is displaced to the second valve depth injection gas begin entering the tubing from the second valve. The combined injection of both the first and second valves exist the throughput of the surface input choke resulting in a casing pressure decline. This decline causes the top valve to close. Injection continues from the second valve as the well continues to unload; lifting both the displaced killing fluid and produced well fluids. Note that as the well the well is unloaded to the second valve the bottom-hole pressure is less than the static bottom hole of the reservoir. This drawdown causes reservoir fluids to flow into the wellbore. The same processes is repeated every time the fluid in the casing is unloaded down below an additional valve, allowing the upper valve to close as the unloading process continues and the well is unloaded to the deepest point of injection. A schematic of the described unloading process is shown in Figure 2.5.

Also it should be noted that, as the liquid level in the casing reduces, the tubing level increases. This will increase the hydrostatic pressure/head in the tubing causing the bottom-hole to increase. Thus back flow can begin in the reservoir which may damage the formation. This can be prevented by installing a check valve at the bottom of the tubing.

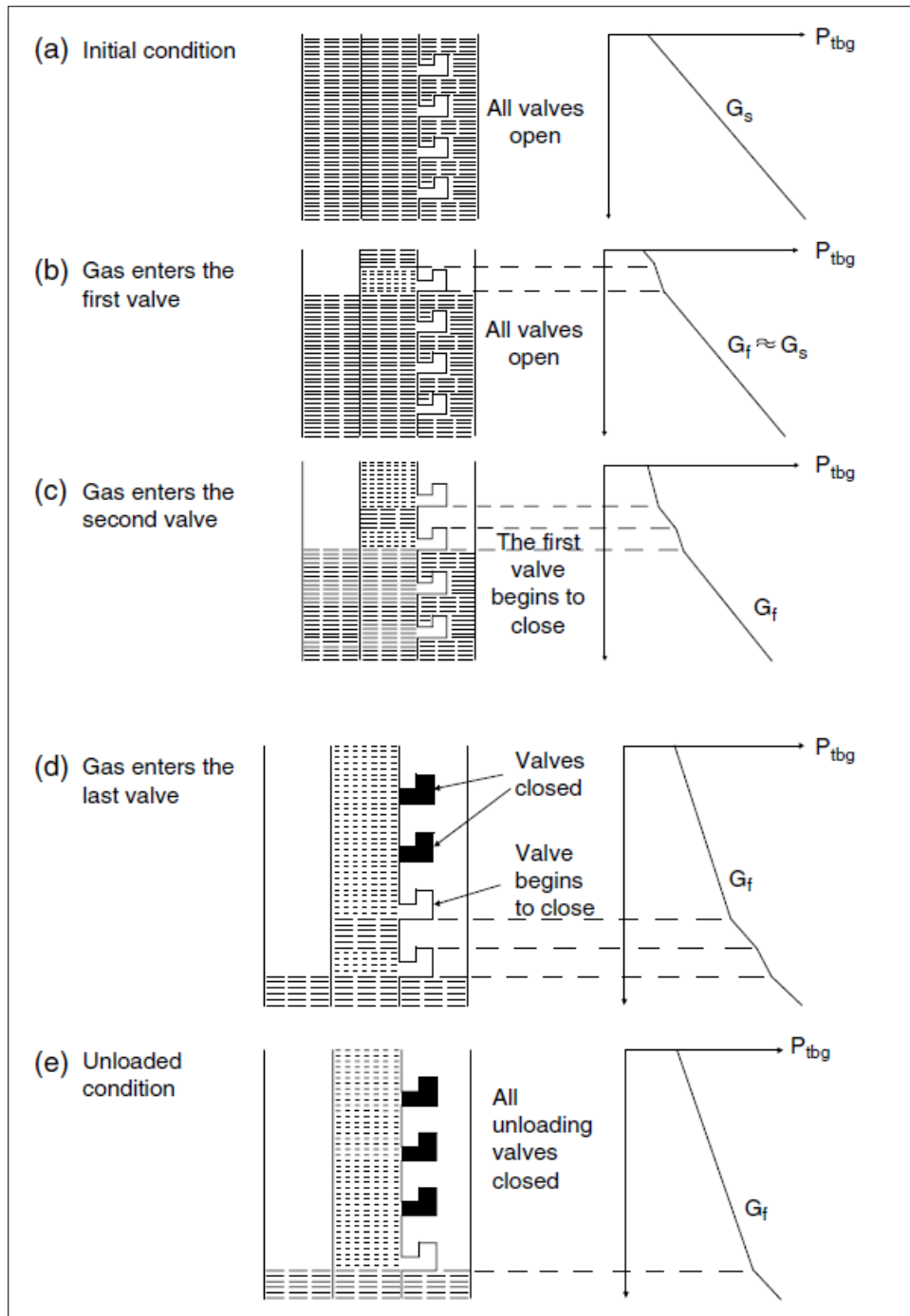


Figure 2.5: Well unloading sequence<sup>7</sup>.

### 2.3.4 Gas Lift Equipment

Gas lift valves located in the tubing are sized and spaced according to the overall design. The method of operation and type of installation depend largely on the type of valves used. It should be pointed out that, apart from the operating valve, additional valves are set along the tubing in predefined positions, according to the completion design. At these positions Side Pocket Mandrels are installed.

These gas lift valves are installed at carefully spaced intervals so that any liquid present above them in the casing/tubing annulus (e.g. due to killing of the well) can be removed by injection of gas at the top of the well annulus leading to the liquid U-tubing into the tubing and its subsequent ejection from the well. The gas injection point into the tubing is then transferred to successively deeper gas lift valves<sup>1</sup>.

There three types of gas lift valves. The difference is by their sensitivity to the casing pressure or the tubing pressure needed to open and close them. The valves are categorized from which pressure has the greater effect on the opening of the valve. The sensitivity is determined by the mechanical design of the valve because it is the pressure exposed to the larger area in the valve that controls the valves operation.

#### ***2.3.4.1 The Casing/Injection pressure operated valves (IPO)***

The IPO valves are designed in such a way that the casing pressure is acting on the larger area of the bellows and thus they are primarily sensitive to the casing pressure. The drop in casing pressure which occurs during unloading is used to close the valves in the correct sequence.

#### ***2.3.4.2 Production Pressure or Tubing operated valves (PPO)***

In the PPO valves the flow path is reversed and thus the tubing pressure is acting on the larger area of the bellows making the valve primarily sensitive to the tubing pressure. The drop in the tubing pressure as gas is injected is used to close the valve.

#### ***2.3.4.3 The throttling valve/Proportional Response Valves***

This technique is basically a refined PPO design and utilizes some minor changes to the mechanics of the valve to increase the throttling range<sup>13</sup>.

### 3. Model Input Data

Well construction and production/reservoir data from an onshore well X-1, from Hessi Messaoud field in Algeria has been used for the study.

#### 3.1 PVT Data

Table 3.1 shows the PVT data of the production fluid.

Property	Value	Units
API gravity	27	°API
Gas Specific Gravity	0.851	-
GOR	273	scf/STB
Bubble Point Pressure	1867	psig
Bo @Pb	1.236	cf/scf
Oil's Viscosity @Pb	1.425	cP
Reservoir's Temperature	204	°F

Table 3.1: PVT properties of the fluid.

#### 3.2 Well Data

##### 3.2.1 Well Geometry

X1 is a slanted well with the following deviation characteristics. Initial 1000 ft is vertical and then the kick off starts for the deviation. It has a deviation at an angle of 3° from vertical for every 100 ft from the kick of point. The target inclination angle is 45° and the proposed target (vertical) depth is 12,933 ft. Rotary table has been taken as the reference for all the depths; and is set at a height of 36 ft from the MSL.

Figure 3.2 shows the well deviation calculated based on the given description and has been used in the simulation study.

Point	Measured Depth (feet)	True Vertical Depth (feet)	Cumulative Displacement (feet)	Angle (degrees)
1	0	0	0	0
2	3280	3280	0	0
3	3380	3379.86	5.2336	3
4	3480	3479.32	15.6864	5.99999
5	3580	3578.08	31.3299	9
6	3680	3675.9	52.1211	12
7	3780	3772.49	78.003	15
8	3880	3867.6	108.905	18
9	3980	3960.96	144.741	21
10	4080	4052.31	185.415	24
11	4180	4141.41	230.814	27
12	4280	4228.01	280.814	30
13	6000	5717.58	1140.81	30
14	9000	8315.65	2640.81	30
15	12000	10913.7	4140.81	30
16	14331.7	12933	5306.66	30

Figure 3.1: Deviation survey of the well.

A schematic description of the well is shown in Figure 3.2.

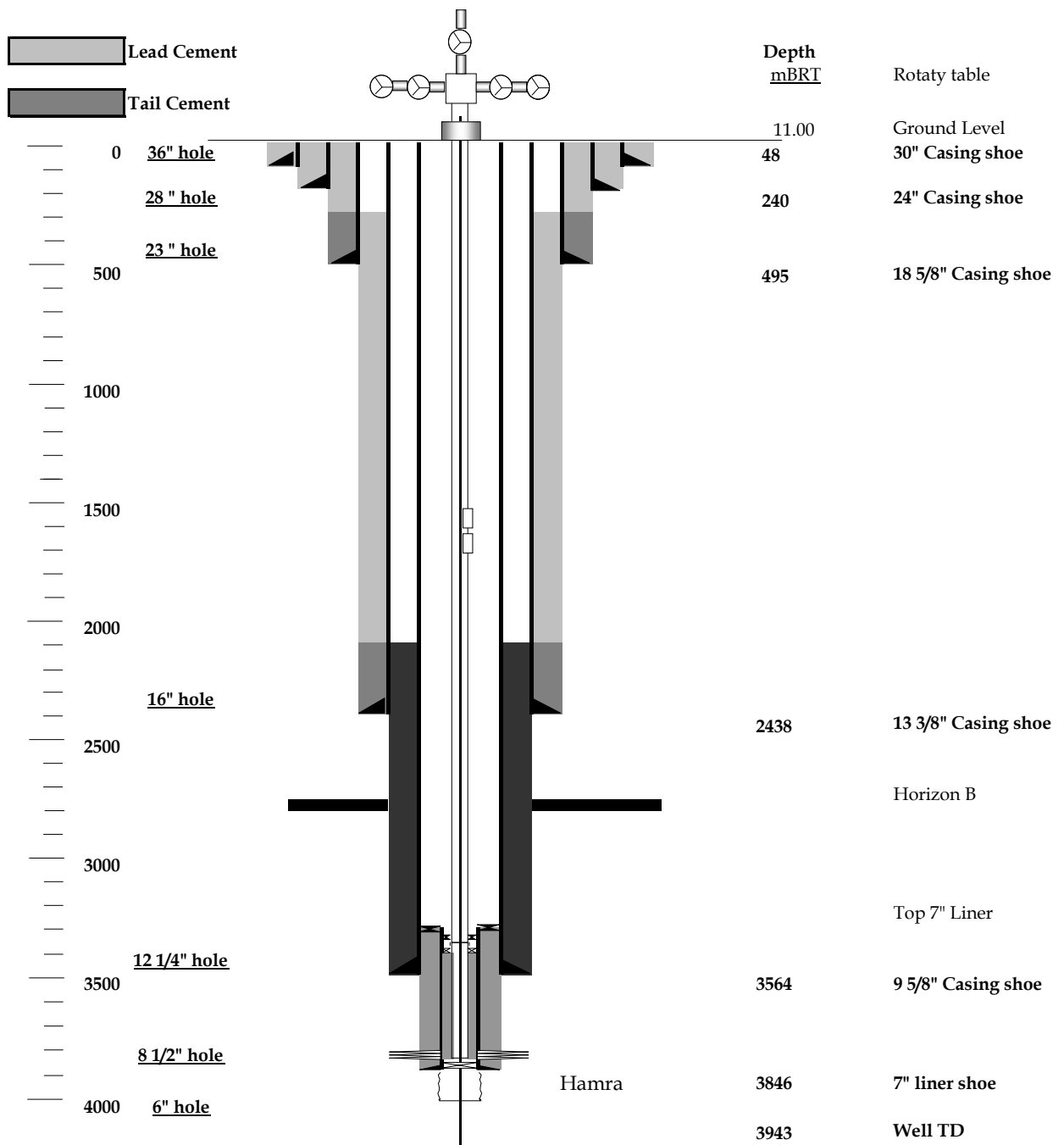


Figure 3.2: Completion Diagram.

### 3.2.1 Mechanical Properties of the tubing

Roughness parameter = 0.0006"

Default commercial value of stainless steel pipe has been used.

Depth of SSSV = 8631 ft

Diameter of SSSV = 3.75"

Tubing Outside Diameter = 4.5"

### 3.2.2 Geothermal Gradient

Table 3.2 shows the formation temperature along the depth of the tubing.

Formation TVD (ft)	Formation MD (ft)	Temperature (°F)
36.08	36.08	68
6560	6972.75	137
8200	8866.46	154
9840	10760.2	171
11480	12653.9	189
12933	14331.7	204

Table 3.2: Geothermal gradient of the well.

### 3.3 Reservoir Data

Reservoir pressure = 3489 psia

Reservoir temperature = 204°F

Productivity's index = 5 STB/day/psi.

### 3.4 Gas Lift Data

It has been supposed that the same produced gas is going to be used as lift gas for injection.

### 3.5 PROSPER Default Values

Water salinity = 23000 ppm

Overall Heat Transfer Coefficient = 8 BTU/h/ft<sup>2</sup>/°F

Average heat capacity of gas = 0.51 BTU/lb/°F

Average heat capacity of oil = 0.53 BTU/lb/°F

Average heat capacity of water = 1.00 BTU/lb/°F

### 3.6 PVT Data Pre-Processing

PVT data in Table 3.1 has been used to verify which of the PVT correlations that are available in PROSPER better matches the well test PVT data. From the low value of GOR and API density the fluid can be characterized as medium volatility to heavy oil.

Figure 3.3 shows Bubble point, Solution GOR, Oil FVF and oil viscosity calculated in PROSPER using different correlations and the closeness of the matching. Glaso equation predicts the Parameter 1 more close to the unity and Parameter 2 more close to zero compared to the other correlations indicating the better match. Hence Glaso equation has been used in the study.

For Oil Viscosity Beal et al has been selected.

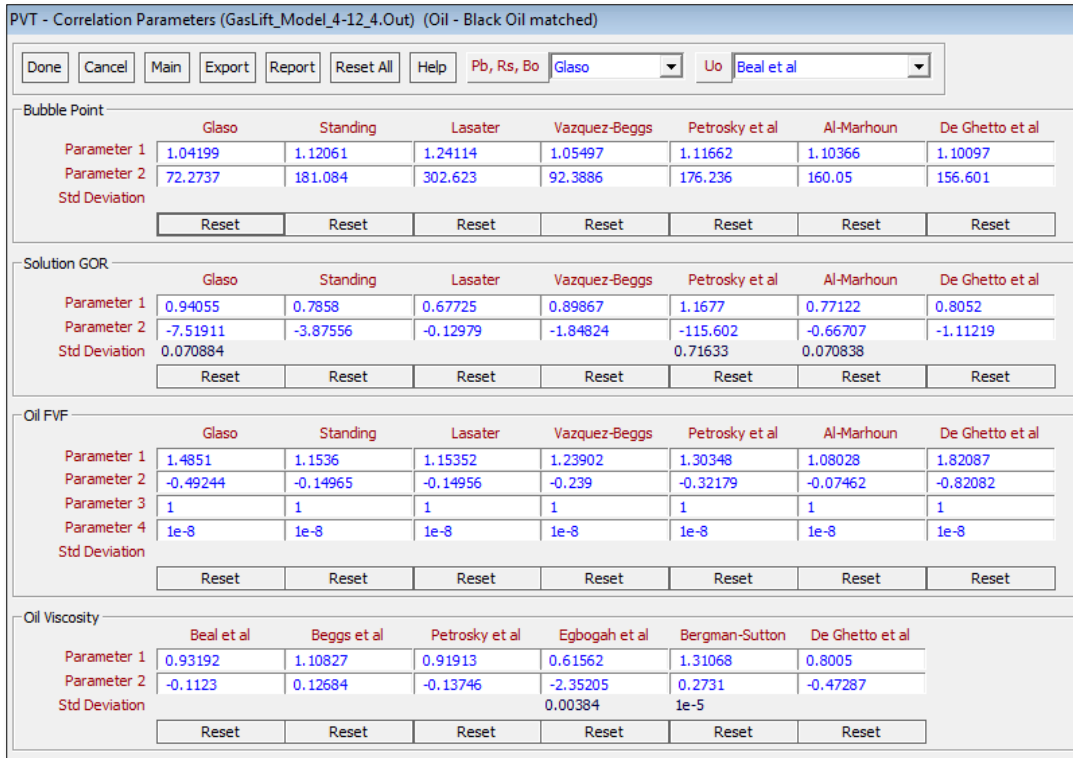


Figure 3.3: PVT matching.

Figure 3.4 through Figure 3.7 show the comparison of various fluid properties predicted by different correlations.

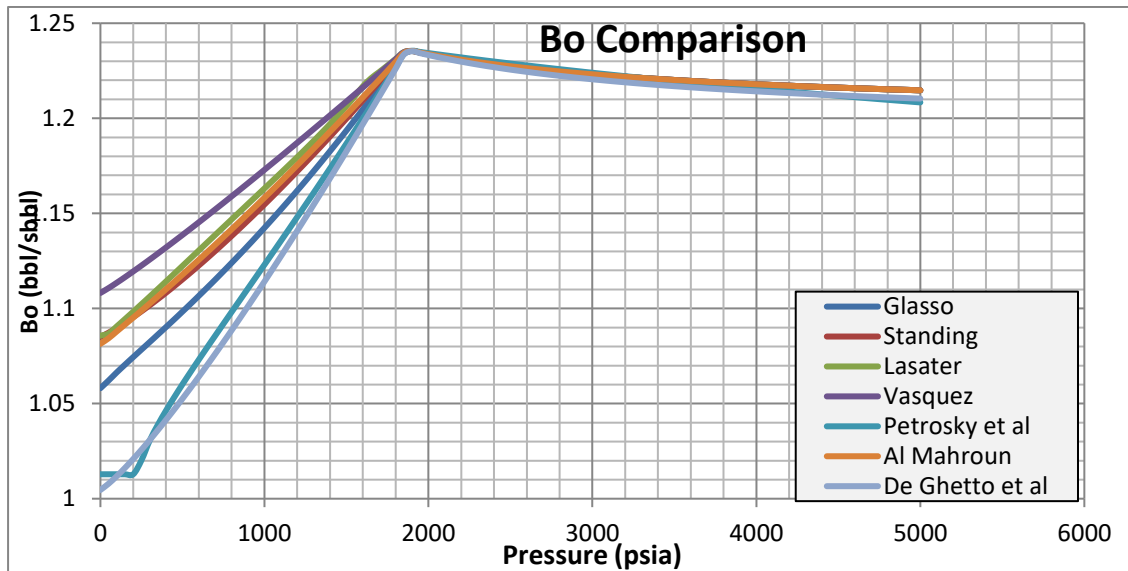


Figure 3.4: Bo comparison.

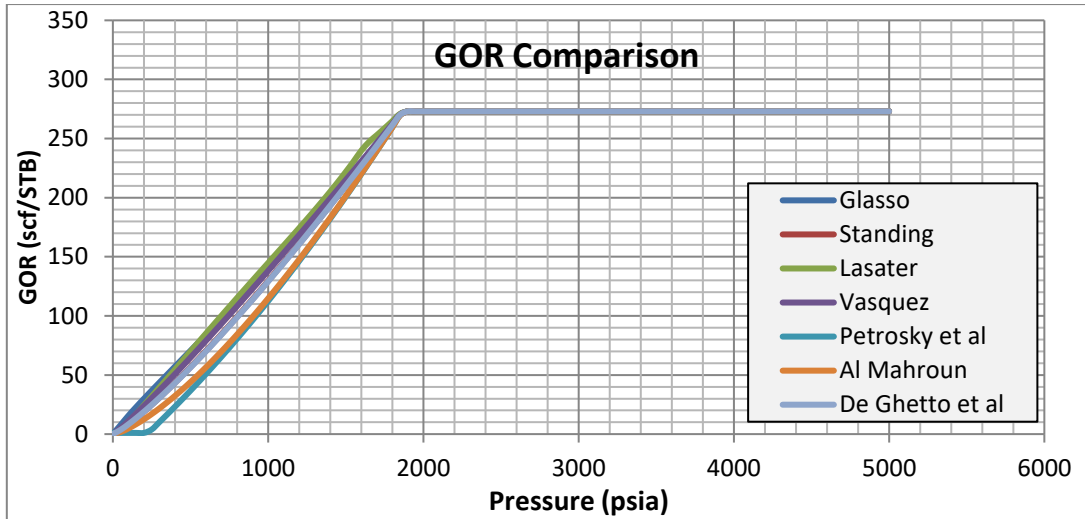


Figure 3.5: GOR comparison.

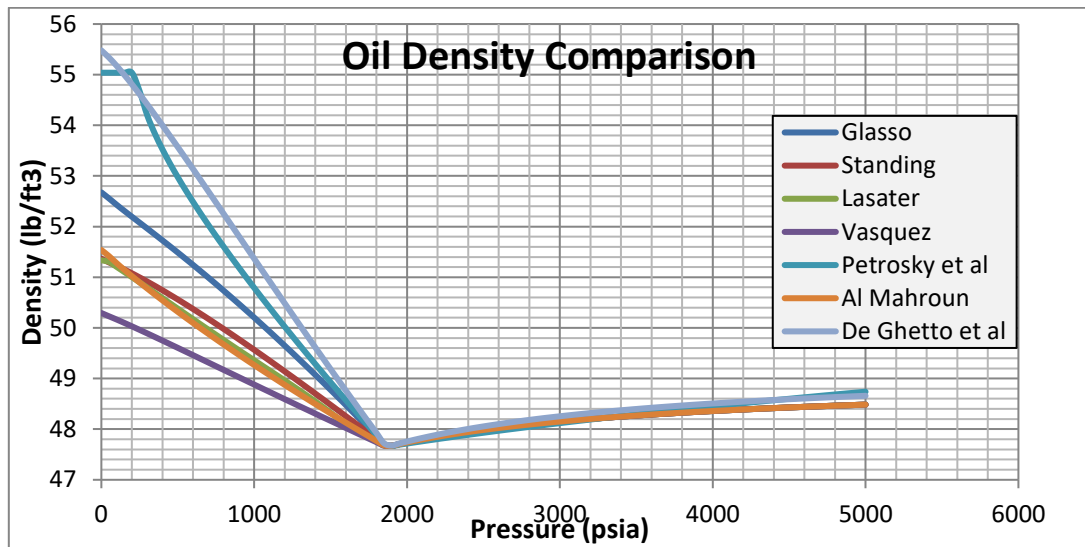


Figure 3.6: Oil density comparison.

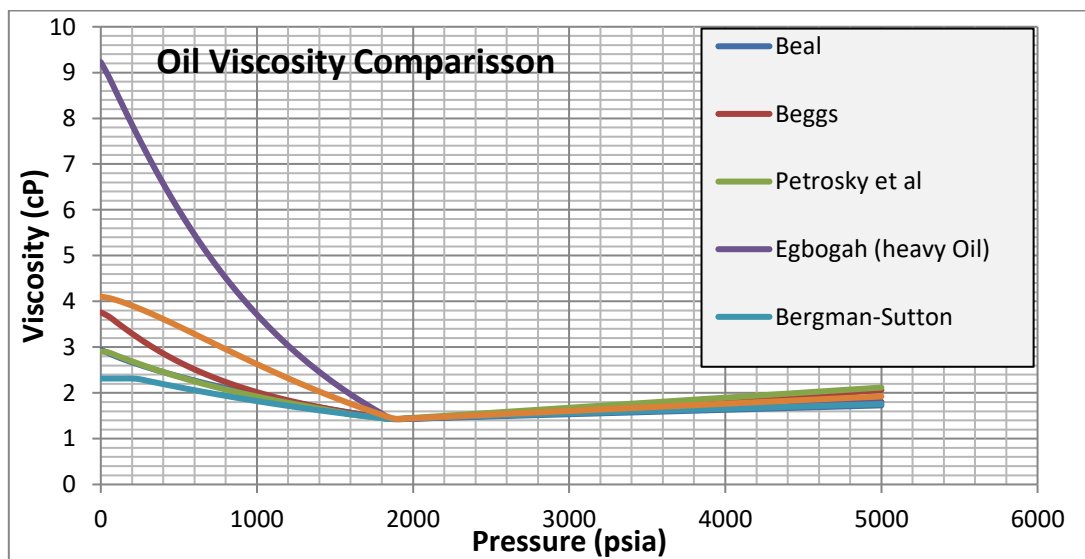


Figure 3.7: Oil viscosity comparison.

### 3.7 Production without Gas Lift

A PROPER model has been developed for the data tabulated in this section. Figure 3.8 shows the IPR and VLP curves. VLP was generated for a wellhead pressure of 250 psia.

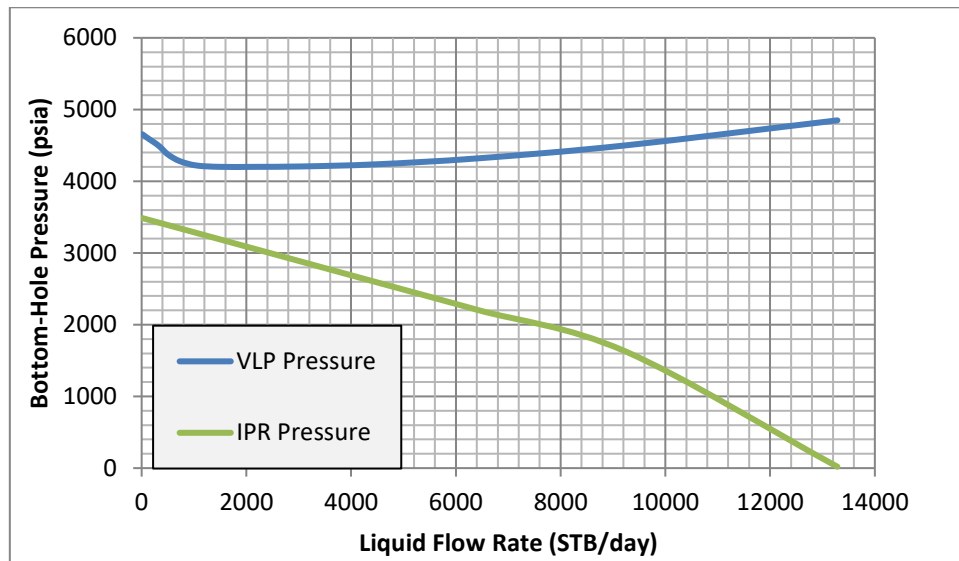


Figure 3.8: Production without gas lift-WHP=250 psia.

It can be observed that there is no point of intersection between the IPR and VLP curves indicating that no production can be possible. Therefore, a gas lift system is needed to make the well flowing.

## **4. Methodology**

The basic purpose of gas lift design is to maximize the oil production. Thus, the objective of this study is to design the gas lift for the maximization of oil production and therefore all the other parameters will be optimized based on/against the maximum oil production.

Maximum production from a single well is part of the overall field operating philosophy and depends on the so many parameters including that effect the reservoir flow, project development plan including the subsurface, subsea and processing plant facilities and the overall economics. Hence, sizing of the tubing has also been considered for the study along with the design and optimization of gas lift and verification of all possible scenarios that sensitize the well production rate. The gas lift design methodology that was followed has been subdivided into 3 sections.

### **4.1 Section 1: Design Methodology**

#### ***4.1.1 Section 1: Sizing of the Tubing and Gas Lift Design***

Three different tubing sizes vis-à-vis 3.5", 4.5" and 5.5" have been considered for the study and each option will have a different maximum production rate; the final tubing size can be decided based on the overall project development philosophy. For each tubing option, the maximum optimized gas injection rate, maximum pressure in the casing and the maximum injection pressure have been established.

Since the wellhead operating pressure is an outcome of the downstream facilities and overall evacuation philosophy a range of WHP pressures from 250 psia to 650 psia has been considered for the study.

A WHP of 250 psia gives the maximum production rate for the optimized gas injection rate and may have the highest bottom-hole pressure owing to the higher flow rates and hence may be the design case for the injection pressure and the maximum casing pressure. WHP of 650 psia may also trigger the higher bottom-hole pressure which may decide the design of the above parameters but the lower production that causes the lower injection rates in turn may lower the injection and casing pressures; and the combination of these two phenomena may warrant the design at a pressure in between 250 psia and 650 psia.

Water cut also plays a significant role since water will have a different density than the oil and hence alters the bottom-hole pressure for the same overall liquid production thus altering the injection rates and pressures. Hence a range of water cuts from 0% to 80% have been considered for the study. To make the study analysis simpler it is better to refer to the total liquid production rate instead of oil production rate.

#### ***4.1.2 Simulation Methodology***

Keeping the injection depth to the maximum i.e. equal to the depth of the casing is the best scenario for any gas lift operation. PROSPER keeps changing the injection depth based on the specified injection pressure to the maximum possible depending on the available gas rate and the rate of production from the reservoir. To arrive at the minimum required

injection pressure for the given gas rate and to inject at the maximum depth the injection pressure has to be changed manually in an iterative process and thus the injection rate has been optimized individually in a manual iterative process.

## **4.2 Section 2: Verification of the Design and Sensitivity Analysis**

Sensitivity analysis has been performed to find the impact of every parameter on the overall design and operation of the system.

Complete range of scenarios have been simulated and the results have been plotted. Keeping to the true definition of Nodal Analysis, the system has been broken into two parts. 1) Flow in the reservoir 2) Flow in the tubing and keeping the bottom hole as the point of conjunction. IPR curves and VLP curves have been generated differently with the different sensitivity parameters and by superimposing them correspondingly will give the maximum achievable production rate, required gas injection rate, gas injection pressure and maximum casing pressure.

### **4.2.1 Parameters Affecting the Inflow Performance**

#### **4.2.1.1 Reservoir Pressure**

As the reservoir depletes it is obvious that the average reservoir pressure declines and hence the reservoir will exhibit different inflow performance. Means different bottom-hole pressures for different liquid production rates. Various reservoir pressures from 4700 to 2250 psia have been considered to study.

#### **4.2.1.2 Water cut in the reservoir**

To verify the effect on IPR curve due to water cut increase in the reservoir, range of water cuts from 0 to 100% have been considered.

#### **4.2.1.3 Productivity Index**

For several productivity index values from 0.5 to 10 STB/day/psi different IPR curves have been generated.

In this study, only the value of productivity index is known. That limits the further investigation of every parameter individually in many parameters of the Darcy's equation. Since  $k * h$  product is implicit in nature; it is treated as a single parameter and the change in  $k * h$  has been considered to find the change in PI and hence in IPR.

Since there is no information about external drainage radius of the reservoir it is very difficult to explicitly divide the skin factor and the  $\ln \frac{r_e}{r_w}$  and hence it was not considered further for the sensitivity analysis. Since a range of PI value has been considered any change in skin factor and  $\ln \frac{r_e}{r_w}$  will fall supposedly into the range of the minimum and maximum considered PI values.

## **4.2.2 Parameters Affecting the Tubing Performance**

### **4.2.2.1 Sensitivity on Wellhead Pressure and Water Cut**

Different VLP curves have been generated for a range of wellhead pressure from 250 to 650 psia and for the water cut from 0 to 80%. For each scenario/combination the injection gas rate has been set to vary within a range of 2 to 13 MMSCFD.

### **4.2.2.2 Tubing Roughness**

PIPESIM has been used to simulate several tubing roughness values; ranging from 0.01 to 0.03 mm.

### **4.2.2.3 Overall Heat Transfer Coefficient**

PIPESIM has been used to simulate several OHTCs from 5 to 60 W/m<sup>2</sup>\*K.

### **4.2.2.4 Tubing Diameter**

Different tubing diameters have been considered as part of the design as explained in section 4.1 and shown in Table 4.1.

<b>Nominal Size (in.)</b>	<b>Weight per Foot (lbm)</b>	<b>ID (in.)</b>	<b>Drilling Drift (in)</b>	<b>Slickline Drift (in.)</b>
2 $\frac{3}{8}$	4.70	1.995	1.901	1.875
2 $\frac{7}{8}$	6.50	2.441	2.347	2.313
3 $\frac{1}{2}$	9.30	2.992	2.867	2.750
4 $\frac{1}{2}$	12.75	3.958	3.883	3.813
5 $\frac{1}{2}$	15.50	4.919	4.825	4.750

Table 4.1: ID and wall thickness data<sup>8</sup>.

## **4.3 Section 3: Unloading Process**

For the calculation of the unloading process both the casing sensitive (IPO) and tubing sensitive (PPO) valves have been considered. In casing sensitive injection valves PROSPER uses two valve spacing methods vis-à-vis the normal and the spacing line procedure. In tubing sensitive valves PROSPER uses one valve spacing method.

Completion fluid gravity of 0.53 psi/ft has been used in unloading calculations. Various injection pressures from 1500 to 2100 psia have been analyzed with the minimum number of unloading valves with corresponding depths. Select of final unloading design is subject to the economic considerations and is out the scope of this study.

## 5. Results and Discussion

### 5.1 Design and Optimization of Gas Lift System

In this section gas injection rates have been optimized for the maximum production that the overall system can handle. Since no reservoir data except  $PI=5$  stb/day/psi is available, the maximum producible flow rate specific to the GIVEN tubing with the outside diameter of 4.5" has been considered to be the base case design.

#### 5.1.1 Base Case - Tubing OD 4.5"

PROSPER automatically calculates the maximum system flow rate that can be supported by both reservoir and the tubing.

Figure 5.1 shows the intersection points of the VLP curves for different injection rates with the IPR of the reservoir. Wellhead pressure is 250 psia. At 9 MMscfd the liquid flow rate in the system is maximum at 4703 stb/d.

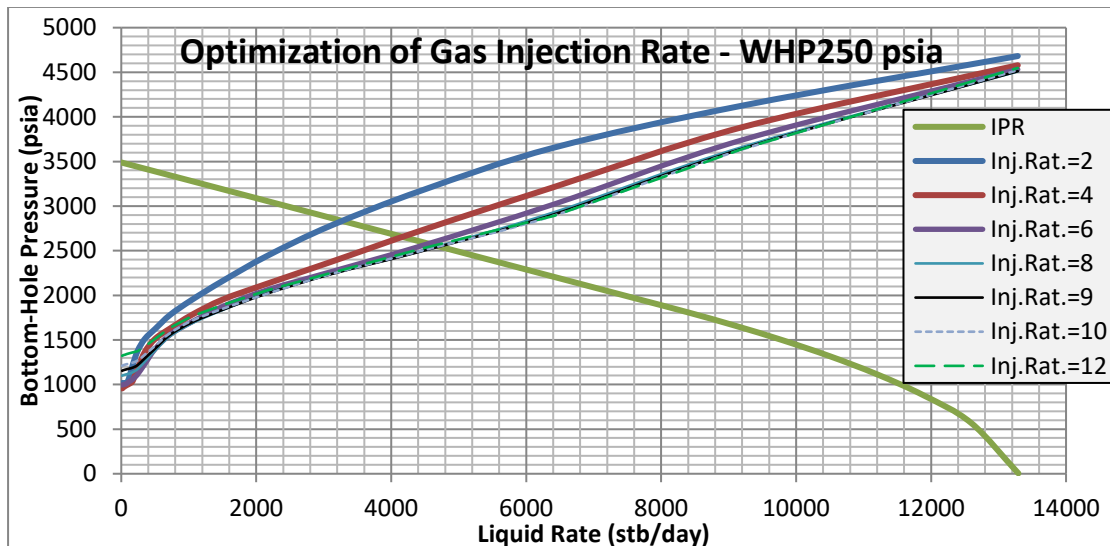


Figure 5.1: Intersection points of the VLP curves for different injection rates with the reservoir IPR.

Figure 5.2 is a different representation of the PROSPER results shown in Figure 5.1, as the gas injection rate is increased the bottom-hole and the injection pressure are decreased until they reach to a minimum value which corresponds to the maximum liquid production. At this point the pressure drop within the tubing is at its minimum for the current conditions/configuration and hence the bottom-hole pressure takes the minimum possible value. After that point the bottom-hole pressure increases since the frictional losses in the tubing dominate, contributing to higher pressure drop in the tubing.

The dip in the injection pressure (blue line in Figure 5.2) at 4 MMscfd is an indication of shift of flow regime from laminar to turbulent in the annulus.

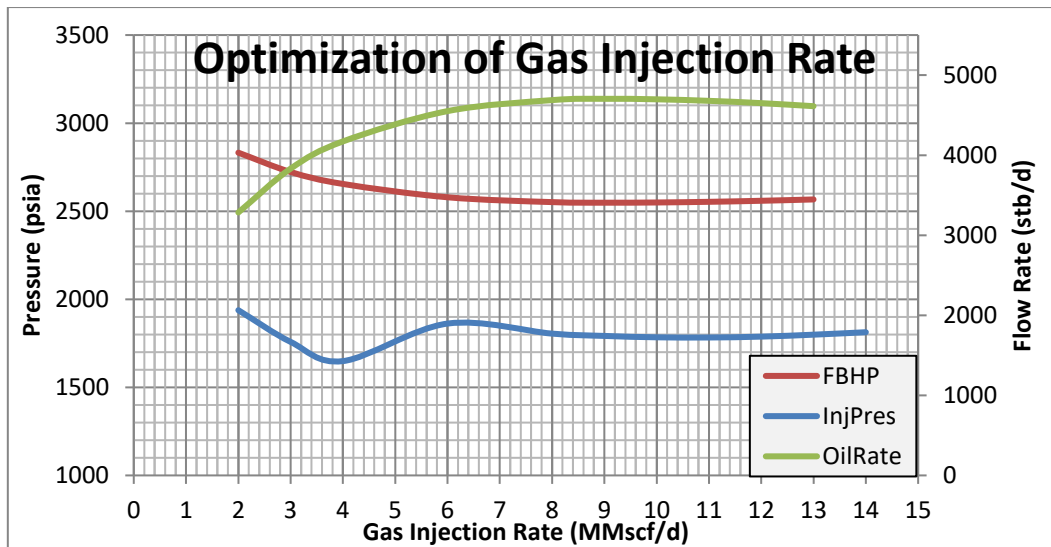


Figure 5.2: Operational Parameters as the injected gas rate is increased for wellhead pressure of 250 psia and 0% water cut.

Table 5.1 shows liquid/ oil production rates along with the bottom-hole and injection pressures for different gas injection rates. For all the injection rates the depth of injection is set equal to the maximum depth of the casing. The wellhead pressure is 250 psia, water cut is 0% and OD of tubing is 4.5”.

It can be observed that at the optimum gas injection rate (highlighted row in grey color) the liquid rate is maximum and the bottom-hole and injection pressures are minimum.

Optimization of Gas Injection Rate						
Inj. Rate (MMscf/d)	Inj. Pres. (psia)	Inj. Depth (ft) MD	Oil Prod. (stb/d)	Gas Rate (MMscf/d)	FBHP (psia)	GLR Injected (scf/stb)
2	1938	12896.2	3284.0	0.897	2832.2	609.0
3	1758	12896.2	3831.8	1.046	2722.6	782.9
4	1649	12896.2	4171.6	1.139	2654.7	958.9
6	1862	12896.2	4549.8	1.242	2579.0	1318.7
8	1805	12896.2	4687.3	1.280	2551.5	1706.7
9	1792	12896.2	4703.7	1.284	2548.3	1913.4
10	1784	12896.2	4697.3	1.282	2549.5	2128.9
11	1783	12896.2	4678.4	1.277	2553.3	2351.2
12	1788	12896.2	4649.6	1.269	2559.1	2580.9
13	1799	12896.2	4611.6	1.259	2566.7	2819.0
14	1813	12896.2	4567.0	1.247	2575.6	3065.5

Table 5.1: Operational Parameters as the injected gas rate is increased for wellhead pressure of 250 psia and 0% water cut.

The required injection flow rate is 9 MMscfd. It also can be noted that the optimum GLR for the maximum oil production for the above conditions is 1913 scf/stb.

Different wellhead pressures and water cut combinations have been considered. For each combination the optimal injection rate and gas injection pressures have been found out along with maximum production that the system can handle.

Table 5.2 shows the optimum gas injection rates for a range of WHPs from 250 psia to 650 psia and for 0% water cut. In all the cases, the injection rates represent the intersection point of IPR and with the VLP of optimized gas injection.

As the wellhead pressure increases the injection gas and pressure requirements also increases, as well as the solution node pressure at the bottom-hole; eventually, decreasing the oil production rate.

Optimal Conditions-4.5" Tubing OD and 0% w.c.							
Pwh (psia)	Inj. Rate (MMscf/d)	Inj. Pres. (psia)	Inj. Depth (ft) MD	Liq. Prod. (stb/d)	Gas Rate (MMscf/d)	FBHP (psia)	GLR Injected (scf/stb)
250	9	1792	12896.2	4703.7	1.28	2548.3	1913
300	9	1840	12896.2	4532.1	1.24	2582.6	1986
350	9	1604	12896.2	4354.6	1.19	2618.1	2067
400	10	1651	12896.2	4173.3	1.14	2654.3	2396
450	10	1696	12896.2	3988.8	1.09	2691.2	2507
500	10	1742	12896.2	3801.9	1.04	2728.6	2630
550	11	1791	12896.2	3613.8	0.99	2766.2	3044
600	11	1836	12896.2	3426.3	0.94	2803.7	3210
650	11	1884	12896.2	3237.0	0.88	2841.6	3398

Table 5.2: Gas lift optimization-OD 4.5" and 0% water cut.

Figure 5.3 is the graphical representation of Table 5.2.

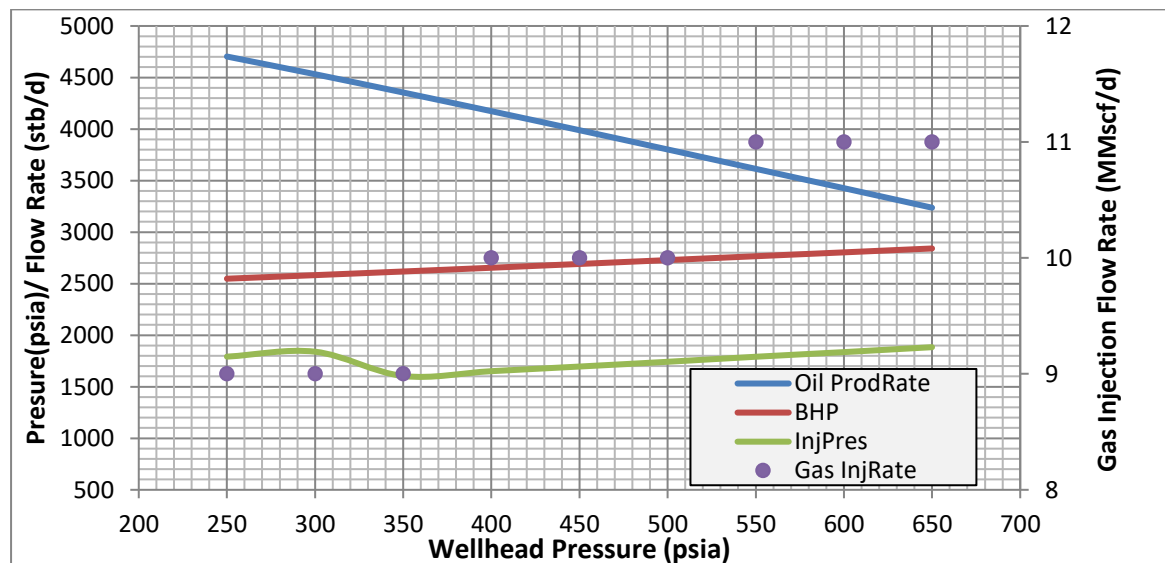


Figure 5.3: Gas lift optimization-OD 4.5" and 0% water cut.

The optimum gas injection rates are about 9 to 11 MMscfd and the maximum oil production rates are from 4700 stb/d to 3200 stb/d. The required injection pressures are approximately

in the range of 1600 psia to 1880 psia. These injection pressures can be seen as the minimum (optimized) specific to the conditions as tabulated. Any change in the above conditions will trigger the injection pressures to rise. It does not mean the failure of the design, but the failure of an efficient operation.

The GLRs calculated in the last column is an indication of the efficient gas injection rate that the system should be operated at. It indicates the GLR where the frictional drop in the tubing is minimum. For example let us assume a limited injection gas availability of 9 MMscfd for WHP of 650 psia. In that scenario, system would not produce at 3237 stb/d and at 2842 psia of BHP. Instead system would be able produce at a lesser flow rate than 3237 stb/d and if the GLR is maintained at 3398 scf/stb will have an injection pressure less than 1884 psia. The actual amount of oil that can be produced can be referred from the sensitivity analysis (Section 5.2).

Similar to the Table 5.2 the optimal gas injection rates for the maximum liquid production for different set of wellhead pressure and water cuts are presented in Figure 5.4 through Figure 5.7. The optimal injection pressure and gas rates are tabulated in order to produce the maximum amount of oil along with the corresponding bottom-hole pressure.

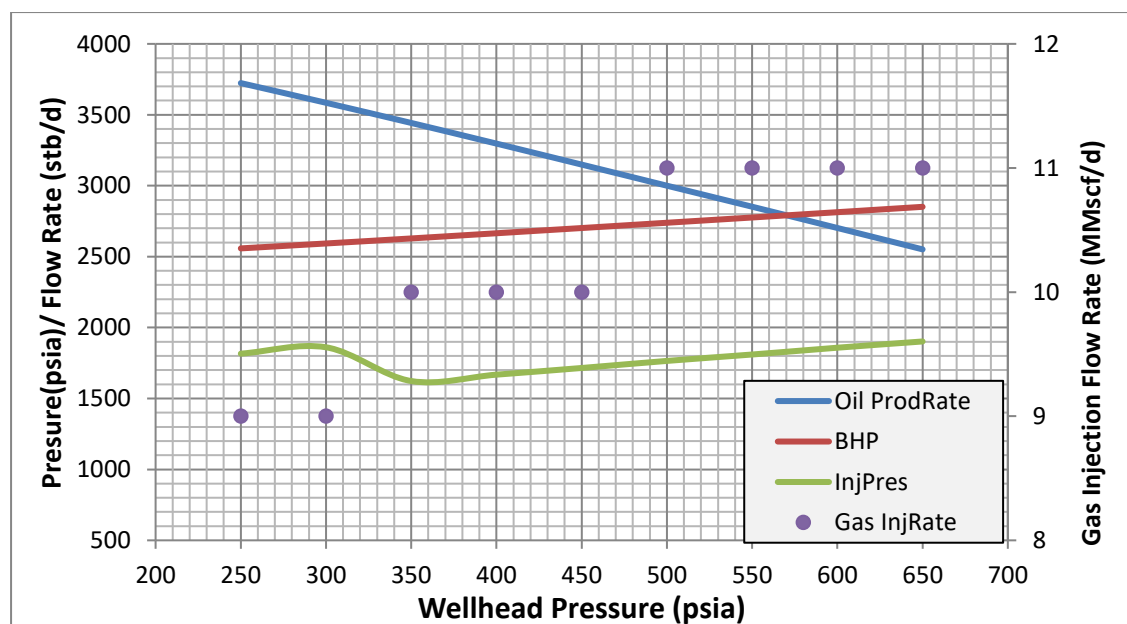


Figure 5.4: Gas lift optimization-OD 4.5" and 20% water cut.

From Figure 5.4 the maximum liquid flow rate is 4655 stb/d at a wellhead pressure of 250 psia. The maximum injection pressure is 1902 psia at a wellhead pressure of 650 psia. The gas injection requirements are varying from 9 to 11 MMscfd.

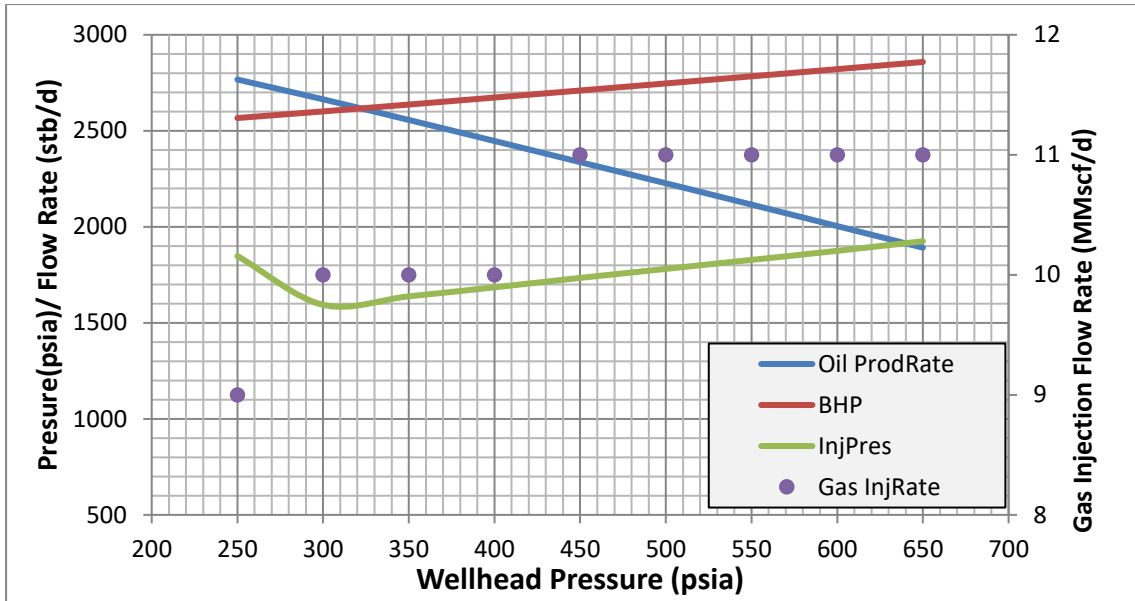


Figure 5.5: Gas lift optimization-OD 4.5" and 40% water cut.

From Figure 5.5 the maximum liquid flow rate is 4612 stb/d at a wellhead pressure of 250 psia. The maximum injection pressure is 1925 psia at a wellhead pressure of 650 psia. The gas injection requirements are varying from 9 to 11 MMscfd.

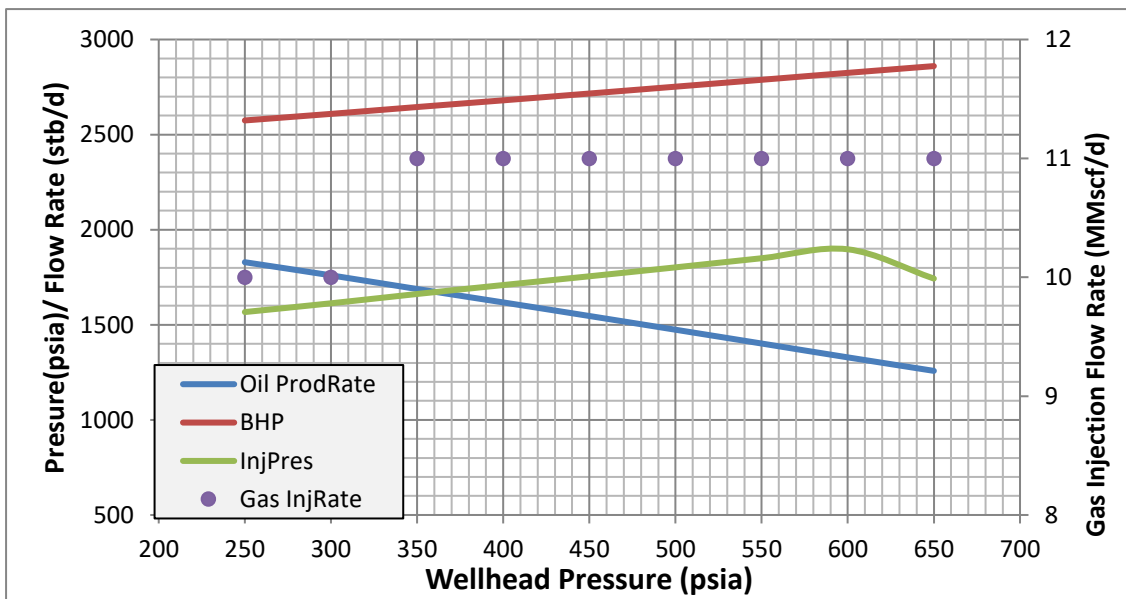


Figure 5.6: Gas lift optimization-OD 4.5" and 60% water cut.

From Figure 5.6 the maximum liquid flow rate is 4573 stb/d at a wellhead pressure of 250 psia. The maximum injection pressure is 1897 psia at a wellhead pressure of 600 psia. The gas injection requirements are varying from 10 to 11 MMscfd.

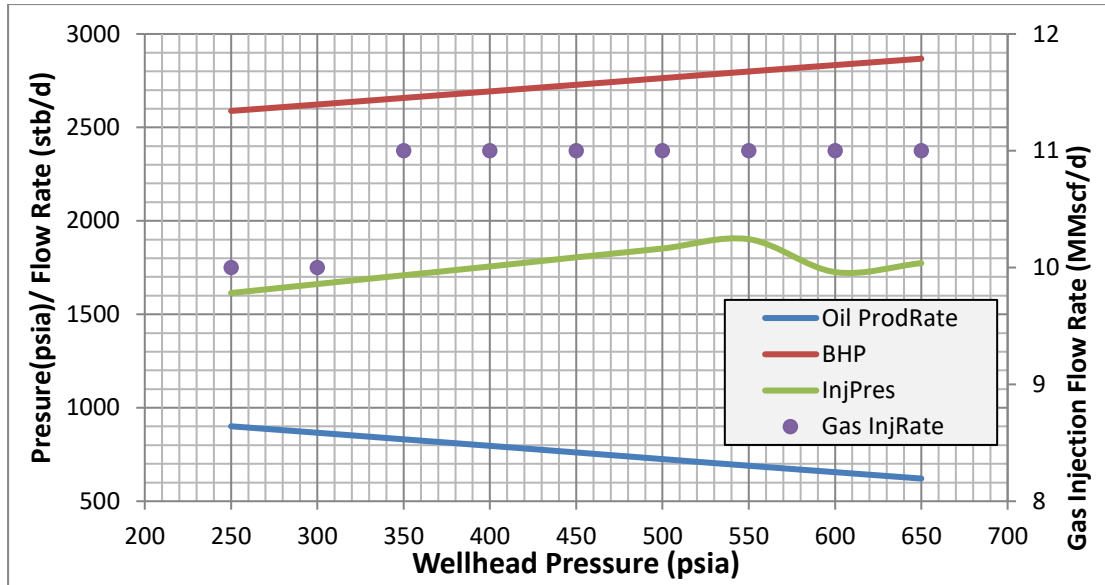


Figure 5.7: Gas lift optimization-OD 4.5" and 80% water cut.

From Figure 5.7 the maximum liquid flow rate is 4504 stb/d at a wellhead pressure of 250 psia. The maximum injection pressure is 1902 psia at a wellhead pressure of 550 psia. The gas injection requirements are varying from 10 to 11 MMscfd.

The required injection pressure increases with the water cut and happens to be the maximum when water cut is 40% and the wellhead pressure is 650 psia corresponds to a value of 1925 psia(Figure 5.5). The maximum gas that needs to be injected is about 11 MMscfd. These values are considered as the boundaries that may occur during the life of the field and the final selection of the compressor will be based on these operational conditions. Every other possible change will fall within the range of the already considered cases. Therefore, the system has been designed for the worst-case scenario.

### 5.1.2 Tubing OD 3.5"

Results of 3.5" OD and 0% water cut have been presented in Table 5.3 and Figure 5.8. The required gas injection is between 6 to 7 MMSCFD for the maximum oil production. Compared to the base case of 4.5" OD, the gas requirements are lesser and about 6 MMscfd. The maximum oil production is 1810 stb for wellhead pressure of 250 psia and the minimum oil production is 1261 stb for 650 psia. This is due to the increase in bottom-hole pressure that caused due to smaller size of the tubing and hence the higher frictional losses compared to base case of 4.5". The injection pressures are also increased due to the higher bottom-hole pressures.

The spike in injection pressure (green line in Figure 5.4) at 550 psia is due to the decreased velocities in the annulus and hence the change of flow regime from turbulent to laminar.

Optimal Conditions–3.5” Tubing OD and 0% water cut							
Pwh (psia)	Inj. Rate (MMscf/d)	Inj. Pres. (psia)	Inj. Depth (ft) MD	Oil Prod. (stb/d)	Gas Rate (MMscf/d)	FBHP (psia)	GLR Injected (scf/stb)
250	6	1833	12896.2	2893.6	0.790	2910.3	2073.6
350	6	1925	12896.2	2670.5	0.729	2954.9	2246.8
450	6	2026	12896.2	2443.1	0.667	3000.4	2455.9
550	6	2130	12896.2	2219.7	0.606	3045.1	2703.1
650	6	1926	12896.2	1975.9	0.539	3093.8	3036.6

Table 5.3: Gas lift optimization-OD 3.5” and 0% water cut.

Figure 5.4 is the graphical representation of Table 5.3.

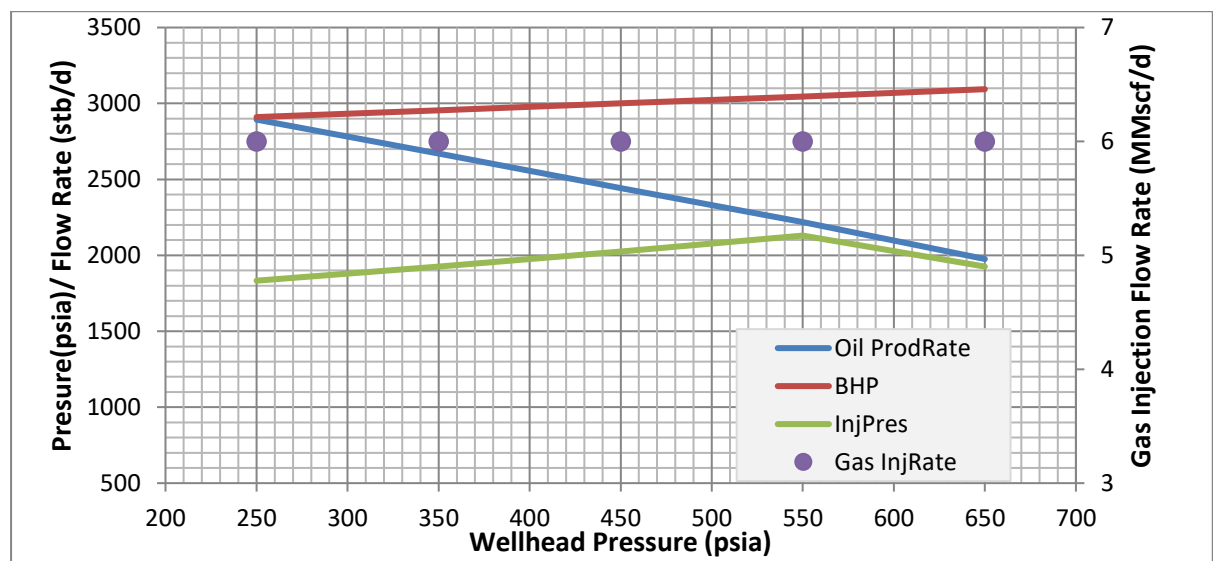


Figure 5.8: Gas lift optimization-OD 3.5” and 0% water cut.

Similar to the Table 5.3 the optimal gas injection rates for the maximum liquid production for different set of wellhead pressure and water cuts are presented in Figure A.5 and Figure A.6 (in Appendix). The optimal injection pressure and gas rates are tabulated in order to produce the maximum amount of oil along with the corresponding bottom-hole pressure.

### 5.1.3 Tubing OD 5.5”

Maximum oil production rates with the required gas injection rates have been presented in Table 5.4 for 5.5” OD for 0% water cut. In this case, the injection gas requirements are considerably higher about 15 to 20 MMSCFD although the increase in oil production is noticeable. Though the production rates are higher it is up to the overall economics of the workovers or incremental costs against production increase, owing to the higher injection rates of 15 to 20 MMscfd and sometimes it may not be feasible to have an OD of 5.5”.

Optimal Conditions–5.5” Tubing OD and 0% water cut							
Pwh (psia)	Inj. Rate (MMscf/d)	Inj. Pres. (psia)	Inj. Depth (ft) MD	Oil Prod. (stb/d)	Gas Rate (MMscf/d)	FBHP (psia)	GLR Injected (scf/stb)
250	15	1376	12896.2	6329.8	1.73	2223.0	2369.7
350	16	1470	12896.2	5871.7	1.60	2314.7	2724.9
450	18	1568	12896.2	5407.5	1.48	2407.5	3328.7
550	19	1662	12896.2	4939.1	1.35	2501.2	3846.9
650	20	1755	12896.2	4467.1	1.22	2595.6	4477.1

Table 5.4: Gas lift optimization-OD 5.5” and 0% water cut.

The maximum oil production rate is 6330 stb/d for a WHP of 250 psia. The maximum injection pressure required is 1755 psia for a WHP of 650 psia.

Figure 5.9 is the graphical representation of Table 5.4.

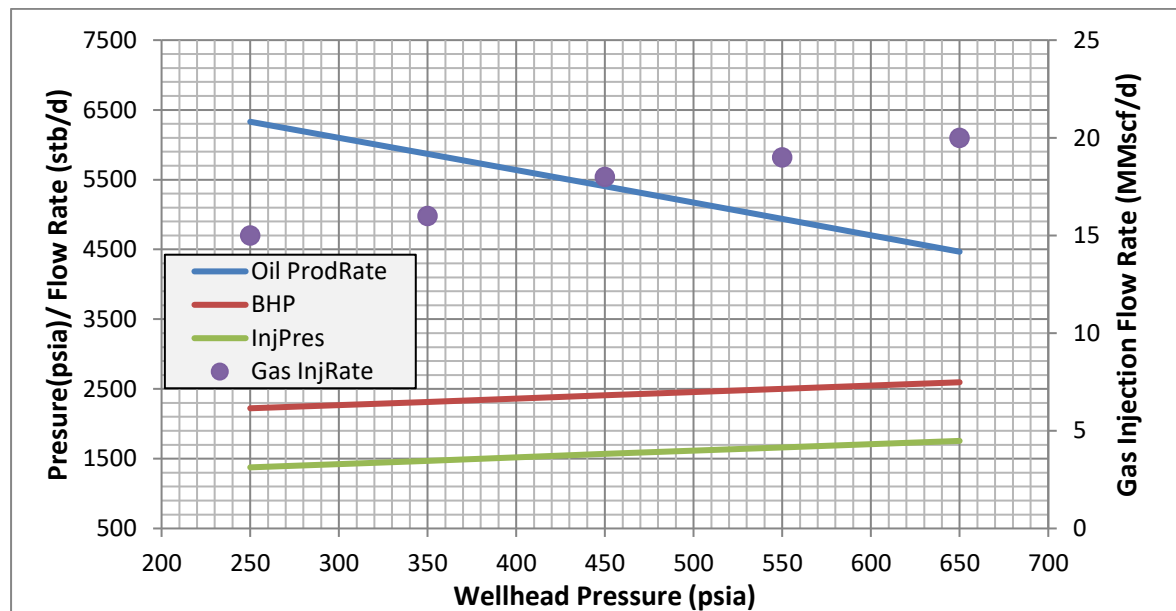


Figure 5.9: Gas lift optimization-OD 5.5” and 0% water cut.

## 5.2 Sensitivity Analysis

The optimum gas lift operation conditions have been presented in Section 5.1 for the given data as in Chapter 3 combined with the most appropriate and obvious field data for the wellhead pressure and tubing diameters. Any change in the above conditions will alter the operating conditions and will have a different maximum oil production rate and corresponding gas injection rate and pressure. In this section other parameters that have the potential to change the operating conditions directly or indirectly have been studied. Also, some parameters such as PVT properties may contain uncertainties in measurement/calculation and the effects the overall performance of the system.

Broadly the variables that affect the flow performance of the system have been divided into two groups. While few parameters affect only the inflow performance of a reservoir, others will influence the vertical lift performance. Few parameters such as viscosity will affect both IPR and VLP.

### 5.2.1 Parameters Affecting the Inflow Performance

Following are the main parameters that affect the inflow performance of the reservoir and will not affect the vertical lift performance directly.

- Reservoir pressure
- Water cut
- Skin factor
- $k \cdot h$  product
- Oil viscosity

#### 5.2.1.1 Average Reservoir's Pressure

As the well keeps producing, the reservoir pressure declines. This decline will result in a decrease in the bottom-hole pressure and thus the deliverability of the reservoir. It means the reservoir will exhibit a different inflow performance (different IPR curves) for every pressure during the life of the reservoir.

Figure 5.10 shows different IPR curves for different reservoir pressures. The triangular markers on the IPR ( $P_R=3489$  psia) represent the maximum production rates and bottom-hole pressure points for the optimized gas injection specified conditions in section 5.1.1. From this graph the (available) bottom-hole pressure for a given liquid rate for any considered change in reservoir pressure can be read. It can be observed that as reservoir pressure decreases the bottom-hole pressure decreases to maintain the same liquid rate.

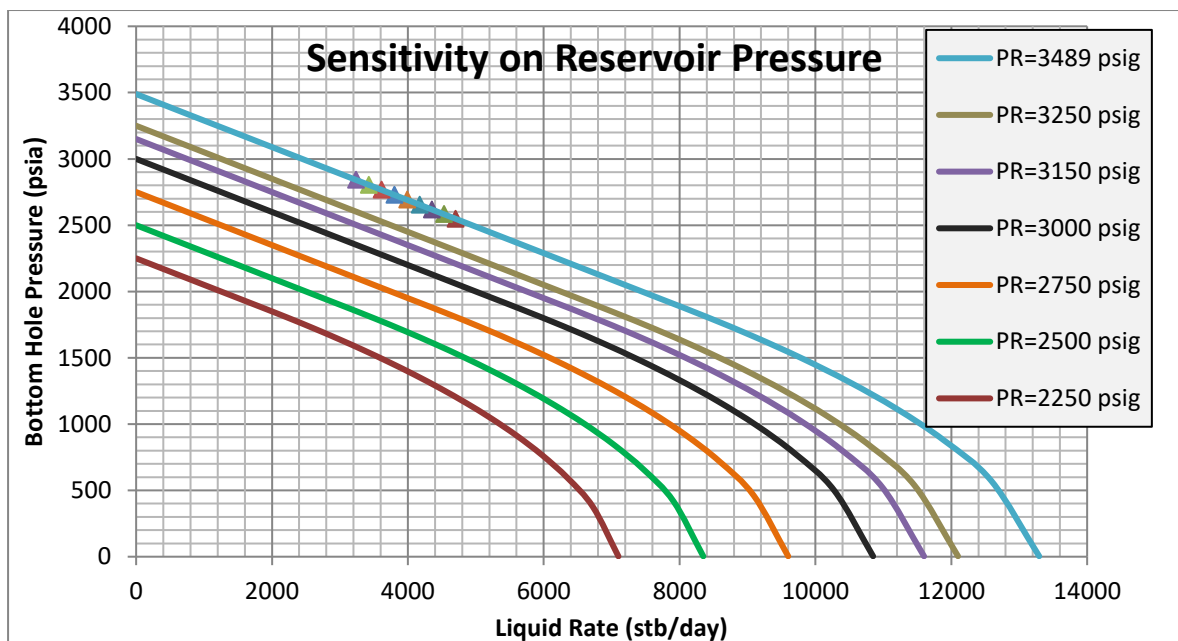


Figure 5.10: Effect of reservoir pressure on inflow performance.

#### 5.2.1.2 Water Cut

As the reservoir depletes the oil saturation decreases that increases water saturation and hence relative permeability of water that eventually triggers the water flow along with the oil. As the pressure reduces more, more water breaks through into the flow. Waterflooding is one of the techniques that is commonly employed in the industry to improve the recovery

of oil from the reservoir. So, it is natural to produce some water along with oil and the water cut increases as the reservoir depletes as explained above. This increase in water cut in reservoir causes increase of water cut in production systems as well.

The IPR curves for different fractions of water cut in the reservoir are illustrated in Figure 5.11. The increase in water cut has no effect on the inflow performance i.e. bottom-hole pressure, above the bubble point; below the bubble point the increase in water cut results in lower bottom-hole pressures for the same liquid rate.

This behavior can be/is explained through Darcy's law. As water saturation increases in the pores, the fractional flow of water is increased also. The parameters that change in Darcy's equation are the relative permeabilities, the viscosities and the formation volume factors. Above the bubble the total flow rate of the liquid is the summation of oil and water flow rates and hence the equation with pressure is not affected. When the pressure falls below the bubble point then gas is getting out of the solution and thus decreasing the relative permeabilities of both oil and water. The decreased relative permeabilities, hence contribute to higher pressure losses within the reservoir.

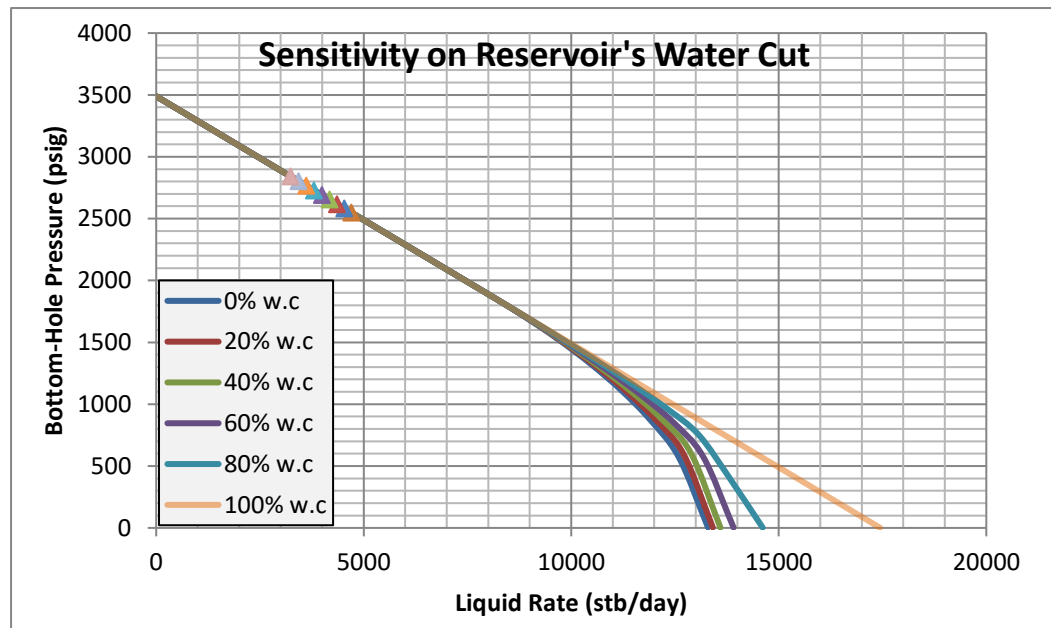


Figure 5.11: Effect of water cut on inflow performance.

### 5.2.1.3 $k * h$ Product

Since permeability ( $k$ ) and pay zone thickness ( $h$ ) are implicit, the product term  $k * h$  is considered as a single parameter and any change in  $k * h$  product proportionally changes the PI. So the  $k * h$  sensitivity has been clubbed with the PI sensitivity in Section 5.2.1.7 (Table 5.5).

### 5.2.1.4 $B_o$

In Darcy's equation  $B_o$  is a variable to translate the stock tank flow rates into reservoir flow rates and is an indication of volatility of the fluid. For a given reservoir fluid and for the purpose of gas lift design optimization,  $B_o$  will not have any influence unless the reservoir fluid changes itself or the wellhead pressure decreases as the reservoir depletes.

### 5.2.1.5 Skin Factor

Skin factor is an implicit parameter in Darcy's equation and cannot be separated unless the other variables are properly specified. Hence the sensitivity has not been considered.

### 5.2.1.6 Viscosity

Viscosity affects both the inflow and vertical lift performances; it is inversely proportional to the flow rate in reservoir and the productivity index. Viscosity is a strong function of temperature and weakly depends on pressure. Viscosity of the residual oil in the reservoir increases as the pressure depletes. Table 5.5 shows the % of effect of viscosity change on the PI.

Change in $\mu_o$ and $B_o$	PI	Change in $k*h$ Product	PI
80%	1	80%	9
70%	1.5	70%	8.5
60%	2	60%	8
50%	2.5	50%	7.5
40%	3	40%	7
30%	3.5	30%	6.5
20%	4	20%	6
10%	4.5	10%	5.5
0%	5	0%	5
-10%	5.5	-10%	4.5
-20%	6	-20%	4
-30%	6.5	-30%	3.5
-40%	7	-40%	3
-50%	7.5	-50%	2.5
-60%	8	-60%	2
-70%	8.5	-70%	1.5
-80%	9	-80%	1

Table 5.5: Effect of viscosity,  $k * h$  product and  $B_o$  on PI.

### 5.2.1.7 Effect of Productivity Index

Darcy's flow equation can be written in terms of PI as follows.

$$q = J * (\bar{P}_R - P_{wf}) \text{ and } J = \frac{k * h}{141.2 * B_o * \mu_o * (\ln \frac{r_e}{r_w} - 0.75 + S)}$$

A range of PI values from 0.5 to 10 stb/d/psi has been considered to generate IPRs and is presented in Figure 5.12. Higher PI is an indication of higher deliverability of the well; it means when PI is higher the bottom-hole pressure is higher for the same flow rate within the reservoir.

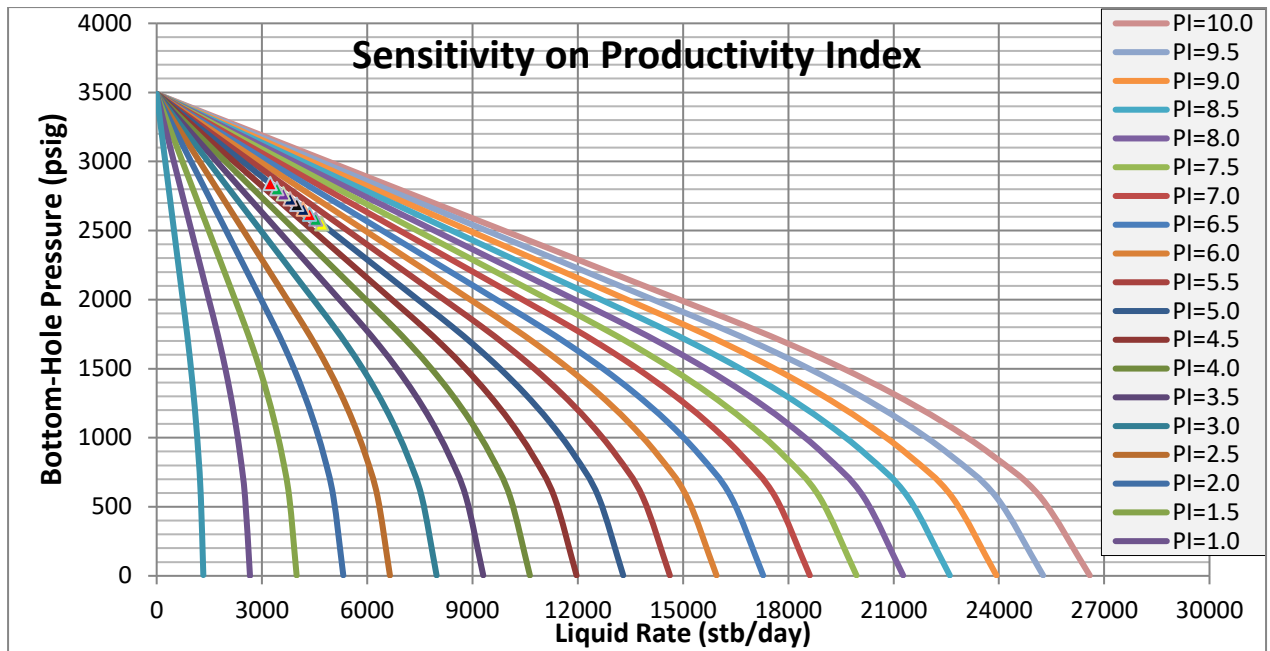


Figure 5.12: Effect of productivity index on inflow performance.

### 5.2.2 Parameters Affecting the Tubing Performance

Parameters that affect the vertical lift performance directly are as below.

- Wellhead Pressure
- Water Cut
- Gas to Liquid Ratio
- Tubing Roughness
- Tubing Diameter
- Overall Heat Transfer Coefficient
- Viscosity

and

- Vertical Lift Performance selected correlation

#### 5.2.2.1 Effect of Wellhead Pressure

Figure 5.13 shows the VLP curves for a range of wellhead pressure between 250 to 650 psia. These VLP curves are generated for 'zero' injection and hence the GLR is constant and equal to the formation GLR in all the cases (If injection is not zero, PROSPER automatically changes the gas injection rate and the VLP curves can't be comparable to show the effect of WHP). Readers caution is advised to make a note that the BHPs in case of VLPs are the required pressures to flow the corresponding rate of the fluid. As the WHP increases, the required pressure at the bottom-hole also increases. These curves in combination with IPR give the maximum flow rate that the system can flow specific to the conditions. Water cut is assumed to be '0' for this case.

Wellhead pressures for 250 to 650 psia have been already considered for the gas lift optimization in section 5.1 for water cuts ranging from 0 to 80% and for three different tubing diameters. All the design parameters including gas injection rate and injection

pressure have been identified specific to the conditions in the section 5.1. The maximum gas production rates are in conformance with the inflow performance of the reservoir. So, the wellhead pressures sensitivity has been already addressed.

In this current section IPR conformance has not been checked and the maximum liquid production rates have been established as a function of wellhead pressure while all the other parameters are constant.

Different VLP curves with different injection flow rates, wellhead pressure and water cut have been plotted and included in Appendix from Figure A.7 to Figure A.41.

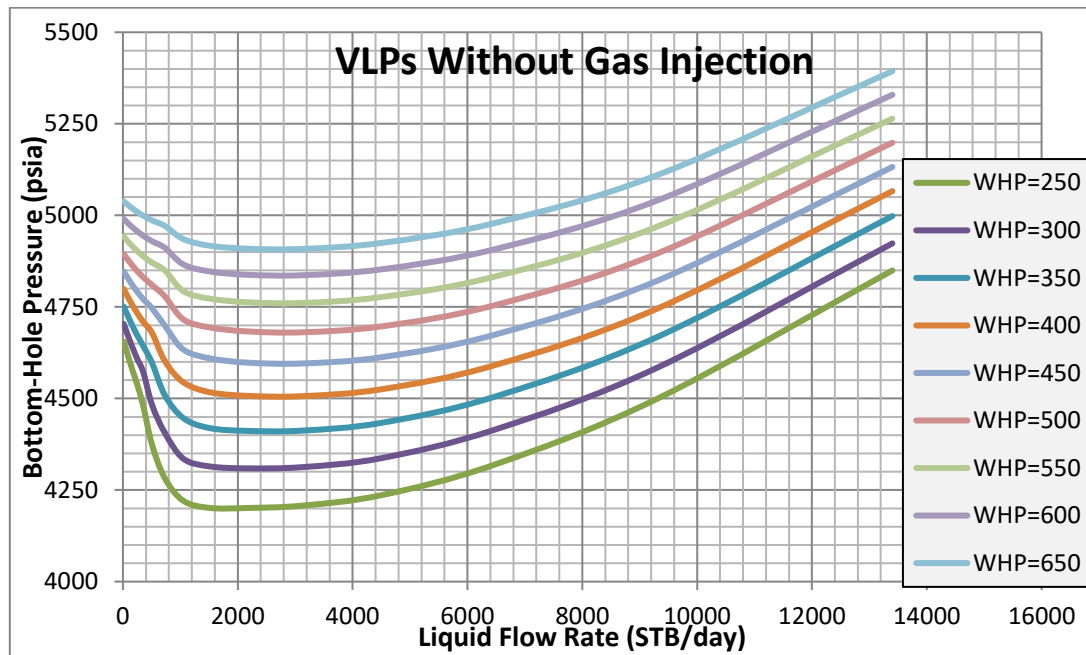


Figure 5.13: Different VLP curves for a range of WHP of 250 to 650 psia, 0% water cut and with formation GLR.

### 5.2.2.2 Effect of Water Cut

The increase in water cut increases the bottom-hole pressures due to the increased pressure drop in the tubing to sustain same total liquid production. It is due to the increased liquid head in the column that increases with the water density when the water cut increases.

$$\rho_{liq} = \rho_o * (1 - WC) + \rho_w * WC$$

Figure 5.14 shows different VLP curves for WHP of 450 psia and for 9 MMscfd of injection gas, as the water cut is increased from 0 to 80%. More pressure drop is observed at the high flow rates due to the high frictional loss caused due to the higher density of increased water cut. Since, the water cut is not affecting the bottom-hole pressure below a rate of 4700 stb/d the gas injection pressure and rate will not be affected.

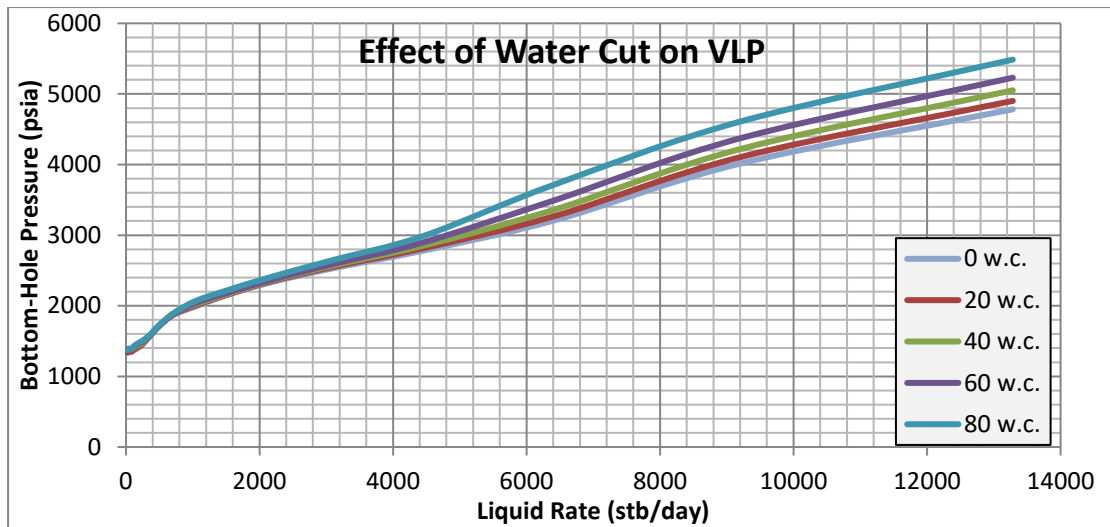


Figure 5.14: The effect of water cut for a WHP=450 psia and gas injection rate=9 MMscfd.

### 5.2.2.3 Gas Liquid Ratio

Figure 5.15 shows the bottom-hole pressures plotted against different GLRs. In all the cases liquid flow rate is constant at 4000 stb/d and three different WHPs have been considered. As the gas injection rate increases GLR also increases.

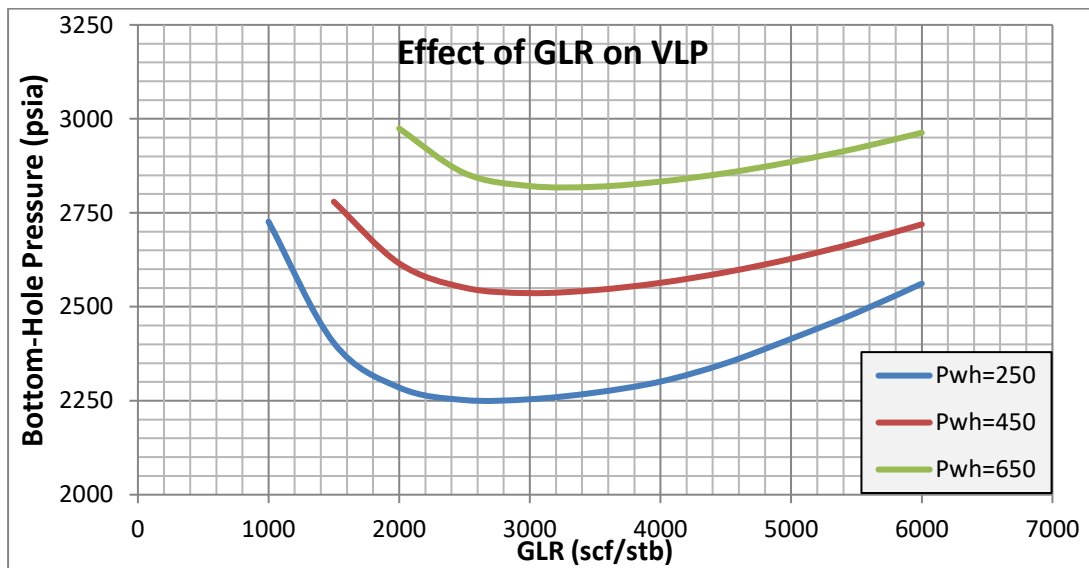


Figure 5.15: Effect of GLR for constant liquid rate of 4000 stb/d and 4.5" OD.

The formation GLR or the GLR of the reservoir fluid is 273 scf/stb and no production is possible with this GLR unless gas is injected. For a WHP of 650 psia the minimum GLR required to start the flow in tubing is approximately 2000 scf/stb; for 450 psia of WHP the minimum GLR required is 1500 psia and it is 1000 scf/stb for 250 of WHP. For 250 psia of WHP and 4000 stb of liquid production a GLR of 2400 scf/stb gives the better lift performance with the minimum pressure drop in the tubing. Below 2400 scf/stb, pressure drop is higher due to higher liquid head and above frictional pressure drop becomes predominant. Similarly for 450 psia of WHP, a GLR of 3000 scf/stb gives the best performance and 650 psia it is at 3200 scf/stb.

For different flow rates for tubing OD of 4.5" are shown in Appendix A from Figure A.42 to Figure A.48.

The GLR sensitivity curves for various production rates for tubing diameter of 3.5" have been included in Appendix A from Figure A.49 to Figure A.52.

#### 5.2.2.4 Effect of Tubing Diameter

Bottom-hole pressures have been plotted against tubing ID in Figure 5.16 while keeping the liquid flow rate and GLR constant. Wellhead pressure is 250 psia and water cut is zero. Liquid flow rate is 4700 stb/d and GLR is 1913 scf/stb.

Smaller tubing diameters result in increasing the frictional losses within the tubing and eventually the pressure drop in the tubing and therefore increases the bottom-hole pressure.

As the OD is increased from 2.875" to 3.5" and from 3.5" to 4.5" the required bottom-hole pressure decreases from 6524 to 4538 psia and then to 2603 psia. To support this required bottom-hole pressure, for the flow rate of about 4700 stb/d the reservoir should be capable of delivering the bottom-hole pressures in the above mentioned range and 4.5" will be the natural selection for this reservoir and the well. If the reservoir is capable of producing this flow rate for a longer period even 5.5" will also be an option. The initial has been marked in the dotted line.

The gas injection optimization has been presented for 3.5", 4.5" and 5.5" in section 5.1.

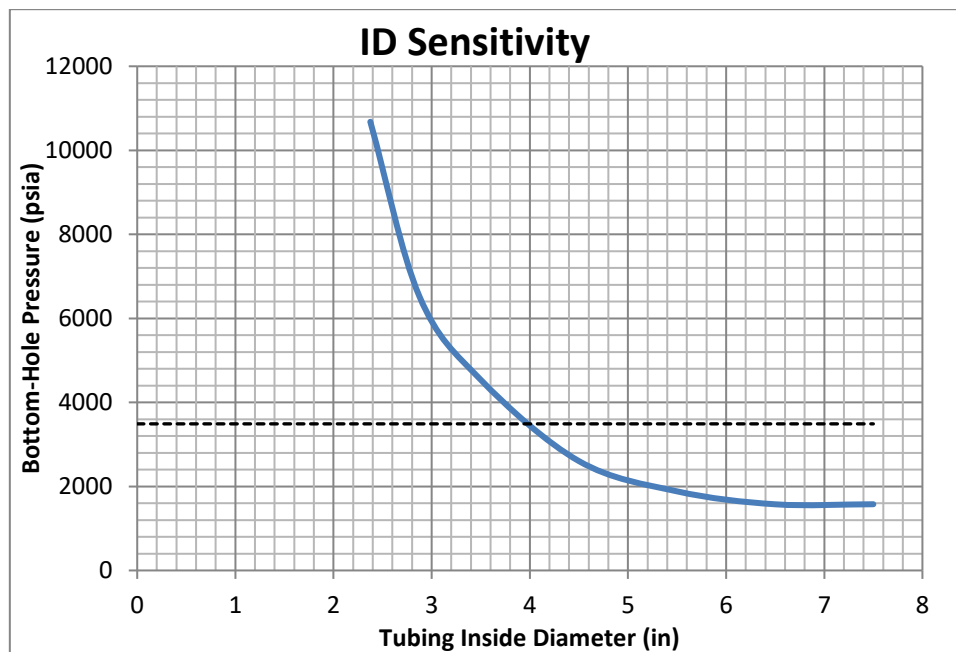


Figure 5.16: Effect of tubing diameter on VLP-.

#### 5.2.2.5 Effect of Tubing Roughness

Tubing roughness directly affects the pressure drop when the flow rates are higher. As long as the fluid is in single phase liquid state, the velocities are lower and the effect of the tubing roughness is not quite visible. When the GLRs are higher, due to the high velocity of gas

phase the effect is clearly visible. In the table below, the GLR is optimized to have minimum frictional drop in the tubing and hence the effect of tubing roughness is not seen predominantly. As it is shown in Table 5.6, the difference is only 10 psia in the solution of BHP and is not going to affect the gas lift design and the liquid production rates.

Wellhead Pres. (psia)	Water Cut (%)	Flow Rate (STB/d)	GLR (scf/STB)	Tubing Roughness (mm)	BHP (psia)
250	0	4704	2186	0.010	2649
				0.015	2652
				0.020	2654
				0.025	2656
				0.030	2659
300	0	4532	2259	0.010	2656
				0.015	2659
				0.020	2661
				0.025	2664
				0.030	2666

Table 5.6: The effect of tubing roughness on VLP.

#### 5.2.2.6 Effect of Overall Heat Transfer Coefficient

Overall heat transfer coefficient (OHTC) is an indication of transferability of heat from/ to surroundings. A higher OHTC means a high rate of heat transfer. Normally in the production tubing, the temperature drops from the reservoir temperature at the bottom to the minimum ambient surrounding temperature at the wellhead.

The impact of the change in the overall heat transfer coefficient on the bottom-hole pressure and in wellhead temperature is shown in Figure 5.17, for a constant liquid rate of 4700 stb/d and GLR equal to 1913 scf/stb. As it can be seen in Figure 5.17 the required bottom-hole pressure is increasing which means that the pressure drop is increasing in the tubing. This increase can be attributed the increase in liquid holdup.

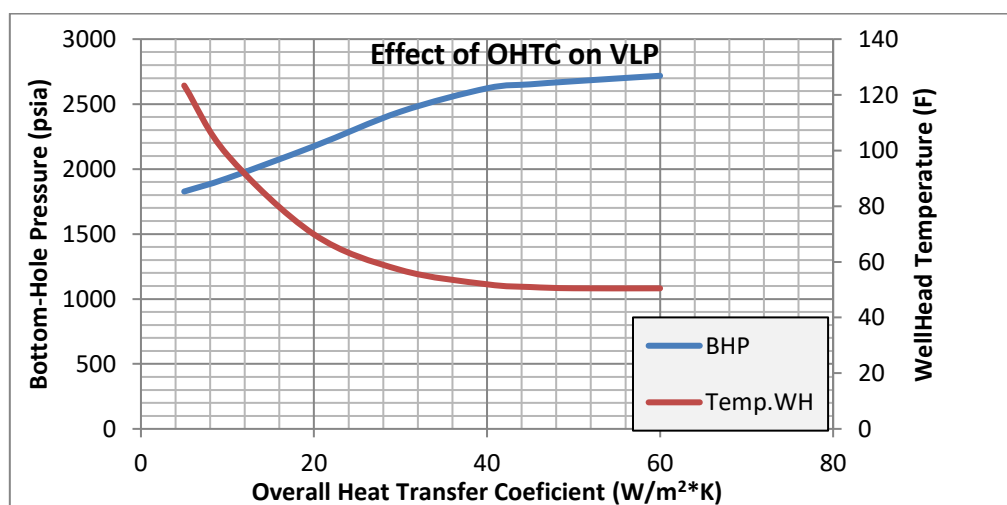


Figure 5.17: Effect of overall heat transfer coefficient on VLP-WHP=250psia.

Figure 5.18 shows the average liquid hold up in the tubing. Increase in liquid hold up is an indication of reduction in GLR in tubing that will adversely affect the bottom-hole pressure. This is due to the cooling down of fluids as the heat is lost to the ambient when the heat transfer coefficient is higher.

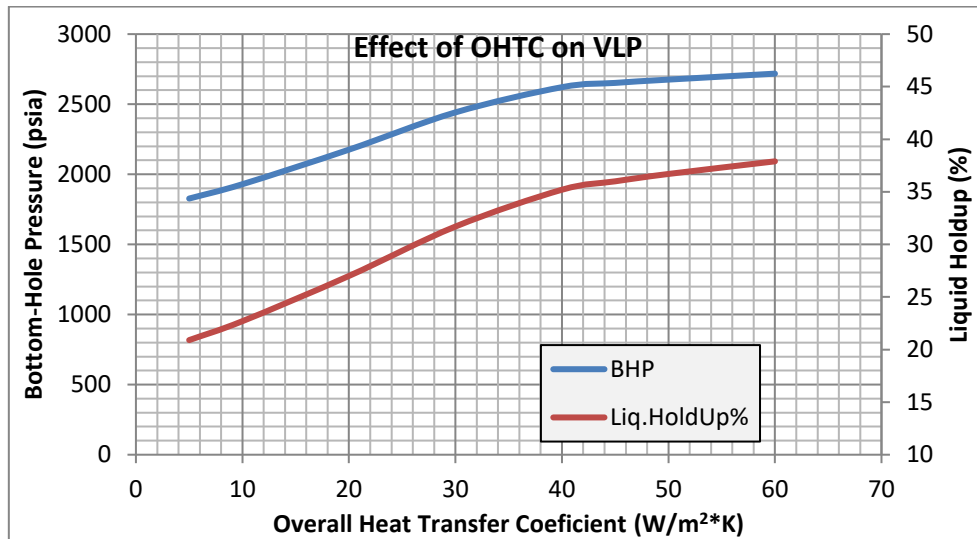


Figure 5.18: Effect of overall heat transfer coefficient on VLP-WHP=250 psia.

From Figure 5.17 it can be observed that any discrepancy in OHTC calculation has a major effect on estimating the pressure drop in the tubing. Therefore, proper care should be taken and OHTC must be determined accurately through the life of the well, to estimate accurately the required bottom-hole pressure and therefore the ability of the well to sustain a certain flow rate.

### 5.2.2.7 Injection Pressure

In Figure 5.19 is shown the required injection pressure against the bottom-hole pressure for different injection gas rates.

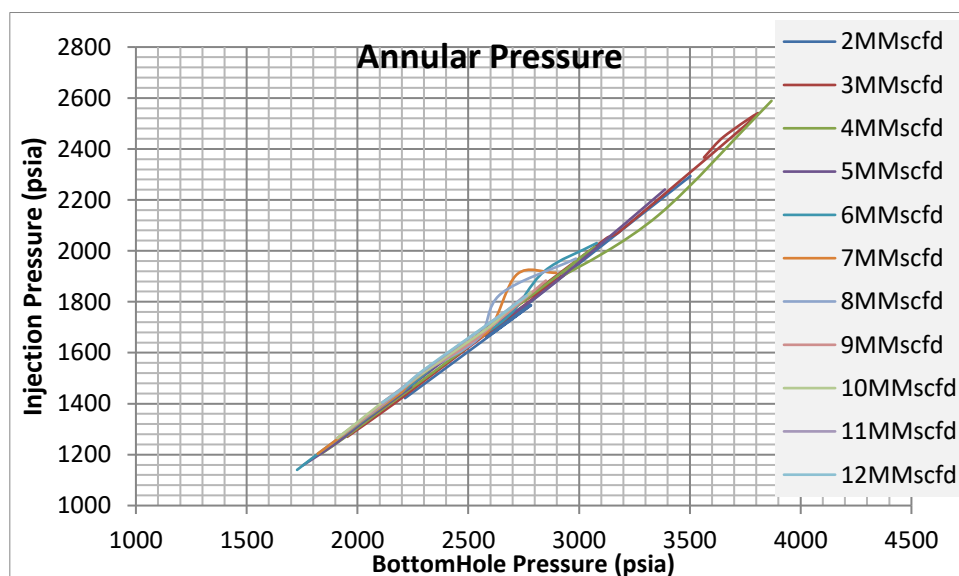


Figure 5.19: Injection pressure versus bottom-hole pressure for different injection gas flow rates

### 5.2.3 Effect of VLP Correlations

For this study the selected vertical lift correlation is Petroleum Experts 2. Since no well test data is available the real pressure drop in the tubing has not been matched with the VLP correlations. In multiphase flow selection of VLP correlation plays significant role in the estimation of the total pressure drop and hence the selection of the design. To verify the effect of various VLP correlations on the tubing performance the liquid rate and the GLR where kept constant and all the available correlations in PIPESIM have been compared. The wellhead pressure is 250 psia. Required bottom-hole pressure to maintain the given liquid rate of 4704 stb/d has been found out and shown in Table 5.9.

<b>Liq.Rate=4704 stb/d GLR=2186 scf/stb</b>	
<b>VLP Correlation</b>	<b>FBHP (psia)</b>
Pet Ex 2	2548
Ansari	3133
No-Slip Assumption	2936
Orkizeski	2594
Duns & Ros	3669
Beggs & Brill (original)	3789
Beggs & Brill (revised)	3678
Govier,Aziz & Fogarasi	2214
Gray (modified)	3001
Hagedorn &Brown	2594

Table 5.7: Comparison of VLP correlations.

All correlations predict different bottom-hole pressures. This is due to empirical nature of all the correlations fitted to different sets of data applicable to different scenarios like angle of elevation of the pipe, GOR and slip effects. Petroleum Experts2 has been used in the study, as it is highly believed for the gas lift system design calculations.

### 5.2.4 Effect of PVT correlation

The selected VLP correlation for the study is the Petroleum Experts 2 and EOS is Glaso correlation for black oil for the estimation of bubble point, GOR, Oil Formation Volume Factor (Bo) and oil density. Beal et al correlation has been used for the viscosity.

PROSPER has another six built in correlations for EOS matching and for viscosity total six correlations are available.

Table 5.7 shows the percentage deviation of GOR between selected correlation and others, for pressures from 250 to 650 psia.

Pressure (psig)	Petrosky et al.	Al Mahroun	De Ghetto et al (Heavy Oil)	Standing	Vasquez-Beggs	Lasater	Glaso
250	-90	-54	-33	-33	-18	-13	0
350	-67	-47	-27	-26	-13	-7	0
450	-53	-40	-22	-22	-10	-2	0
650	-36	-30	-15	-15	-5	2	0

Table 5.8: Deviation (%) of PROSPER EOS correlations in GOR.

All other correlations apart from Glaso under estimate the GOR. The percentage of deviation has been increasing from a WHP of 650 psia to 250 psia. So this under estimation will in turn makes the gas lift operation inefficient and the maximum production rates anticipated in Section 5.1 will be lower.

Table 5.8 shows the percentage deviation of viscosity between selected correlation and others, for pressures from 250 to 650 psia.

Pressure (psig)	Bergman-Sutton	Beal et al	Petrosky et al	Beggs et al	De Ghetto et al (Heavy Oil)	Egbogah (Heavy Oil)
250	-12	0	1	22	47	188
350	-11	0	0	13	41	163
450	-10	0	0	6	35	140
650	-9	0	-1	-7	23	99

Table 5.9: Deviation (%) of PROSPER EOS correlations in oil viscosity.

Increase in viscosity increases the pressure drop in tubing and hence De Ghetto et al, Egbogah, Beggs et al and Petrosky correlations will estimate a higher pressure drop and hence lower production. Bergman Sutton correlation will estimate the higher production.

Density and Bo have very little deviations about  $\pm 5\%$  between the correlations and hence will have little effect.

For any sensitivity analysis considered the IPR and VLP curves must be superimposed to find the liquid rate and the bottom-hole pressure that the well is producing. Because the considered cases are innumerable, separate IPR and VLP curves have been generated in the respective sections. When they are superimposed the maximum production and the required injection gas can be found.

### 5.3 Unloading Process

Table 5.10 shows the minimum gas injection pressure at the surface for unloading the annulus and tubing of the completion fluids along with the number of unloading valves and the corresponding depths. As the injection pressure is increased the number of valves is decreased.

PROSPER allows two methods for the calculation of number of valves and corresponding depths for casing pressure operated valves. 1) Spacing line procedure 2) Normal procedure. For tubing pressure operated valves only normal method is allowed.

Casing Pressure Operated Valves						Tubing Pressure Operated Valves		
Valve Spacing Method	Spacing Line Procedure		Valve Spacing Method	Normal		Valve Spacing Method	Normal	
Inj. Pressure (psia)	# Valves	Depth (MD) of n-1 <sup>th</sup> valve	Inj. Pressure (psia)	# Valves	Depth (MD) of n-1 <sup>th</sup> valve	Inj. Pressure (psia)	# Valves	Depth (MD) of n-1 <sup>th</sup> valve
1500	7+1	11182.6	1500	5+1	9381.55	1500	8+1	11246.1
1600	7+1	11985.8	1600	5+1	10285.4	1600	9+1	12435.3
1700	7+1	12758.1	1700	5+1	11201.1	1700	8+0	12896.2
1800	5+1	12409.4	1800	5+1	12096.9	1800	6+0	12896.2
1900	4+1	12360.2	1900	5+0	12896.2	1900	5+0	12896.2
2000	3+1	11685.1	2000	4+0	12896.2	2000	4+0	12896.2
2100	2+1	10369.5	2100	3+0	12896.2	2100	4+0	12896.2
2200	2+1	11224.2	2200	3+0	12896.2	2200	3+0	12896.2

Table 5.10: Depth and number of unloading valves for different injection pressures

For spacing line procedure in IPO valves for an injection pressure of 1800 psia the total number of unloading valves is 5 and the depth of operated valve is 12409.4 ft. When the injection pressure is increased from 1800 to 1900 psia the number of unloading valves is decreased from 5 to 4 and the depth of injection has been changed to 12360.2 ft. This could be due to the PROSPER's attempt to optimize the overall economics specific to the unloading of the well by optimizing the size of the compressor with the number of valves. Since the operating valve at the maximum depth is the most efficient gas lift operation, and this fact has already been considered in the design itself, unloading from the bottom most depth shall be analyzed.

For normal valve spacing method in IPO valves for an injection pressure of 1900 psia the operating valve is set at the target depth of 12896 ft and the number of unloading valves is 5. When the injection pressure is increased to 2000 the number of unloading valves is decreased to 4 while the depth remains at the maximum.

For PPO valves, since no pressure is lost for closing already unloaded valves, the minimum injection depth of 12896 ft can be reached with a compressor pressure of 1700 psia to and the number of unloading valves is 8.

## 6. Conclusions

### 6.1 Design of the Gas Lift System

Depth of injection has been kept at its maximum equal to the depth of the casing i.e. 12896.2 ft.

For a tubing size of 4.5", the maximum oil production rate is about 4700 stb/d at a wellhead pressure of 250 psia and 0% water cut. At this point the bottom-hole pressure is 2548 psia, the gas injected is about 9 MMscfd and the compressor injection pressure is 1792 psia. The maximum injection pressure is 1925 psia for a water cut of 40% and wellhead pressure of 650 psia. The corresponding oil production rate is 1892 stb/d and the bottom-hole pressure is 2859 psia and the gas injection rate is about 11 MMscfd.

Therefore, the size of the compressor that will be used must be able to handle at least 1925 (+20% for the fluctuations) psia and 11 MMscfd of gas. The depth of the operational valve is set at the depth of 12896.2 ft.

If a tubing size of 3.5" had been selected, the maximum possible oil production would be about 2894 stb/d at wellhead pressure of 250 psia and 0% water cut. The bottom-hole pressure is 2910 psia, the gas injection rate is about 6 MMscfd and the surface injection pressure is 1833 psia. Maximum injection pressure is 2130 psia for a water cut of 0% and a wellhead pressure of 550 psia; corresponding oil production rate is 2219 stb/d, the bottom-hole pressure is 3094 psia and the gas injection rate is 6 MMscfd.

For tubing size of 5.5" the maximum production is again at 250 psia wellhead pressure and 0% water cut and corresponds to a value of 6330 stb/d. The gas requirements are about 15 MMscfd, the surface injection pressure at the compressor is about 1376 psia and the bottom-hole pressure is 2223 psia.

Since no other reservoir data is available except the productivity, it is not possible to predict the plateau period of maximum production to have a justification for higher tubing size. Hence, 4.5" OD of tubing has been selected for the sensitivity analysis.

### 6.2 Sensitivity Analysis

Many IPRs have been generated for a range of possibilities with all the possible changes in parameters such as reservoir pressure, water cut, oil viscosity,  $k * h$  product, oil formation volume factor and productivity index. Similarly, many VLP curves have been generated for a range of variations in parameters such as wellhead pressure, Gas to Liquid ratio, tubing size, tubing roughness and the overall heat transfer coefficient. By superimposing any IPR and VLP the maximum possible production specific to that sensitivity can be read from the intersection point and the injection gas rate, casing pressure and injection pressures can be read from the corresponding sensitivity curves for the gas flow in the annulus. Also, the maximum deviation of the PVT selected correlation is found out and the effect of the VLP correlation on the maximum production for the selected tubing diameter is found out.

### **6.3 Unloading Process**

For normal valve spacing method in IPO valves for an injection pressure of 1900 psia the operating valve is set at the target depth of 12896 ft and the 5 number of unloading valves are required. The usual gas injection valve that has been decided to be at the maximum depth during the design selection can be the 5<sup>th</sup> valve in this case and hence the actual requirement of unloading valves is only 4. If the compressor is designed for an output pressure of 2000 psia only 3 number of unloading valves are required.

For PPO valves, since no pressure is lost for closing already unloaded valves, the minimum injection depth of 12896 ft can be reached with a compressor pressure of 1700 psia and the number of unloading valves is 8 means 7 unloading + 1 operating.

## 7. References

1. Heriot Watt University. *Production Technology*, (2011).
2. Guo, B., Ph, D., Sun, K., Ghalambor, A. & Ph, D. *Well Productivity Handbook Vertical, Fractured, Horizontal, Multilateral, and Intelligent Wells*, (2008).
3. Agrawal, A. Two Phase Flow Patterns and FLOW Maps. *J. Pet. Technol.* 20, 83–92, (2010).
4. Takacs, G. *Gas Lift Manual*. Penn Well Corporation, (2005).
5. Hernández, A. *Fundamentals of Gas Lift Engineering: Well Design and Troubleshooting*, (2016).
6. Economides, M. J. H. *Petroleum Production Systems*, (2004).
7. Guo, B., Lyons, W. C. & Ghalambor, A. *Petroleum Production Engineering. Petroleum Production Engineering*, (2007).
8. API Tubing Table, 152
9. Ahmed, T. *Reservoir Engineering Handbook*. Gulf Professional, (2010).
10. Beggs, H. D. *Production Optimization Using Nodal Analysis*, (1991).
11. Dmour, H. N. Optimization of well production system by NODAL analysis technique. *Pet. Sci. Technol.* 31, 1109–1122, (2013).
12. Vogel, J. V. Inflow Performance Relationships for Solution-Gas Drive Wells. *J. Pet. Technol.* 20, 83–92, (1968).
13. Schlumberger. *Gas Lift Design and Technology*, (1999).

## 8. Appendix

### A.1 Optimization of Gas Lift for Different Wellhead Pressures and Water Cuts

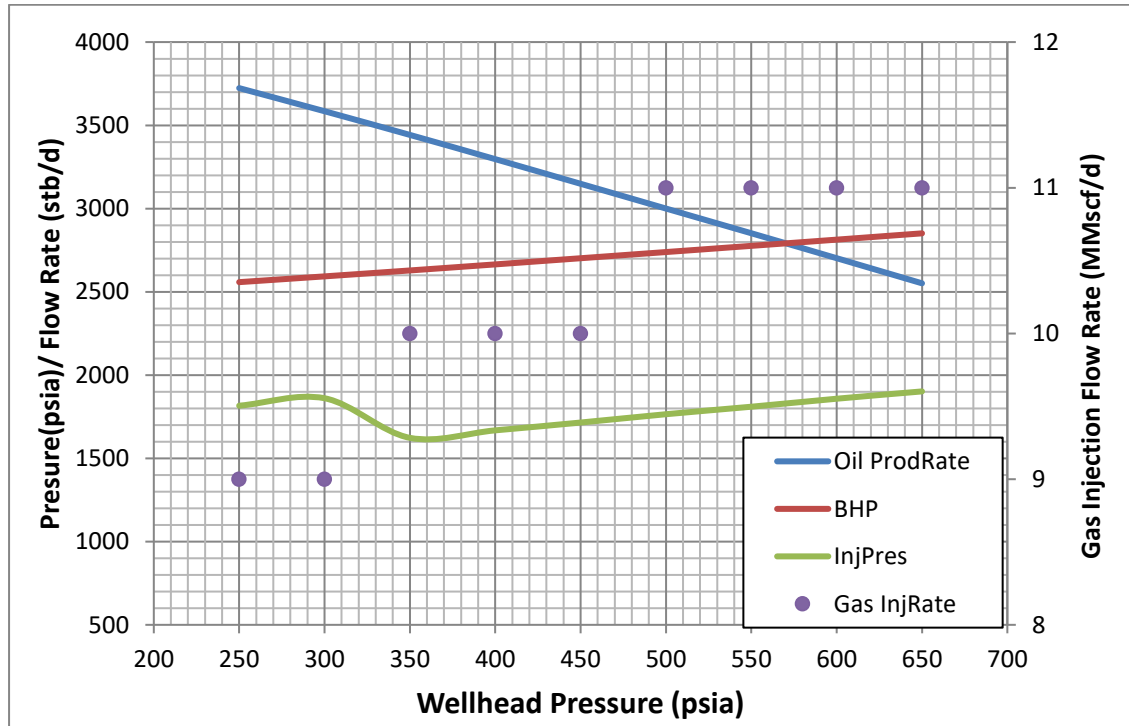


Figure A.1: Gas lift optimization-OD 4.5" and 20% water cut.

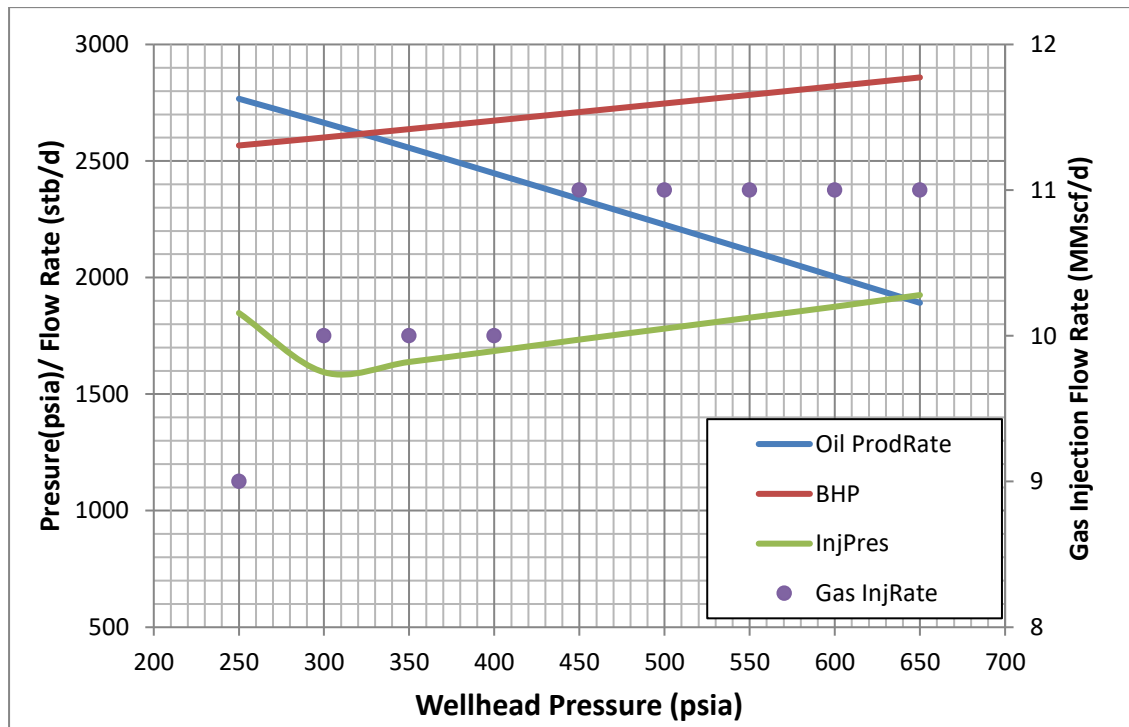


Figure A.2: Gas lift optimization-OD 4.5" and 40% water cut.

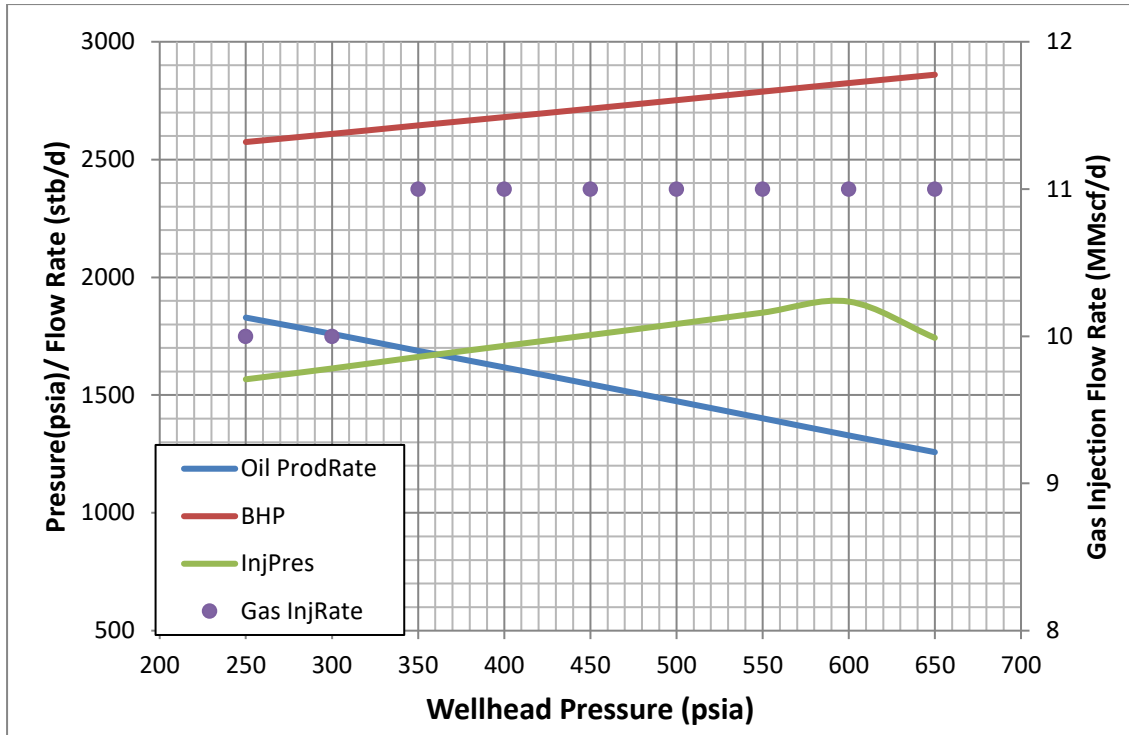


Figure A.3: Gas lift optimization-OD 4.5" and 60% water cut.

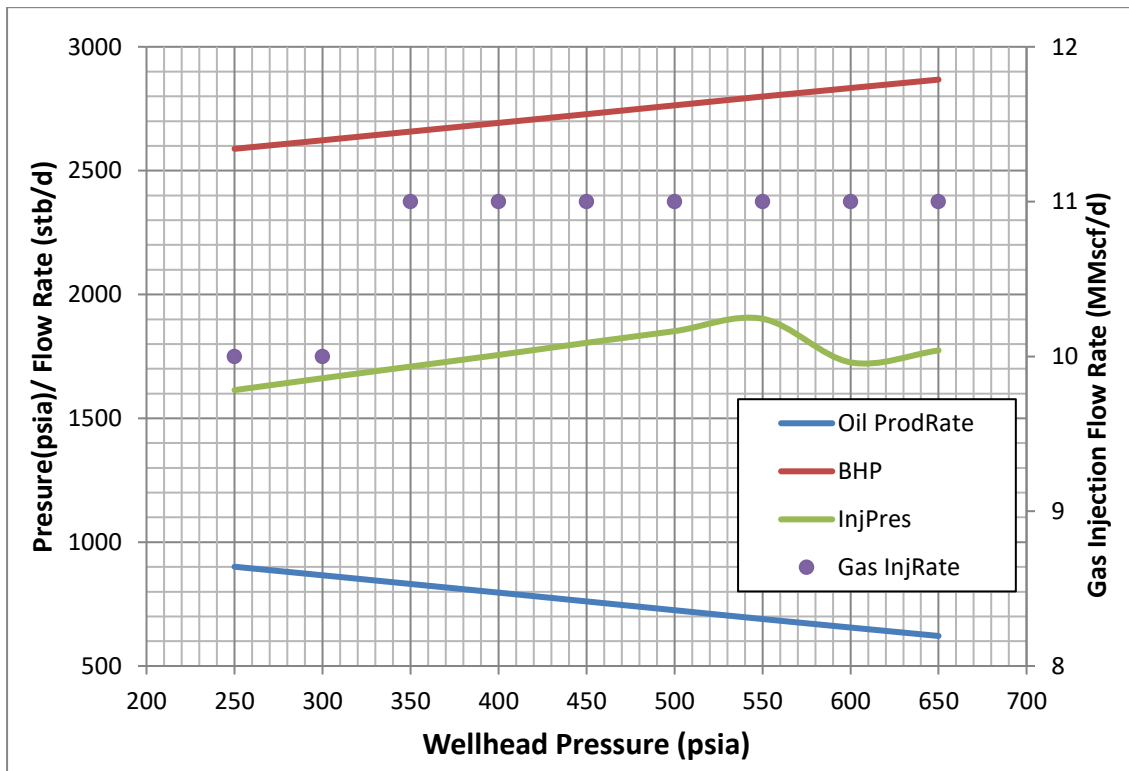


Figure A.4: Gas lift optimization-OD 4.5" and 80% water cut.

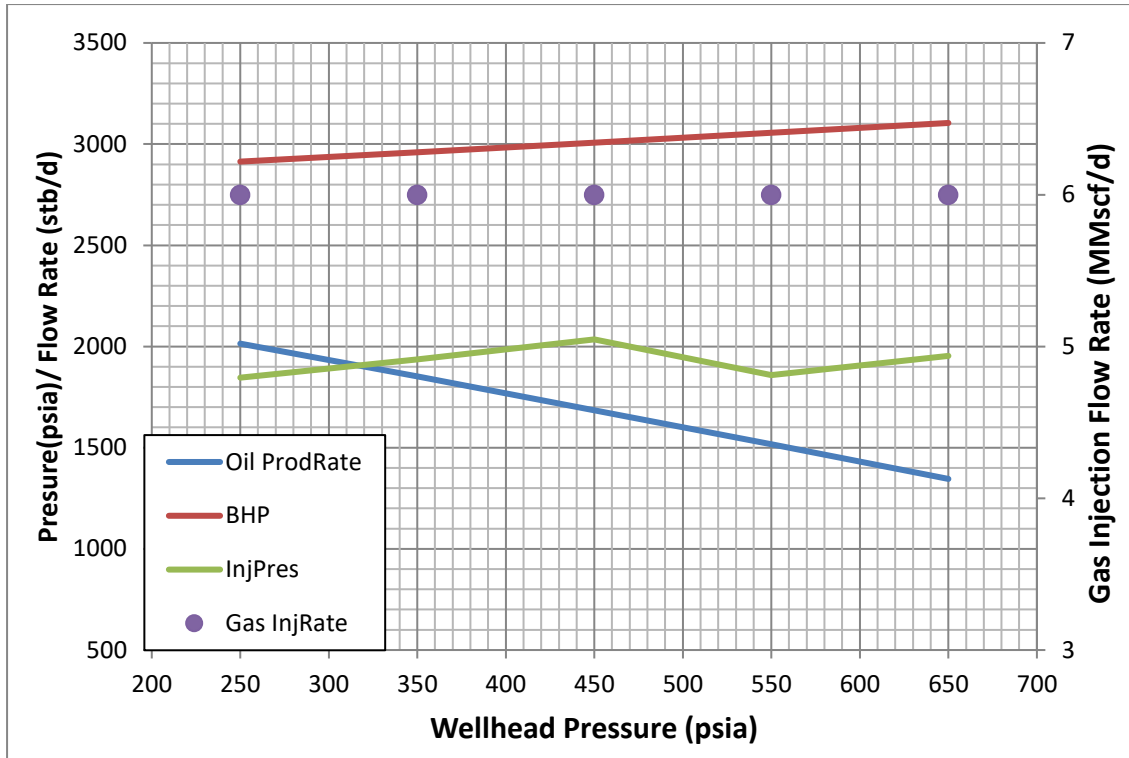


Figure A.5: Gas lift optimization-OD3.5" and 30% water cut.

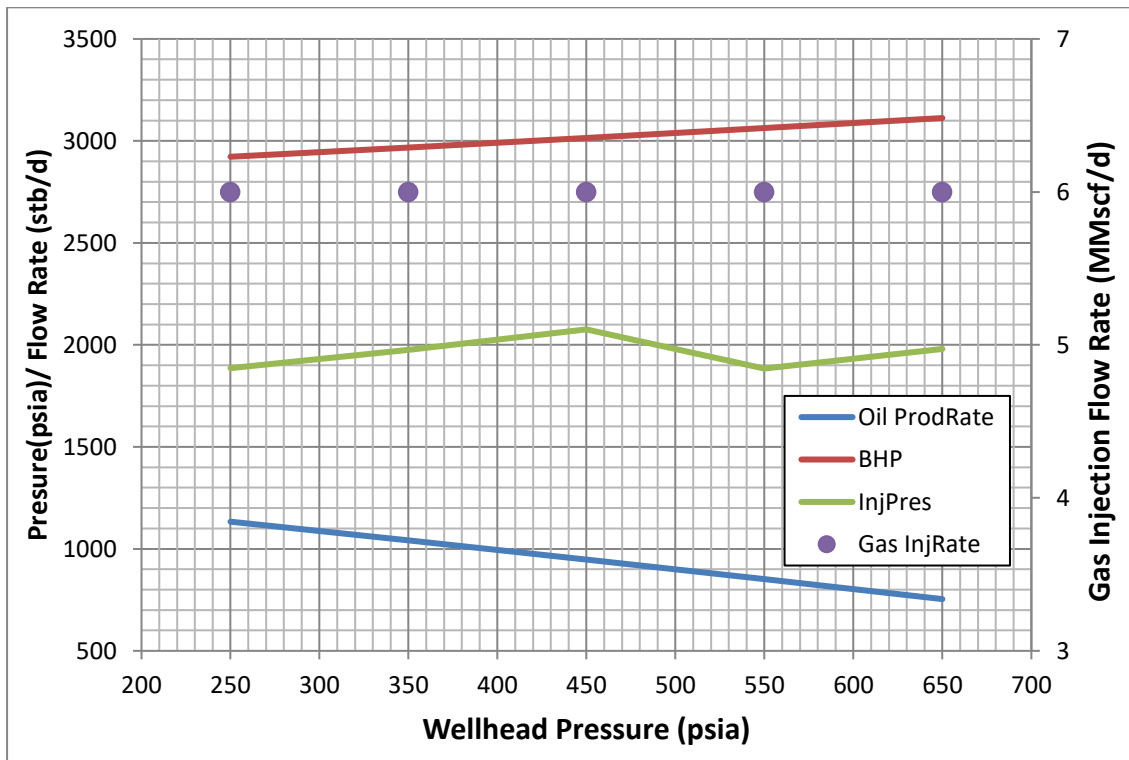


Figure A.6: Gas lift optimization-OD3.5" and 60% water cut- OD 4.5".

## A.2 Sensitivity for different Wellhead Pressures and Injection Flow Rates for 0% Water Cut

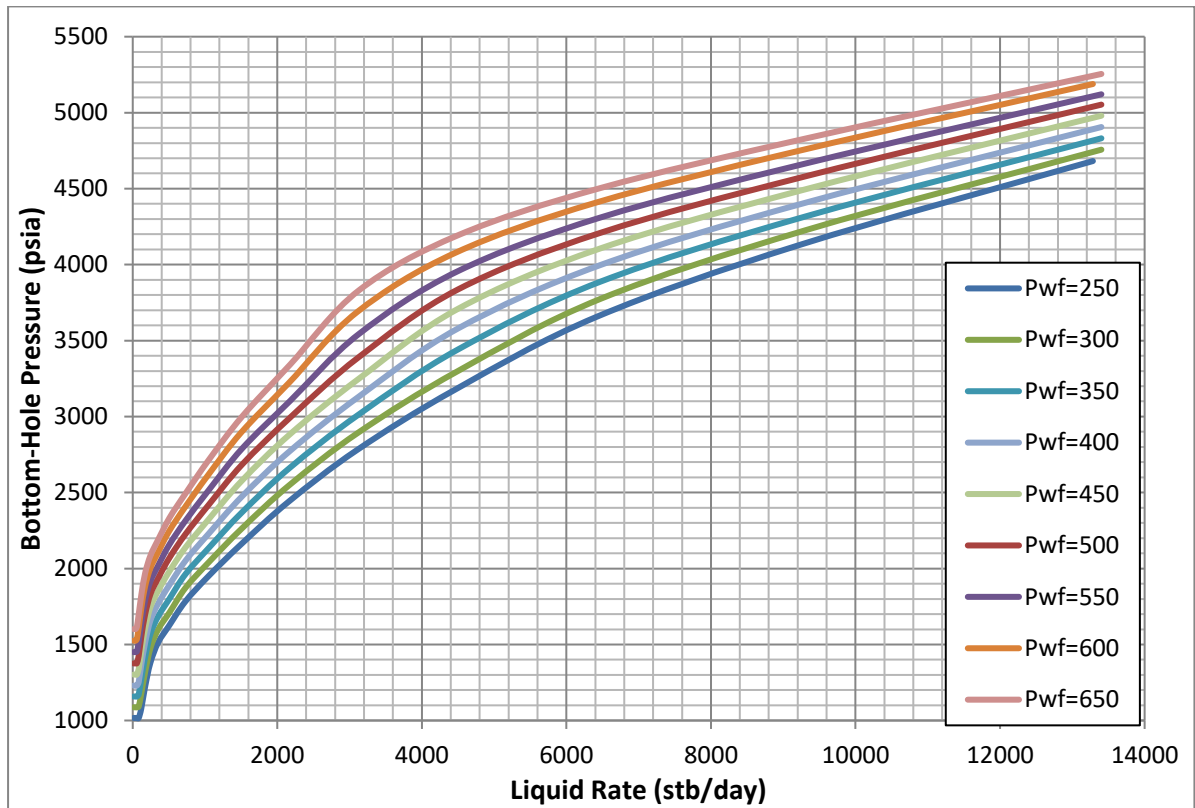


Figure A.7: VLP curves for 2MMscf/d injection rate and 0% water cut.

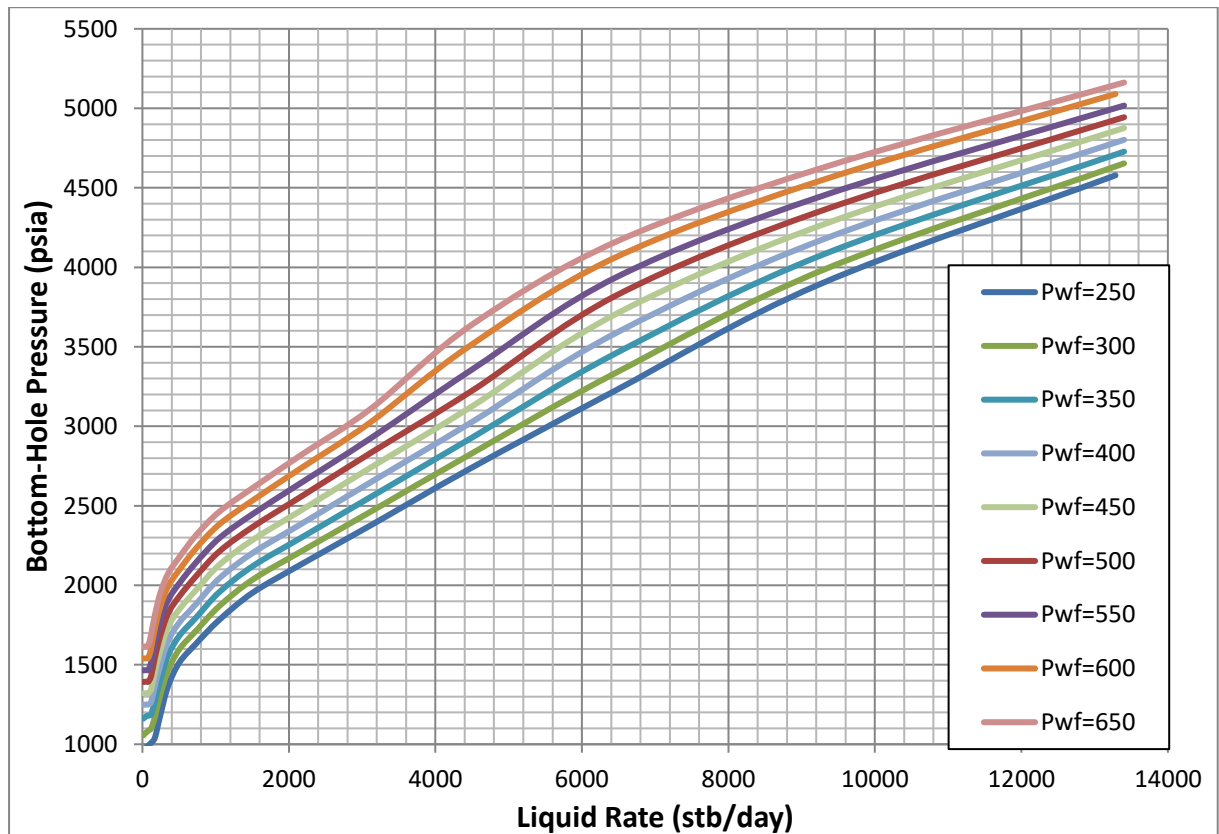


Figure A.8: VLP curves for 4MMscf/d injection rate and 0% water cut

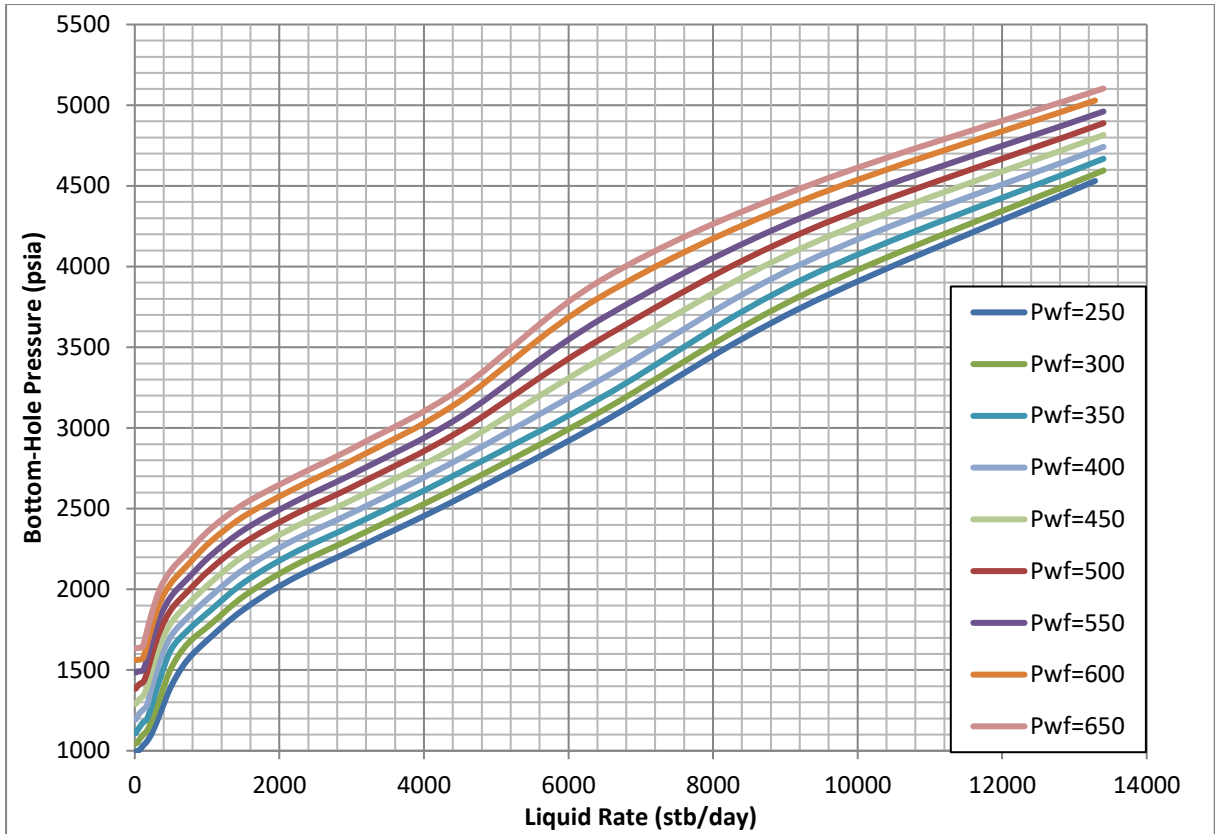


Figure A.9: VLP curves for 6 MMscf/day injection rate and 0% water cut.

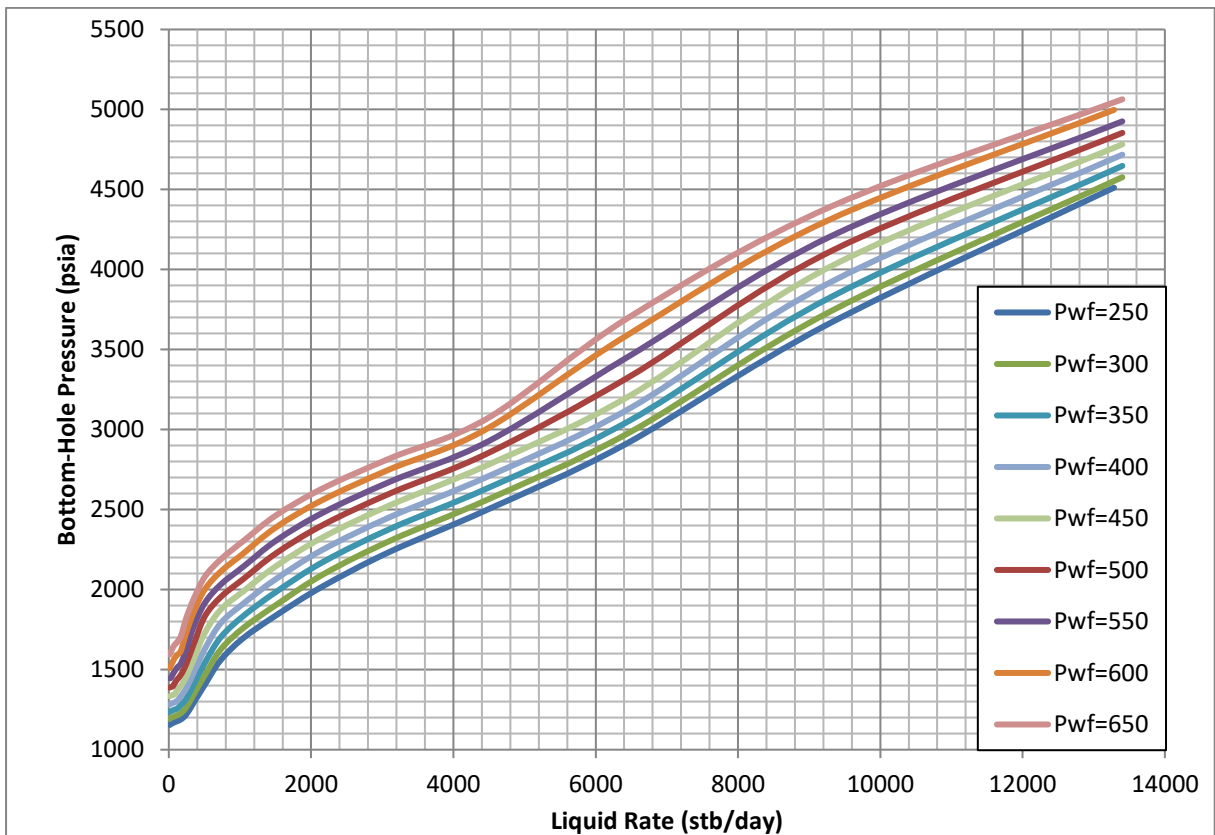


Figure A.10: VLP curves for 9 MMscf/day injection rate and 0% water cut.

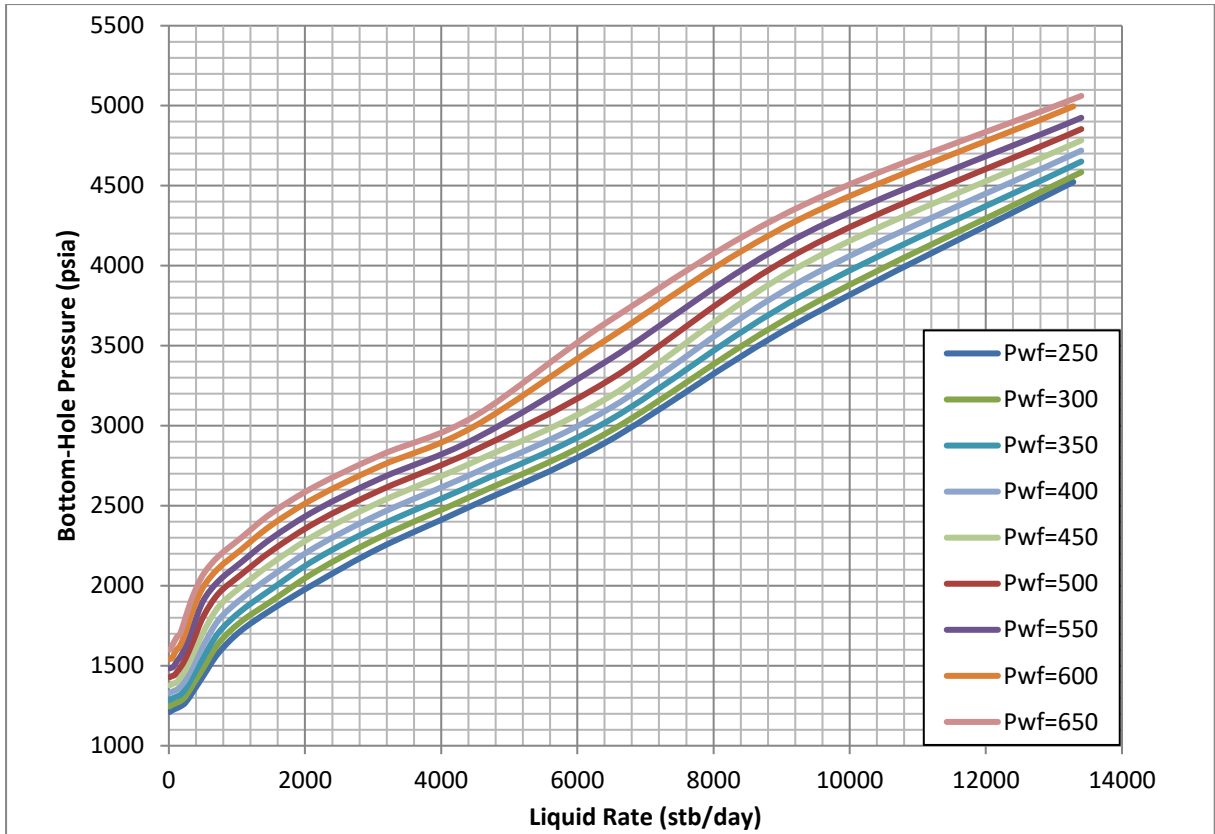


Figure A.11: VLP curves for 10 MMscf/day injection rate and 0% water cut.

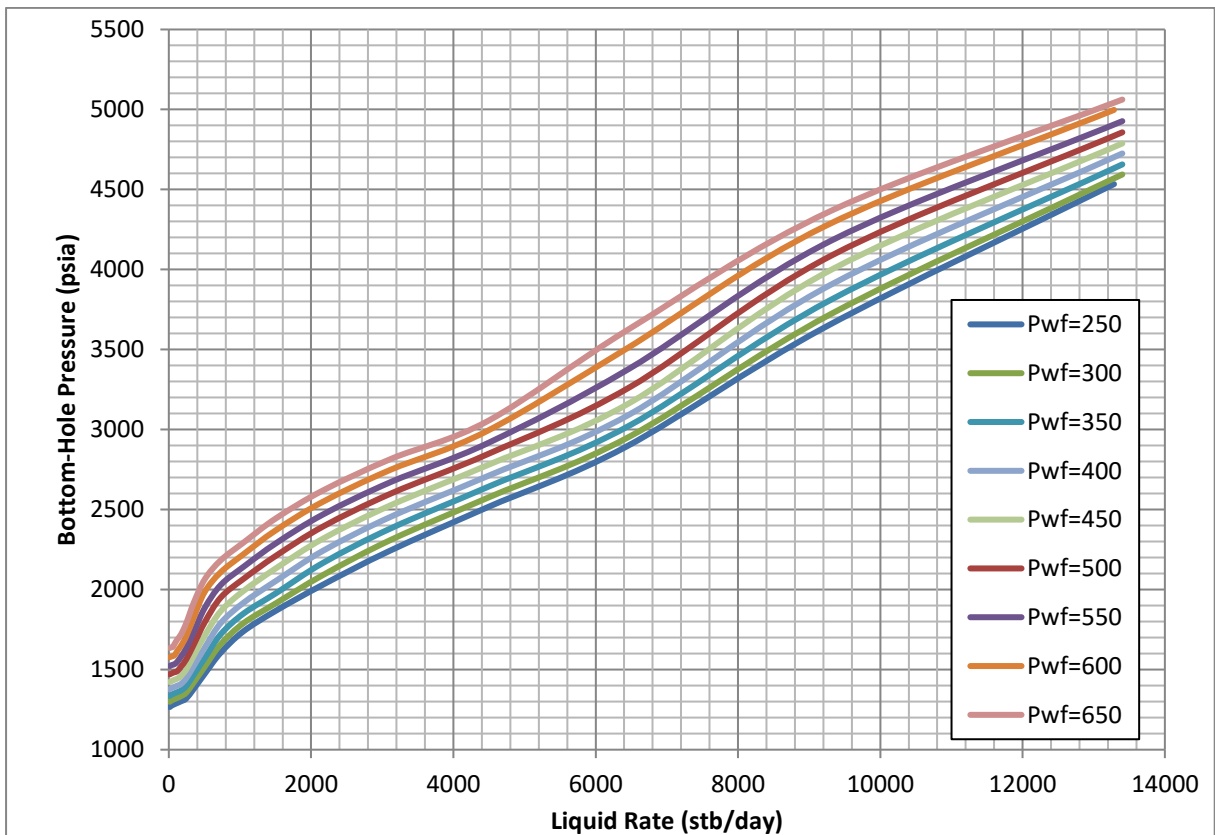


Figure A.12: VLP curves for 11 MMscf/day injection rate and 0% water cut.

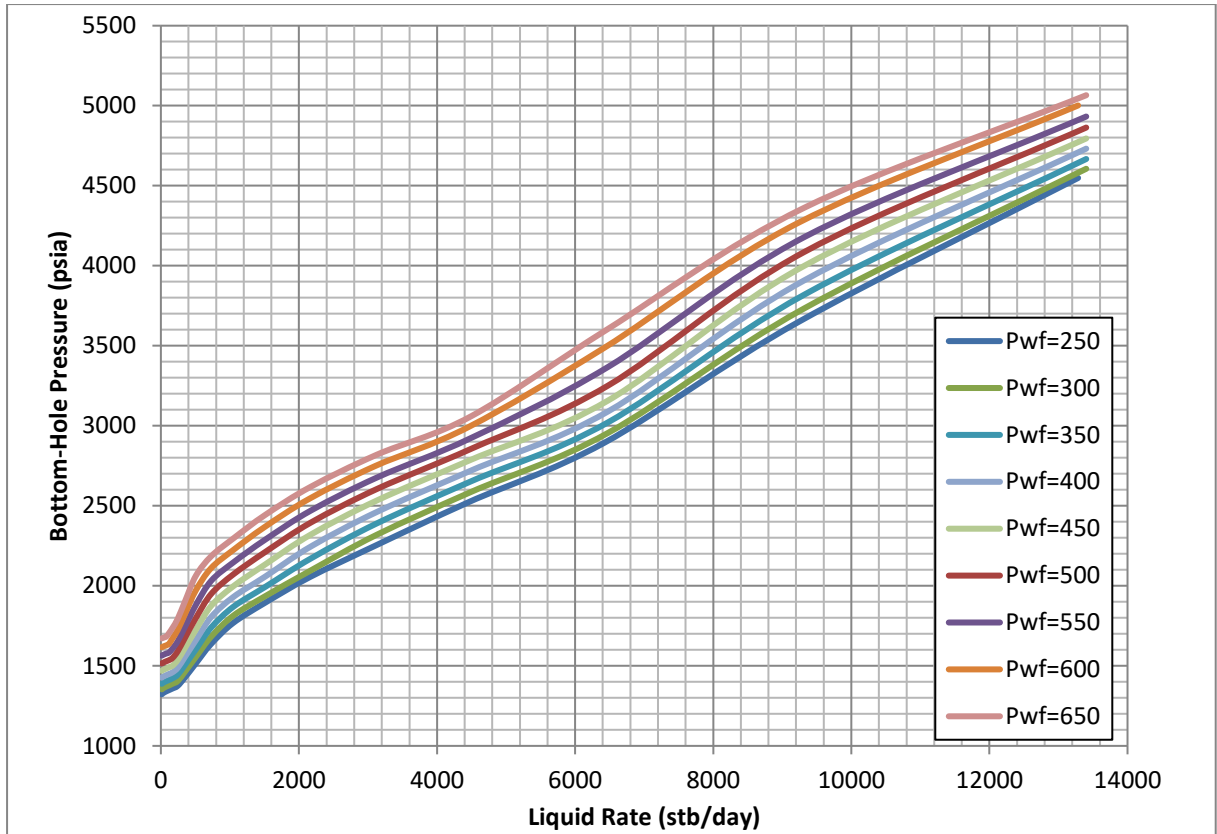


Figure A.13: VLP curves for 12 MMscf/day injection rate and 0% water cut.

### A.3 Sensitivity for different Wellhead Pressures and Injection Flow Rates for 20% Water Cut

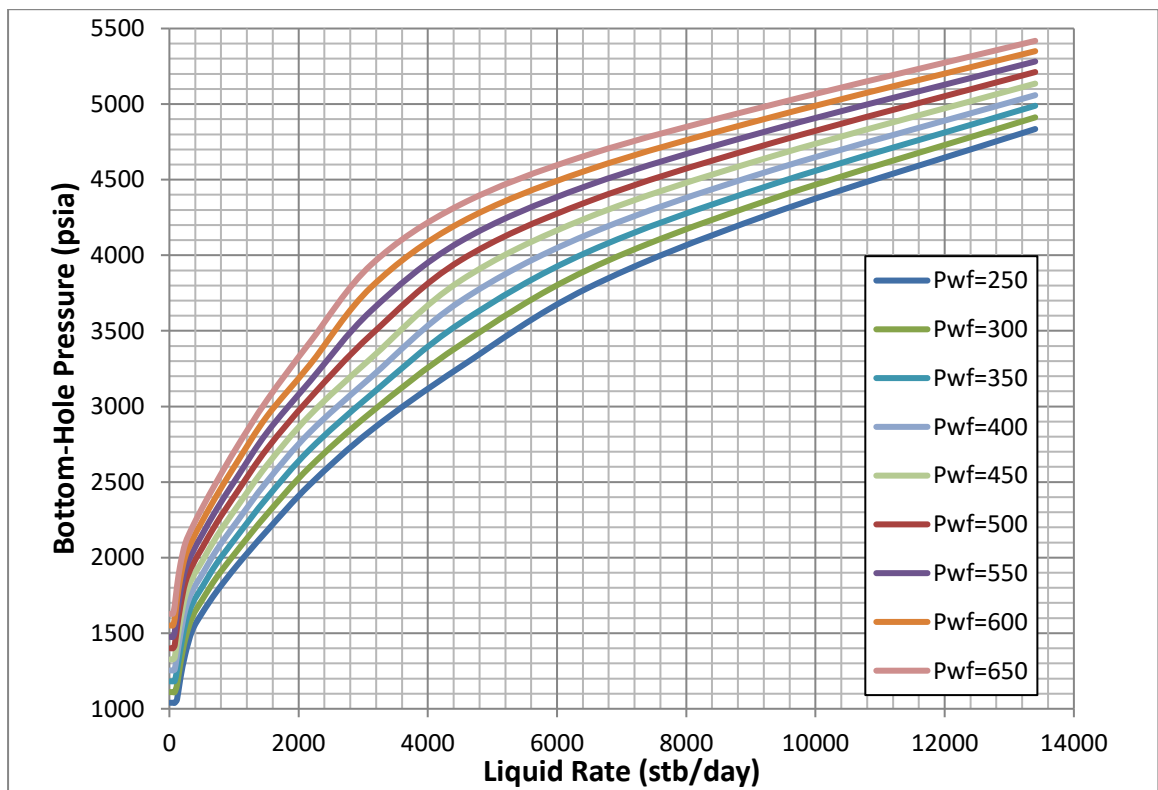


Figure A.14: VLP curves for 2 MMscf/day injection rate and 20% water cut.

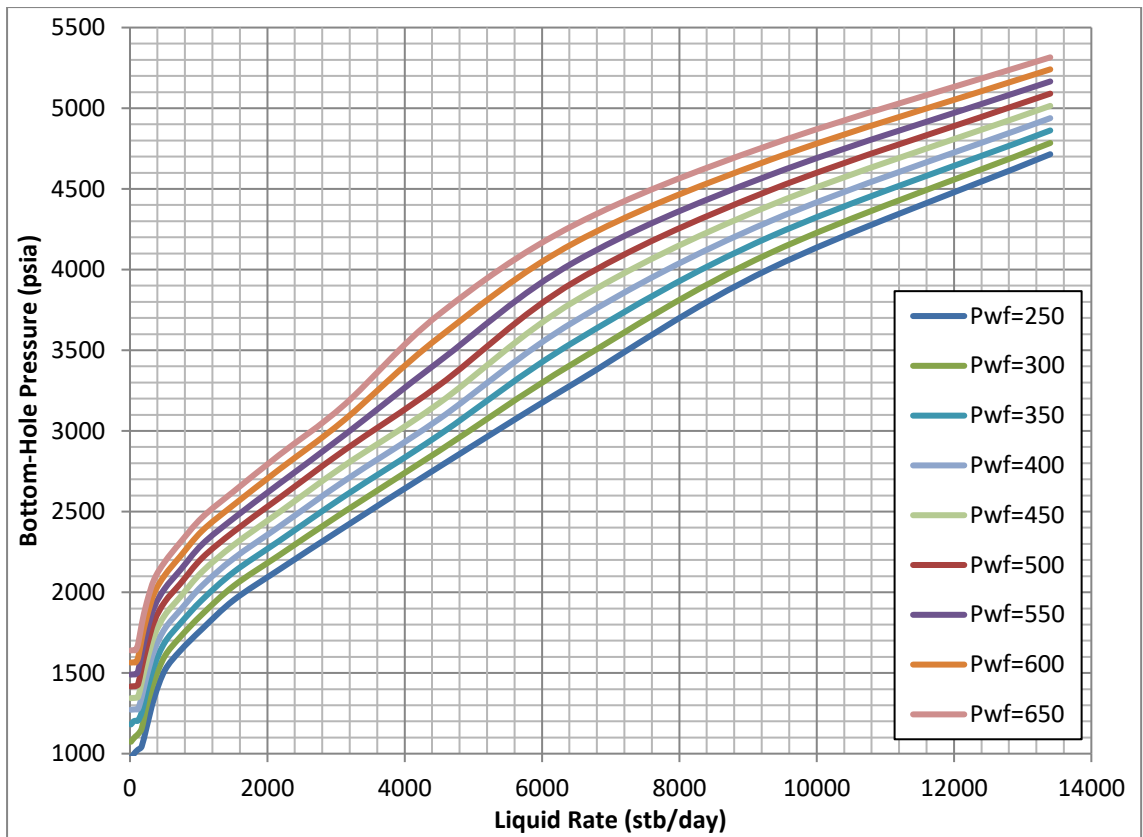


Figure A.15: VLP curves for 4 MMscf/day injection rate and 20% water cut.

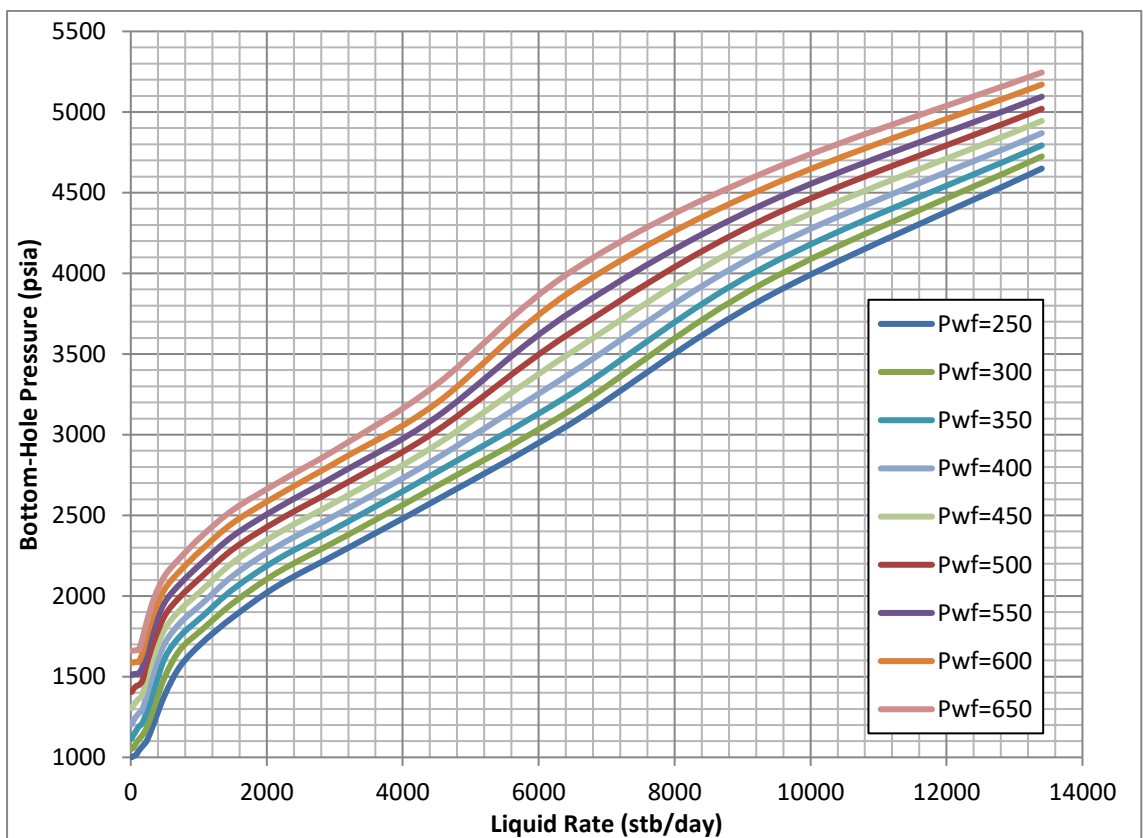


Figure A.16: VLP curves for 6 MMscf/day injection rate and 20% water cut.

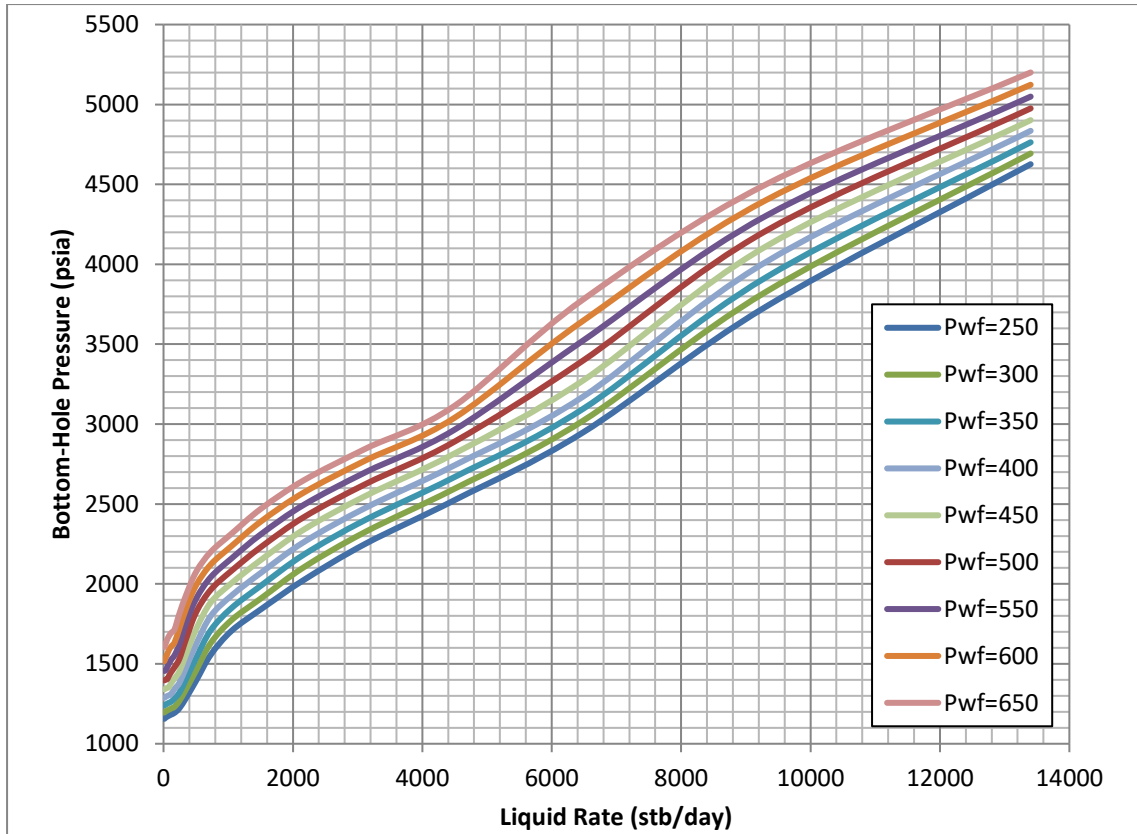


Figure A.17: VLP curves for 9 MMscf/day injection rate and 20% water cut.

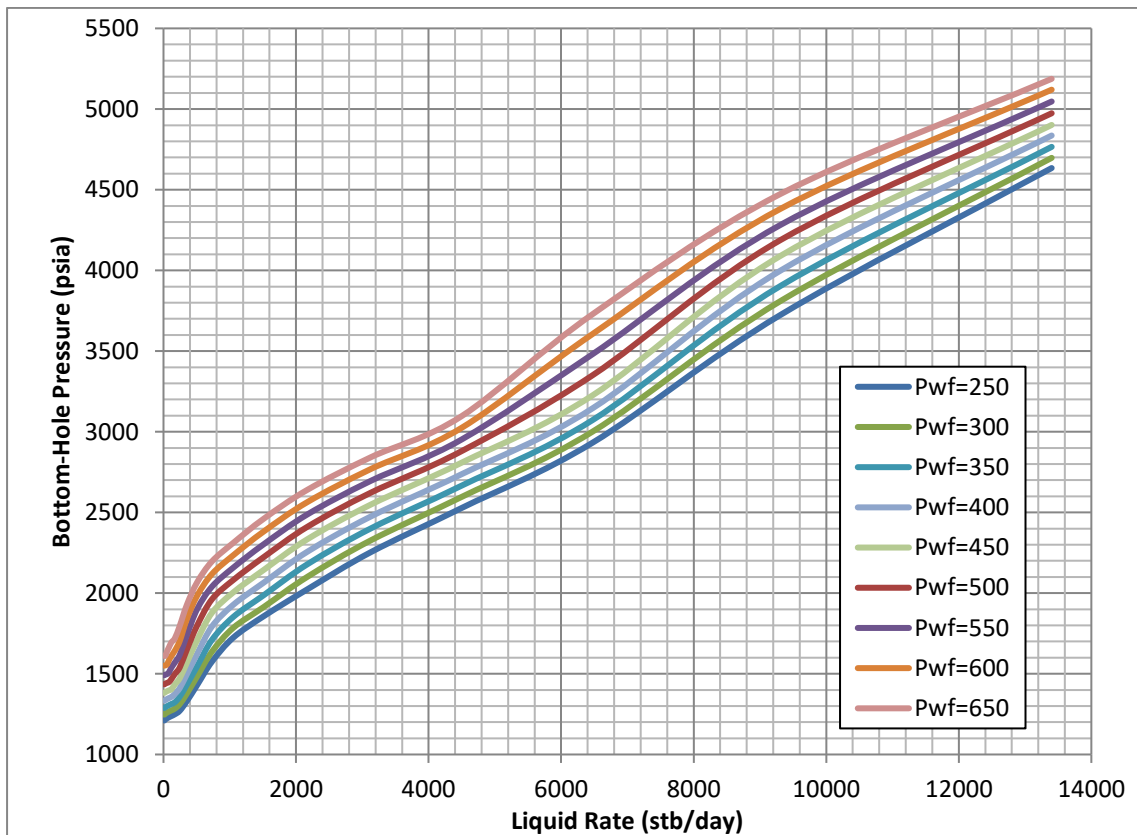


Figure A.18: VLP curves for 10 MMscf/day injection rate and 20% water cut.

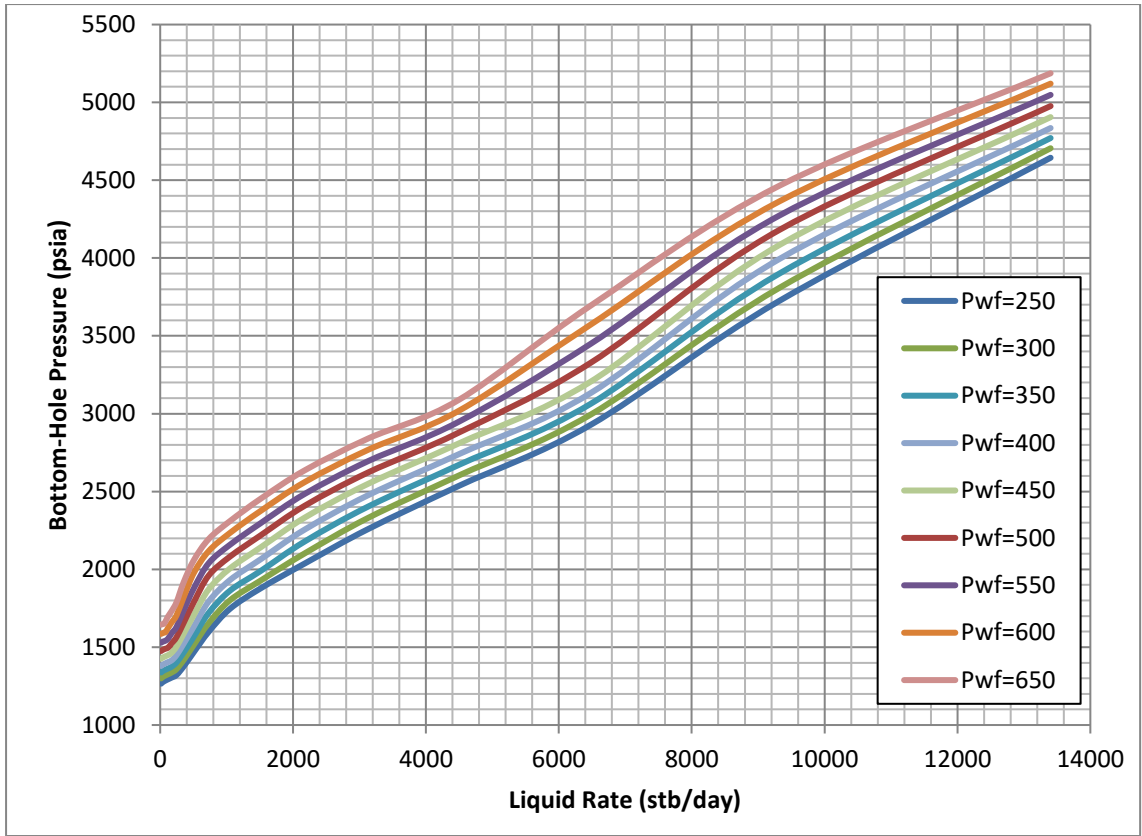


Figure A.19: VLP curves for 11 MMscf/day injection rate and 20% water cut.

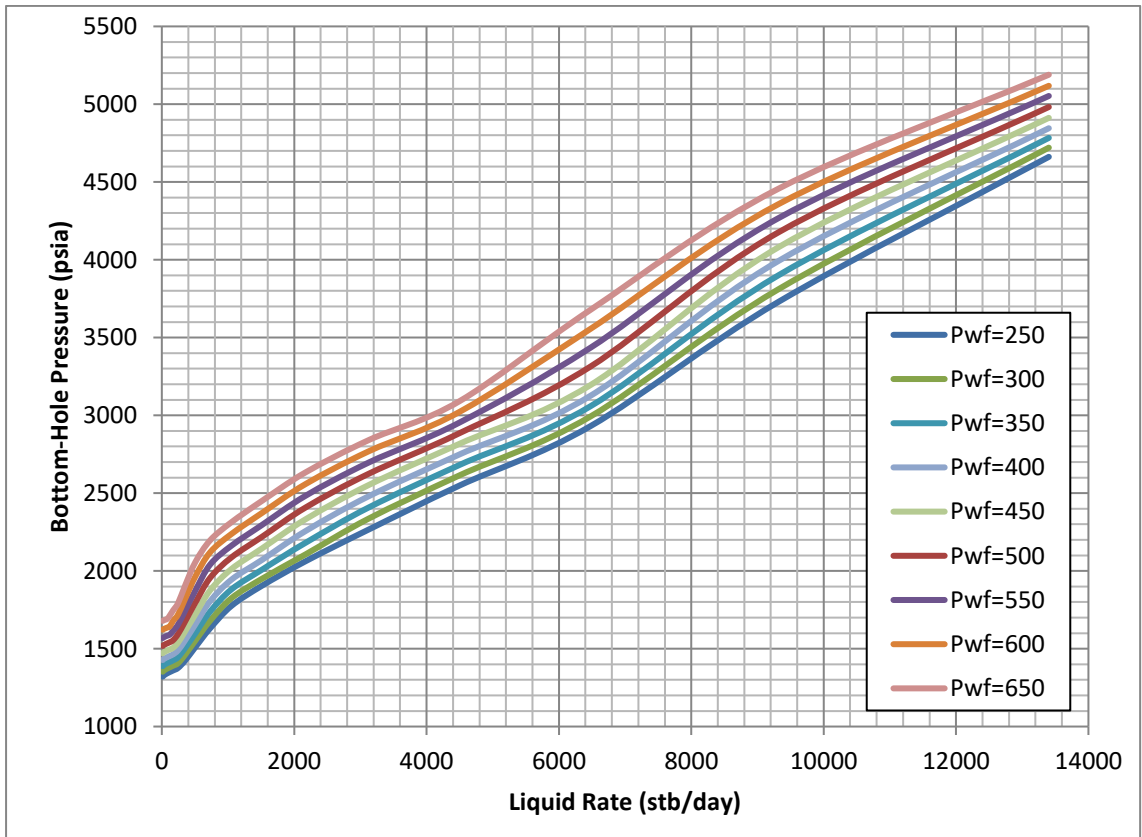


Figure A.20: VLP curves for 12 MMscf/day injection rate and 20% water cut.

### A.4 Sensitivity for different Wellhead Pressures and Injection Flow Rates for 40% Water Cut

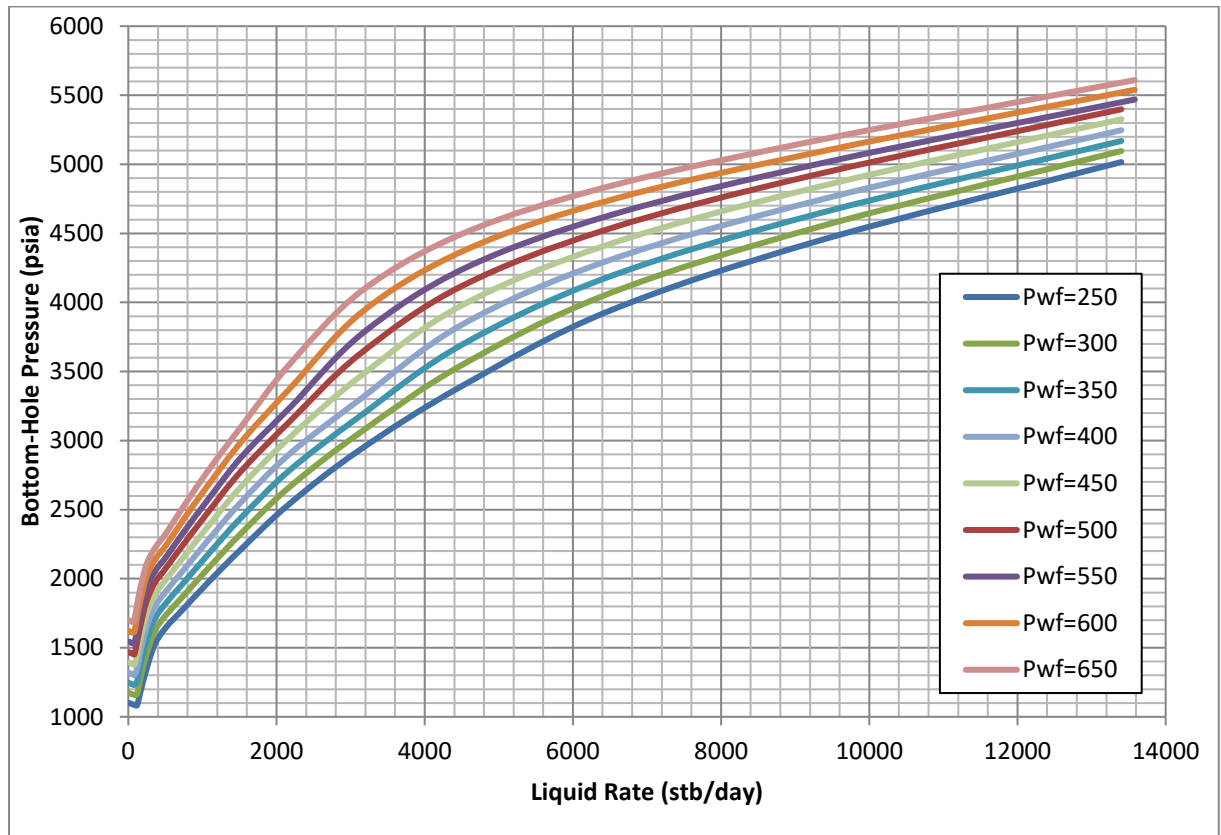


Figure A.21: VLP curves for 2 MMscf/day injection rate and 40% water cut.

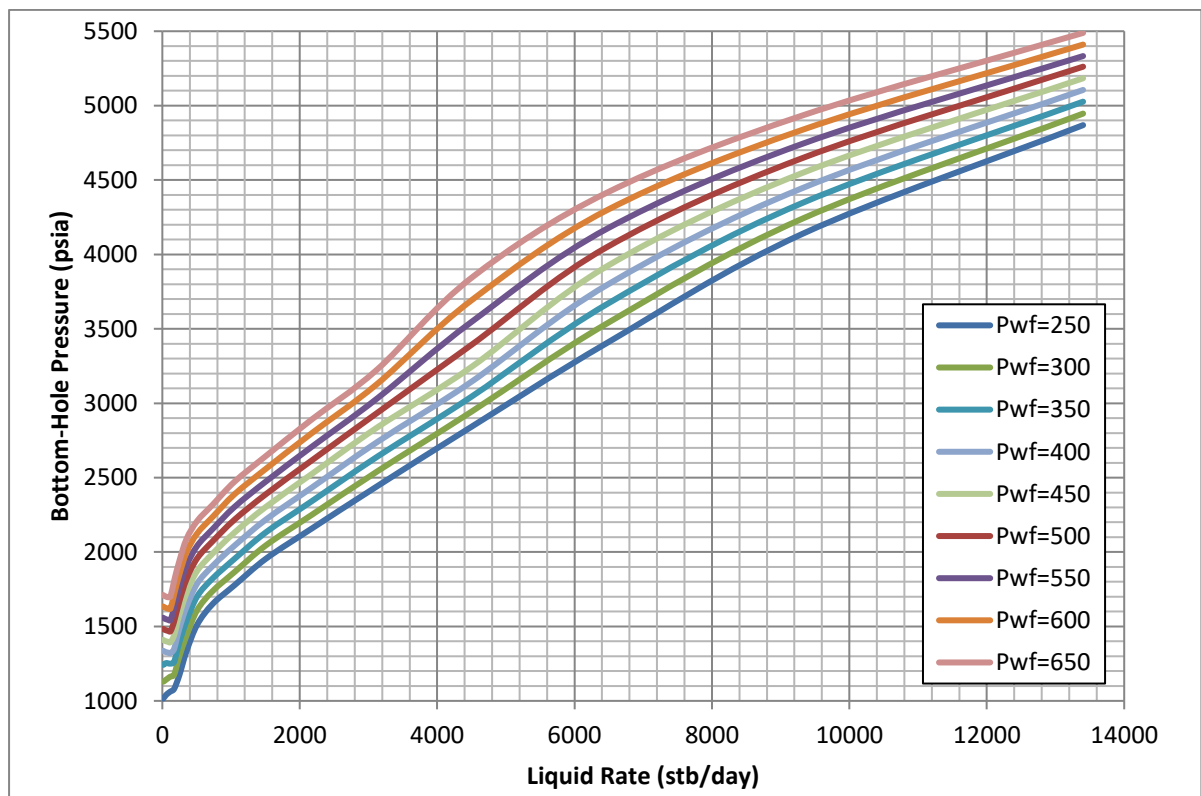


Figure A.22: VLP curves for 4 MMscf/day injection rate and 40% water cut.

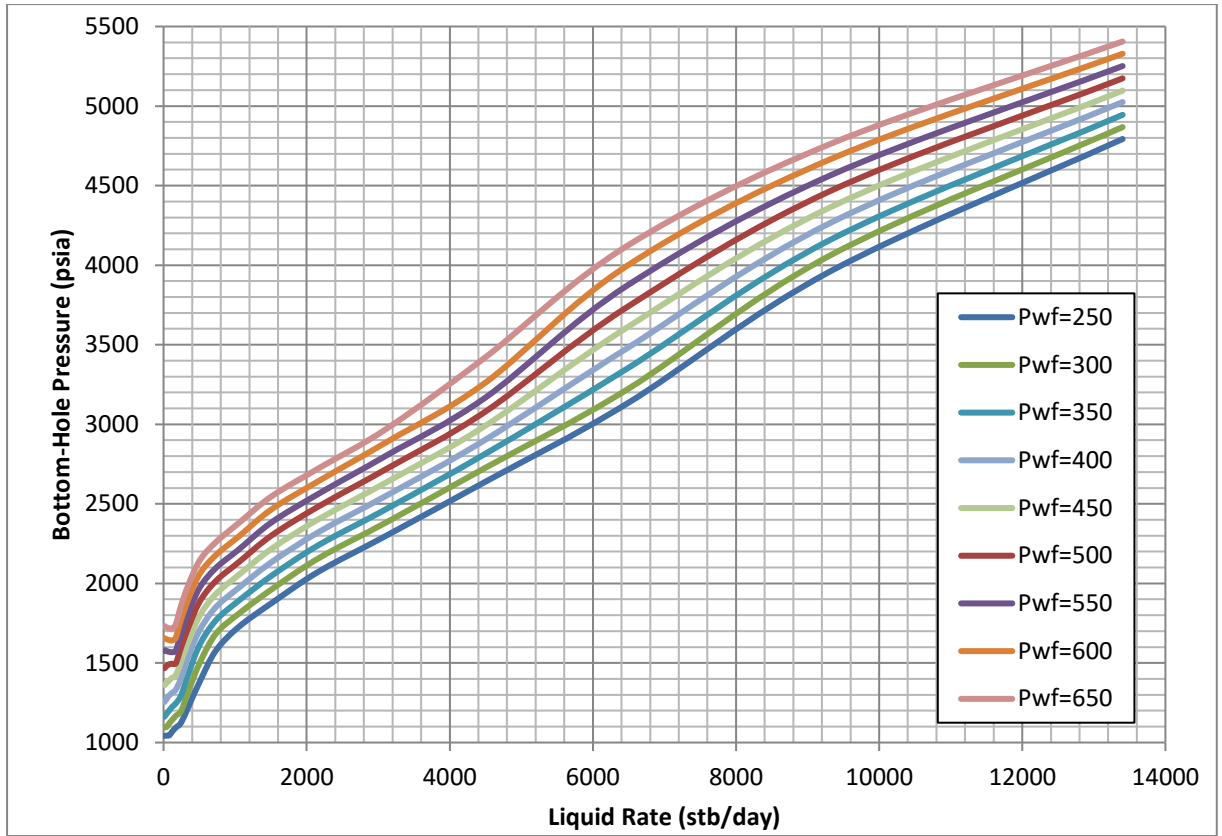


Figure A.23: VLP curves for 6 MMscf/day injection rate and 40% water cut.

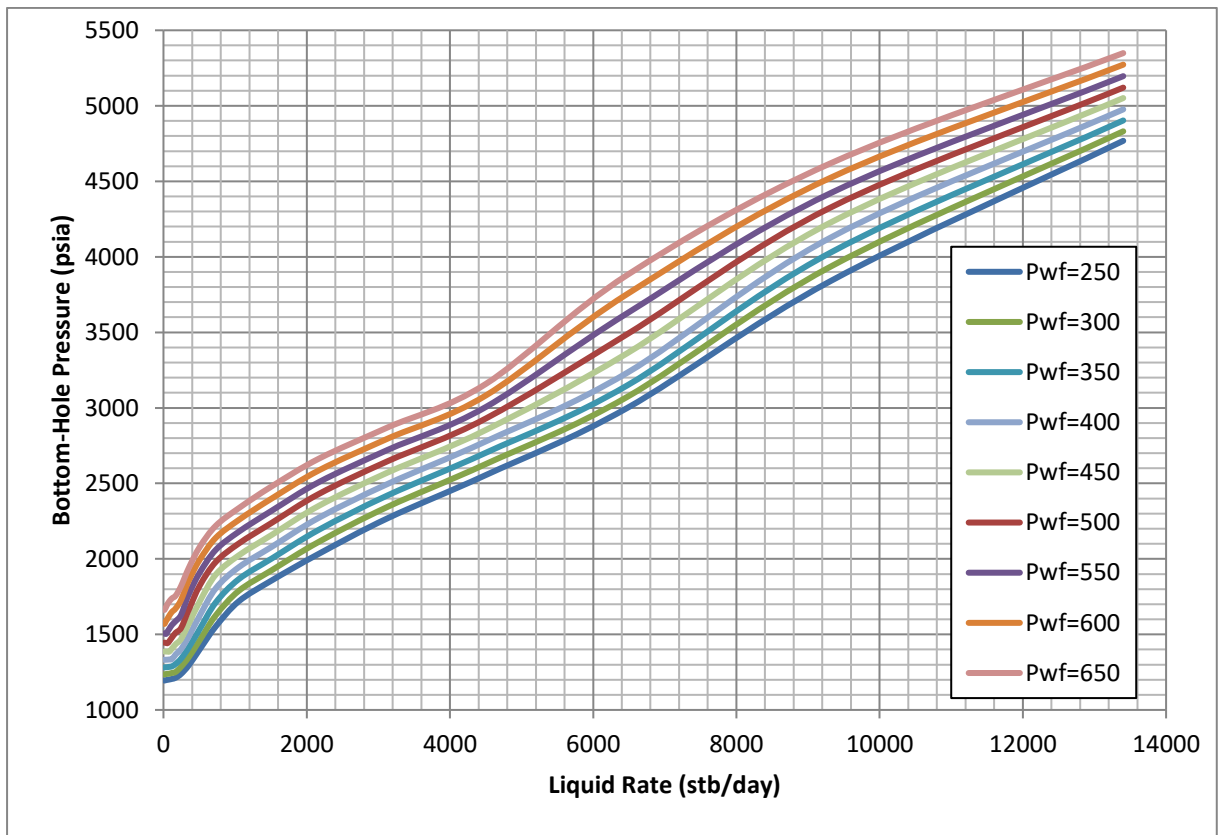


Figure A.24: VLP curves for 9 MMscf/day injection rate and 40% water cut.

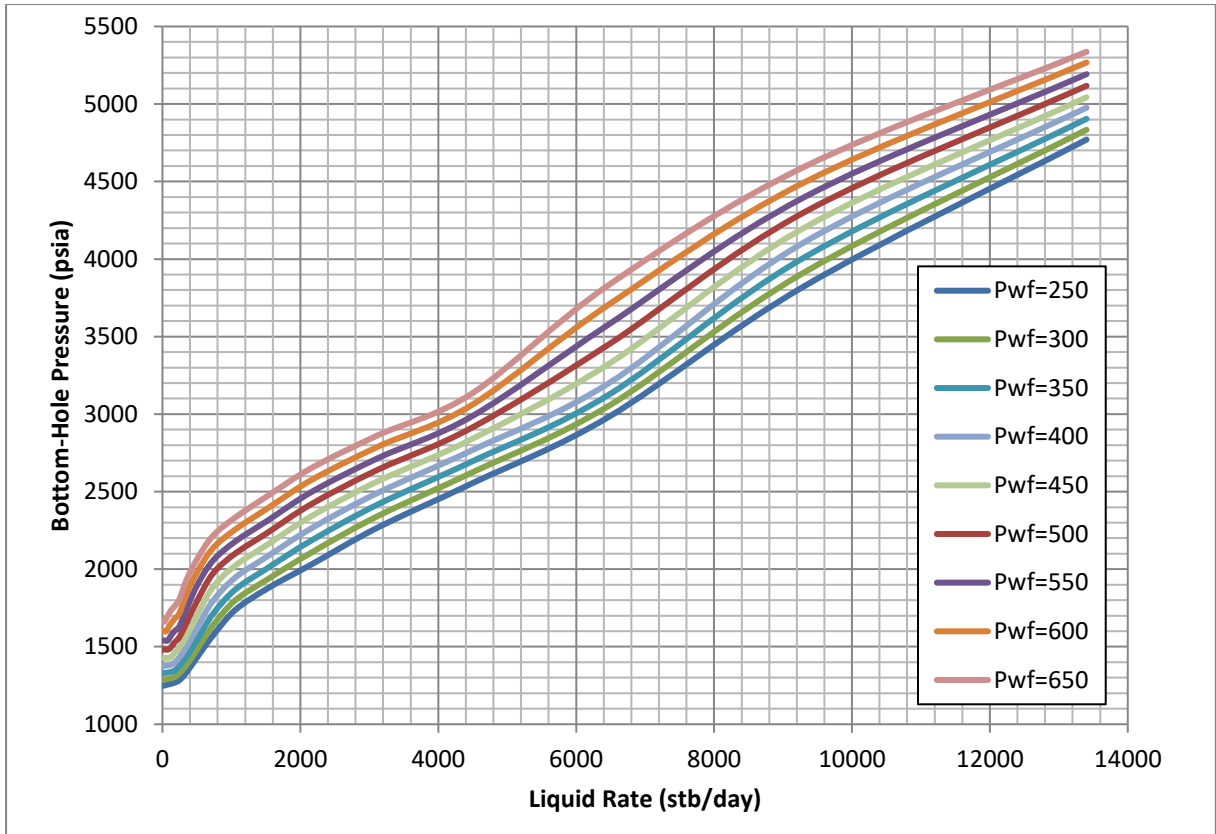


Figure A.25: VLP curves for 10 MMscf/day injection rate and 40% water cut.

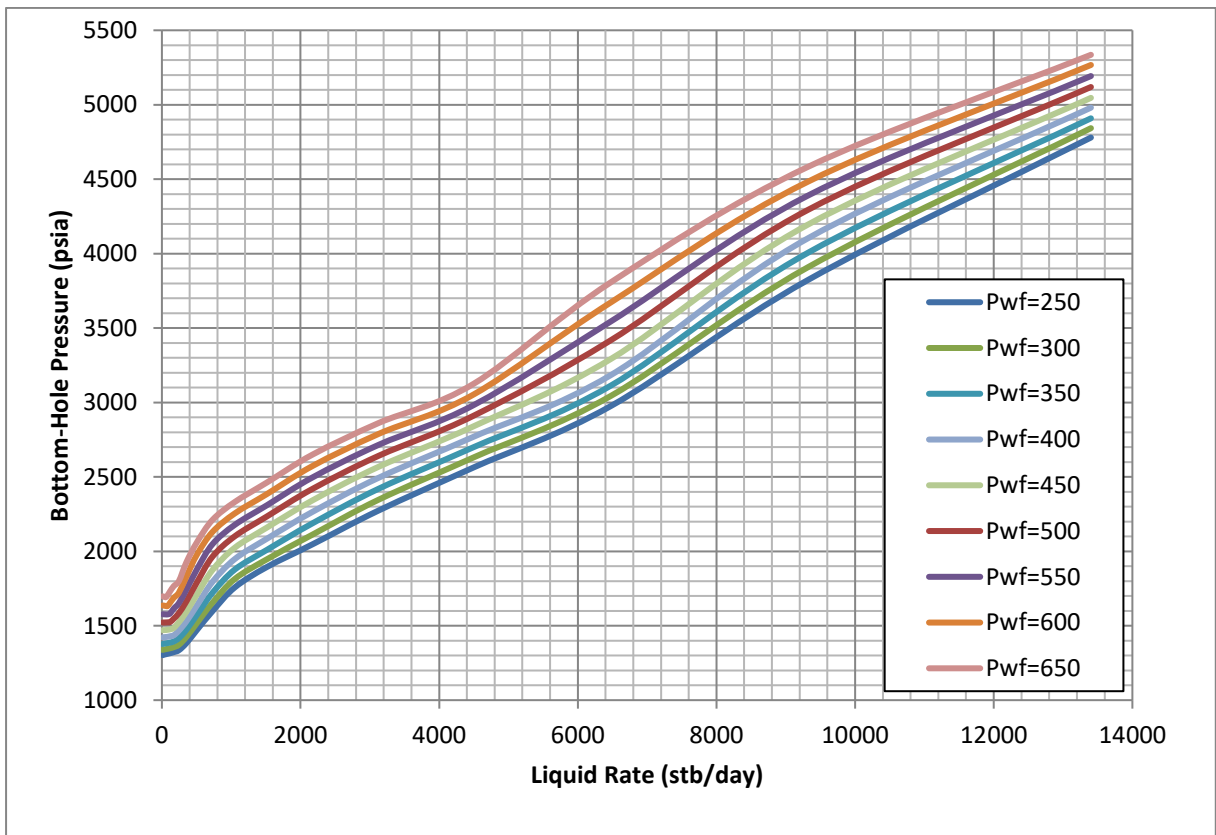


Figure A.26: VLP curves for 11 MMscf/day injection rate and 40% water cut.

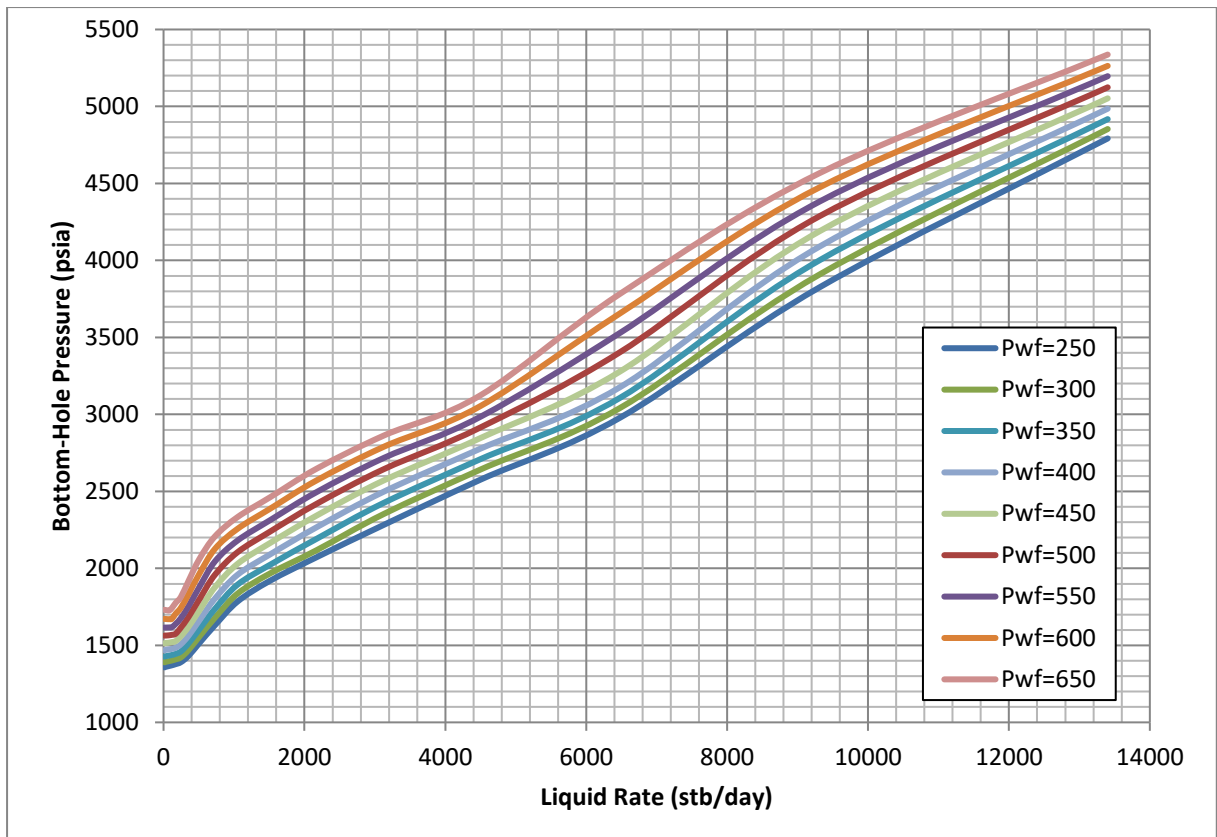


Figure A.27: VLP curves for 12 MMscf/day injection rate and 40% water cut.

**A.5 Sensitivity for different Wellhead Pressures and Injection Flow Rates for 60% Water Cut**

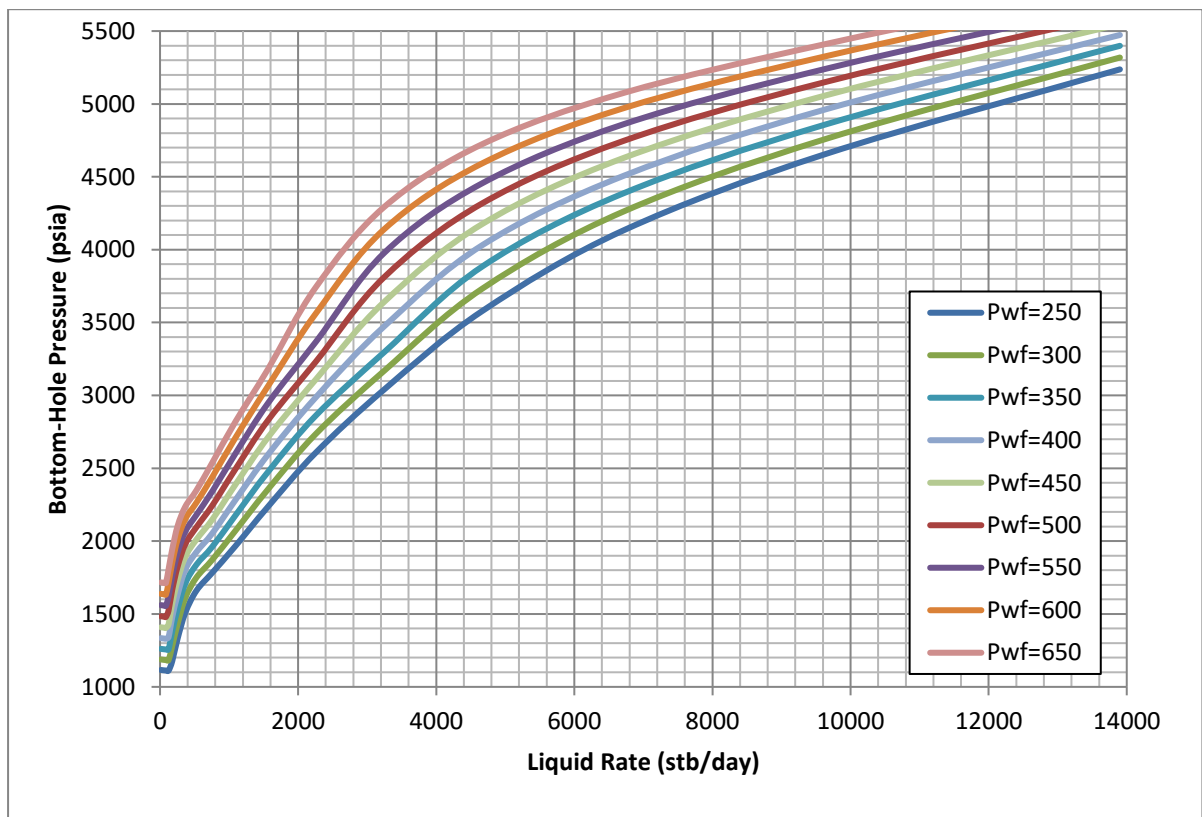


Figure A.28: VLP curves for 2 MMscf/day injection rate and 60% water cut.

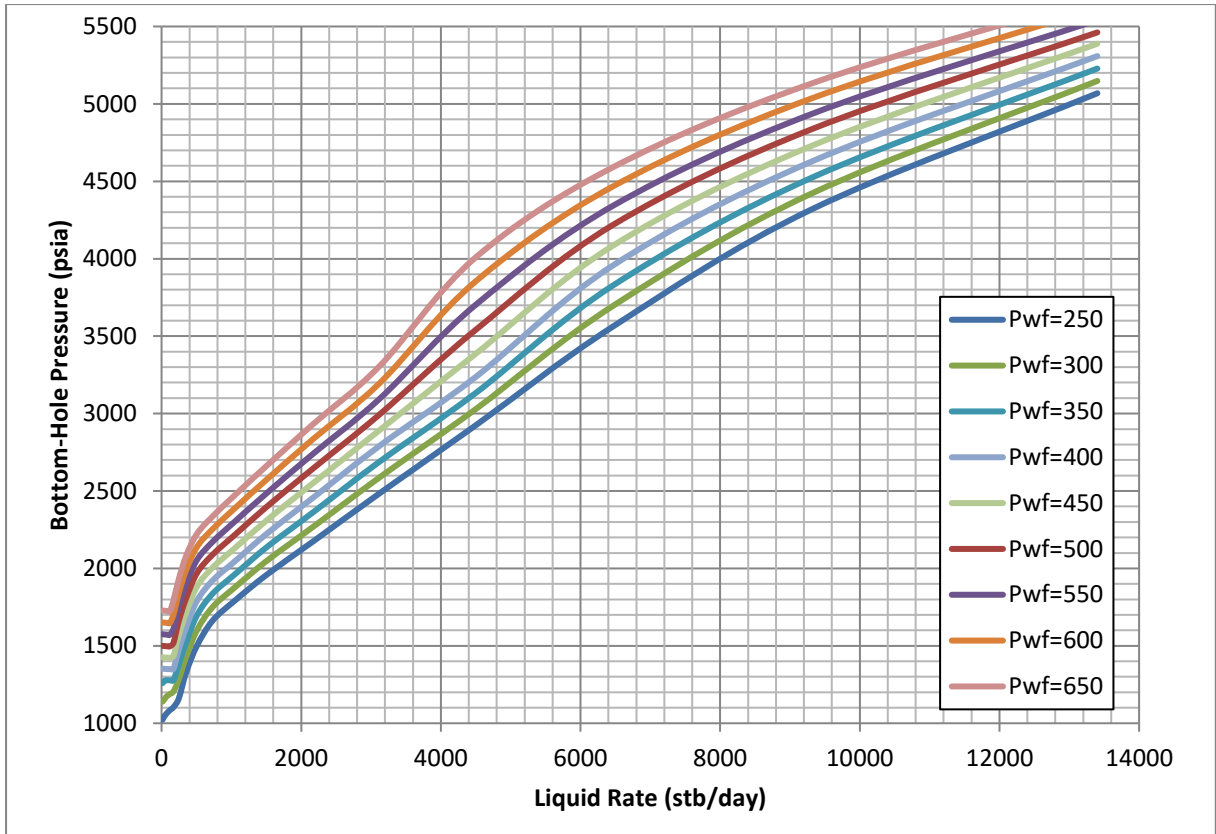


Figure A.29: VLP curves for 4 MMscf/day injection rate and 60% water cut.

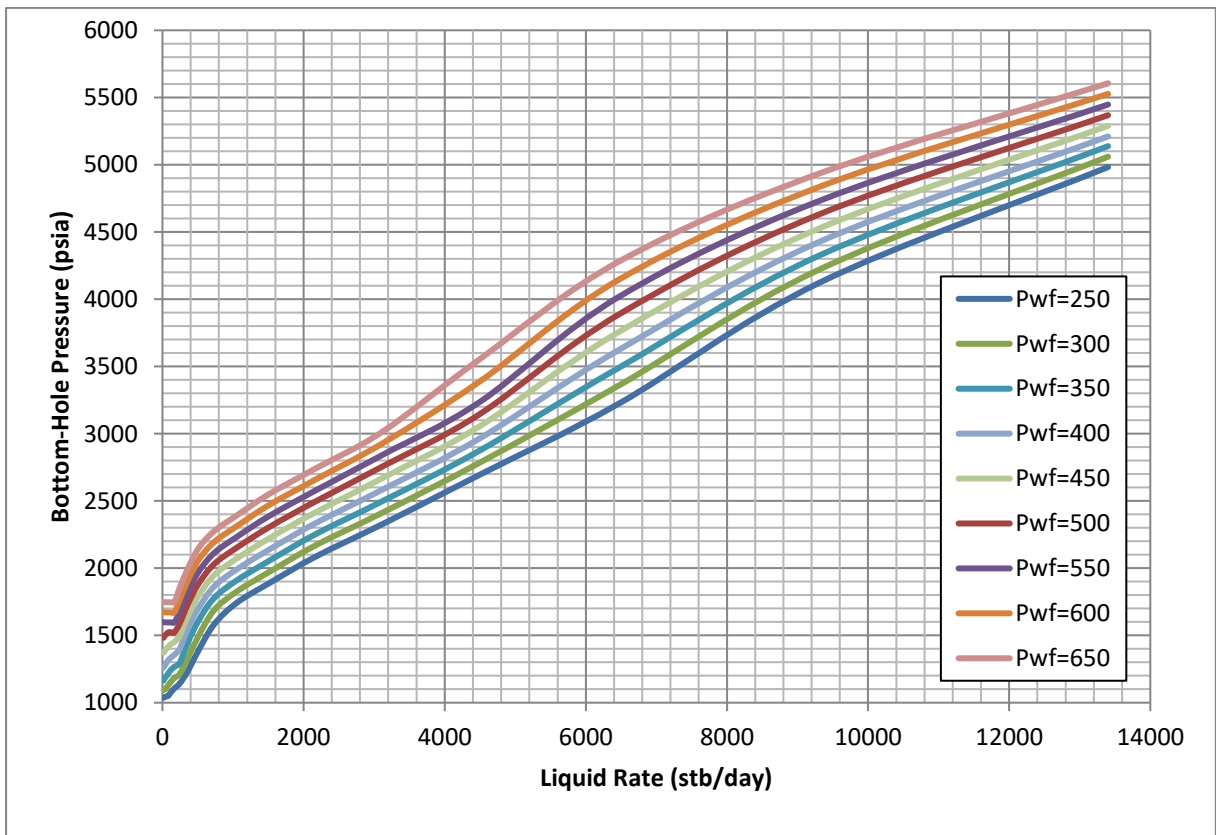


Figure A.30: VLP curves for 6 MMscf/day injection rate and 60% water cut.

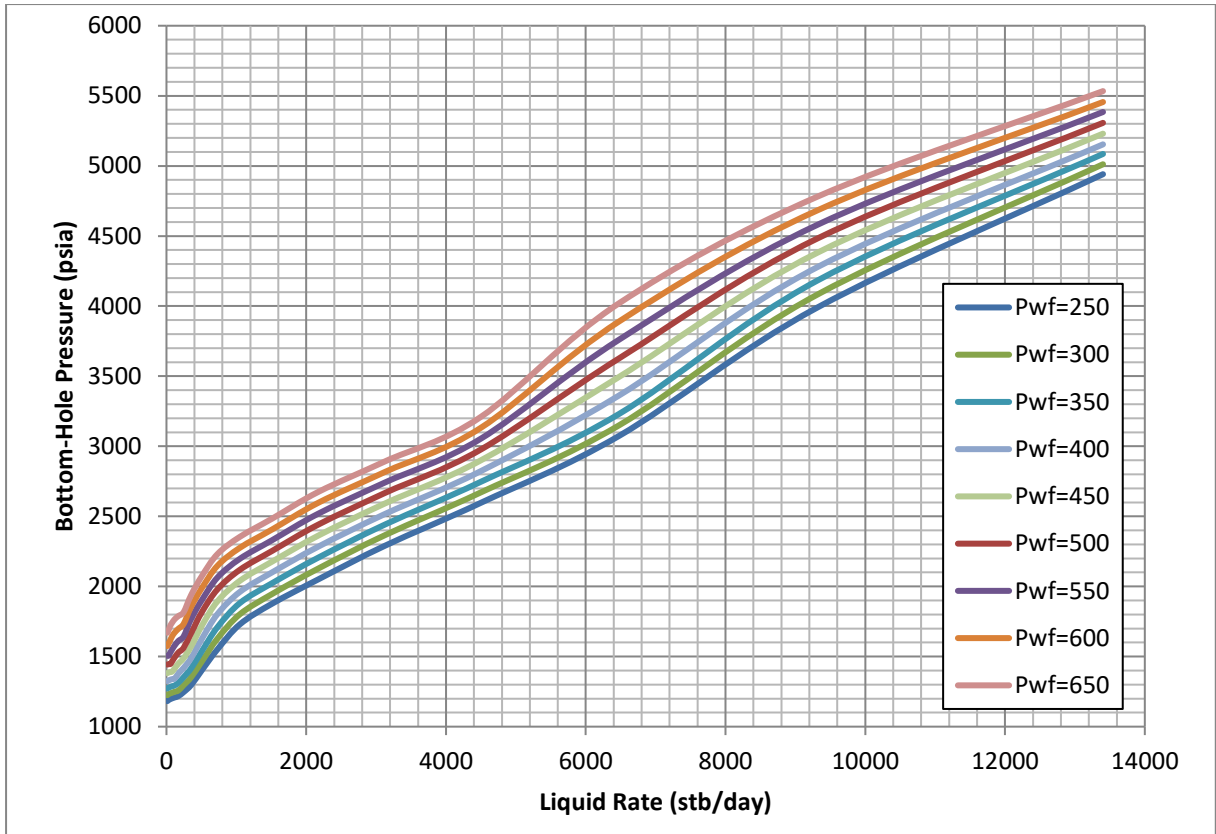


Figure A.31: VLP curves for 9 MMscf/day injection rate and 60% water cut.

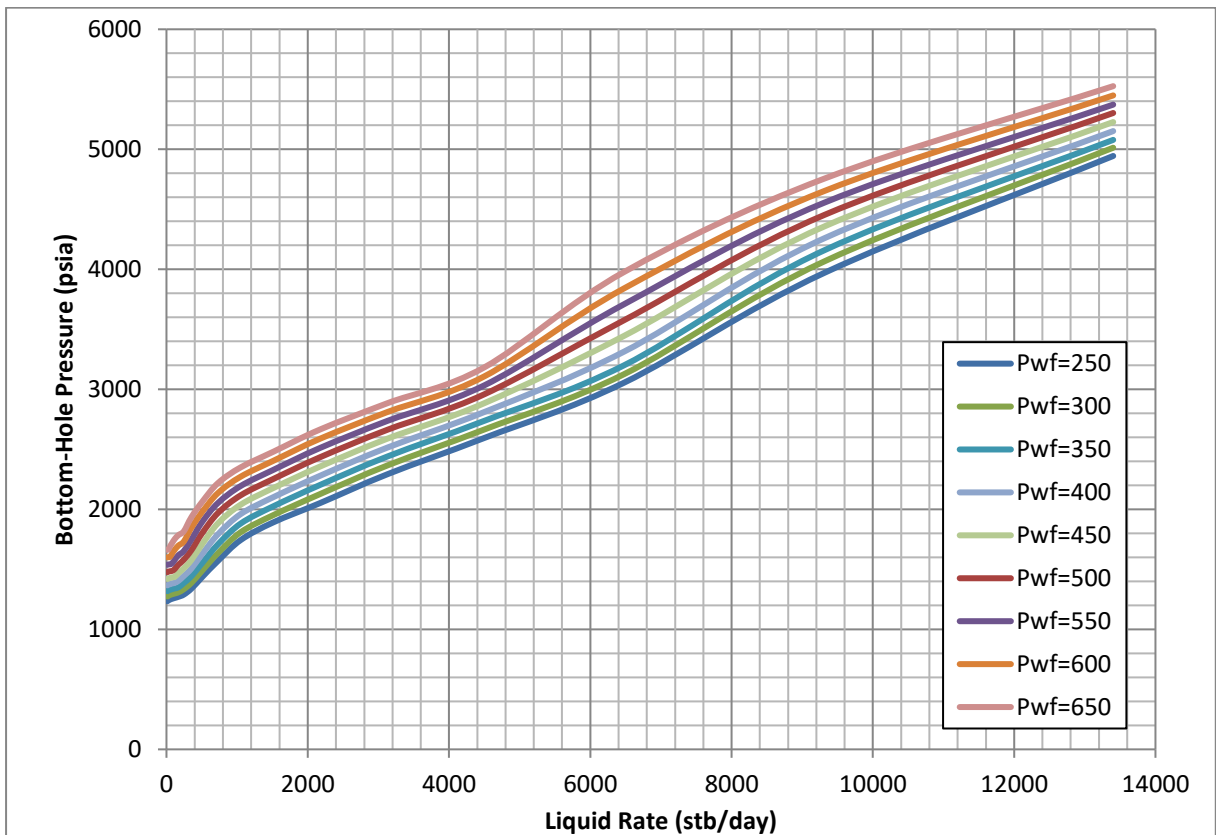


Figure A.32: VLP curves for 10 MMscf/day injection rate and 60% water cut.

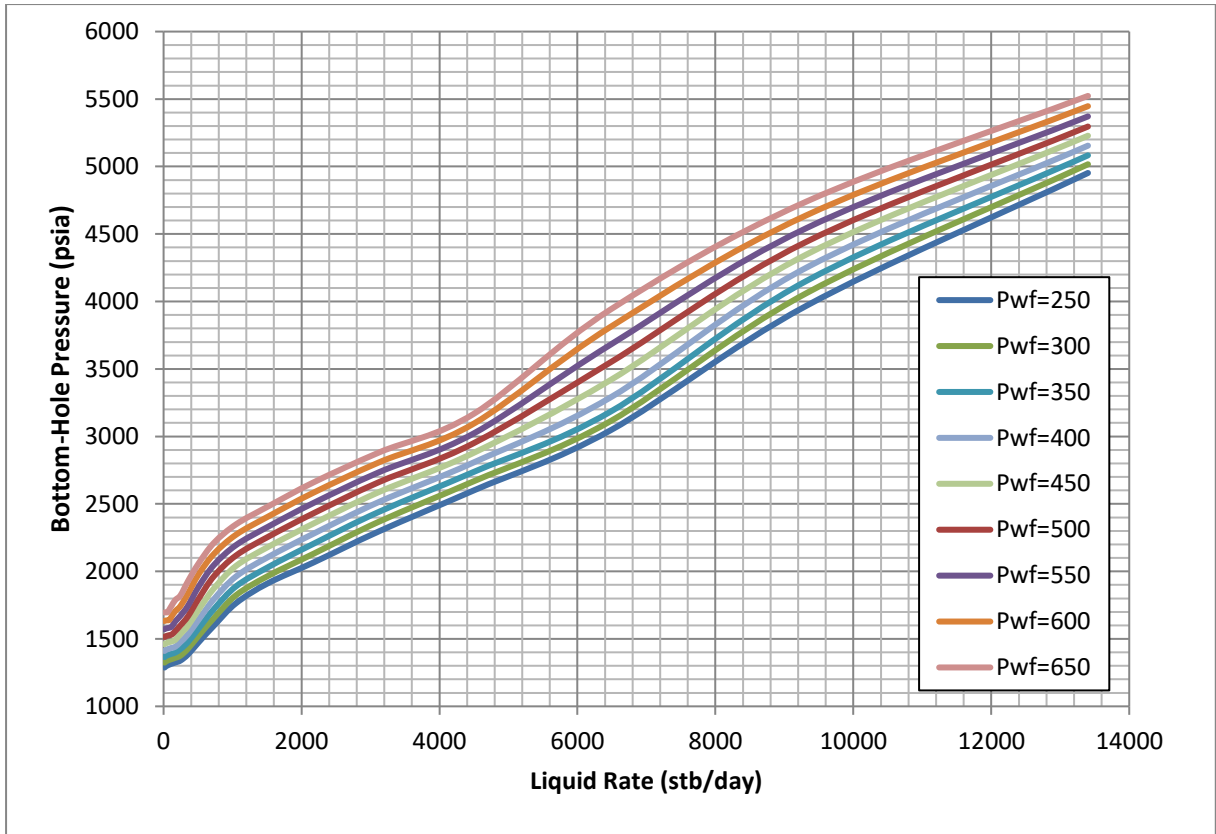


Figure A.33: VLP curves for 11 MMscf/day injection rate and 60% water cut.

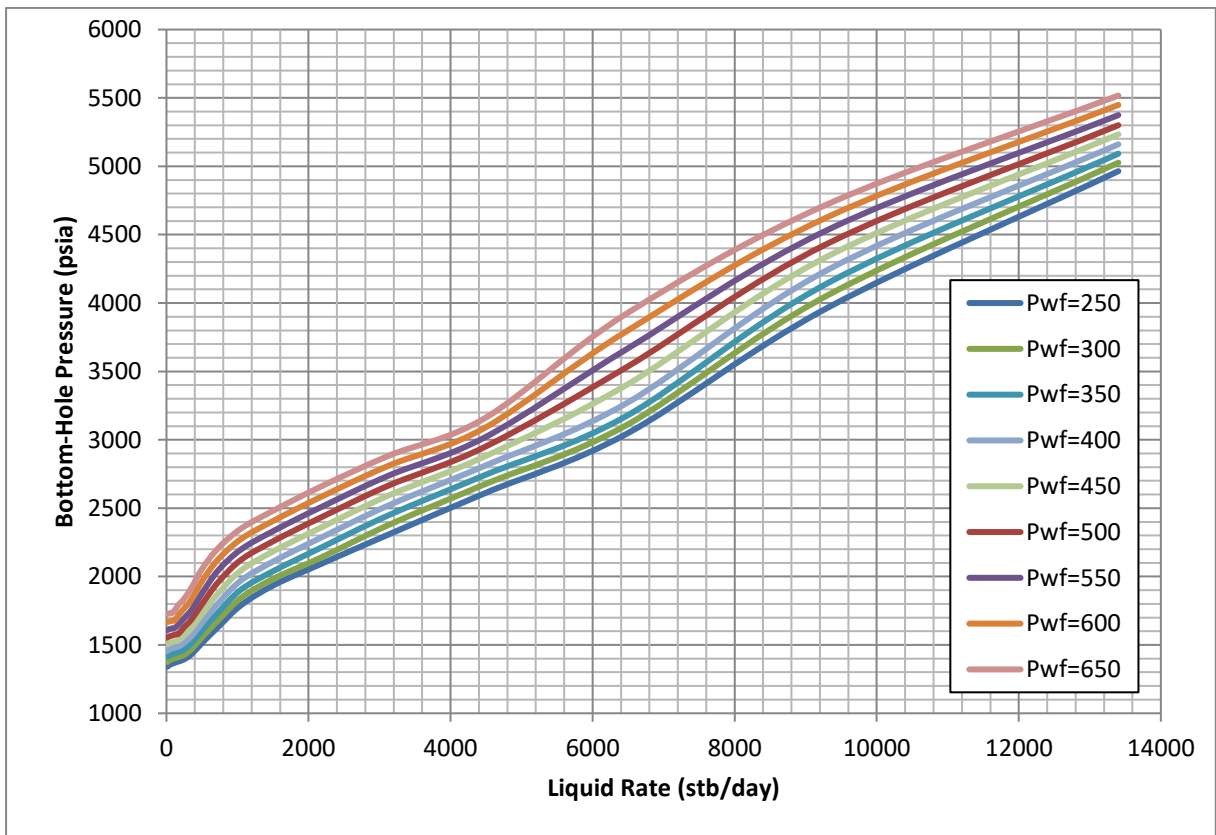


Figure A.34: VLP curves for 12 MMscf/day injection rate and 60% water cut.

### A.6 Sensitivity for different Wellhead Pressures and Injection Flow Rates for 80% Water Cut

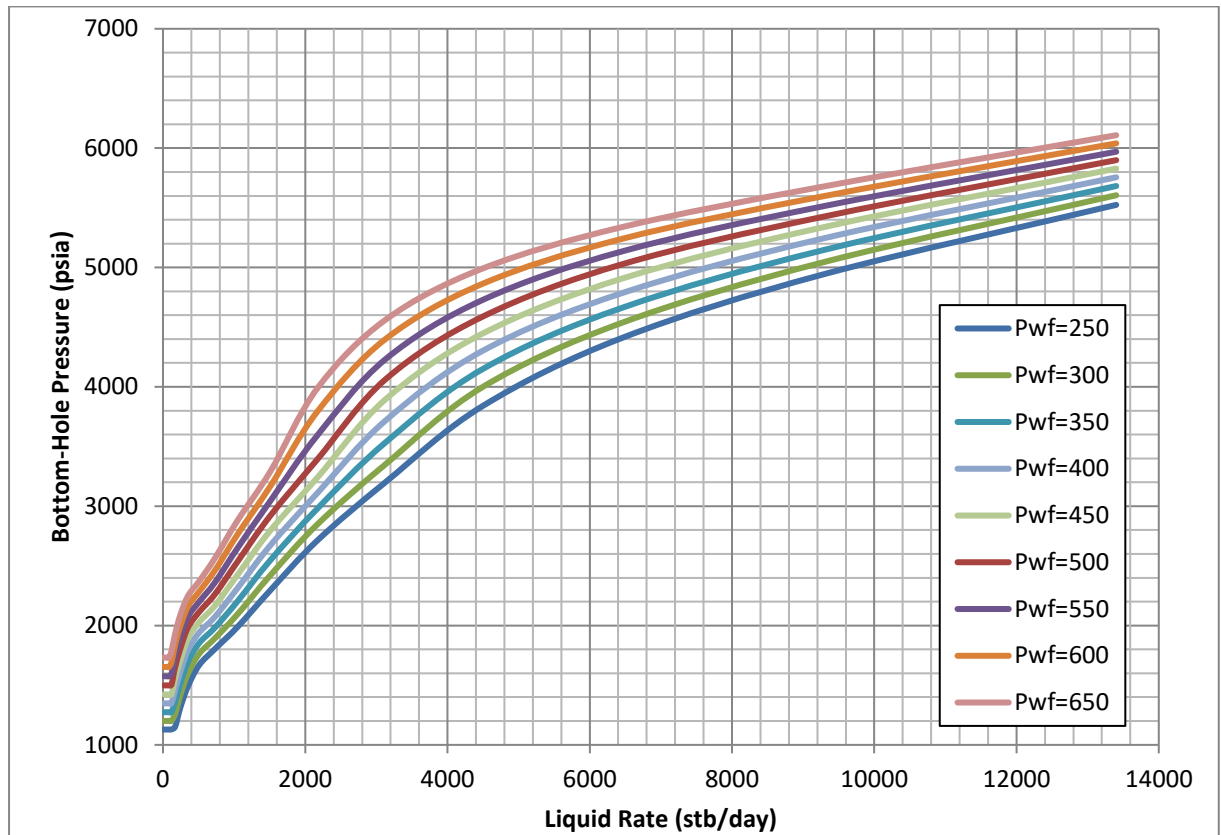


Figure A.35: VLP curves for 2 MMscf/day injection rate and 80% water cut.

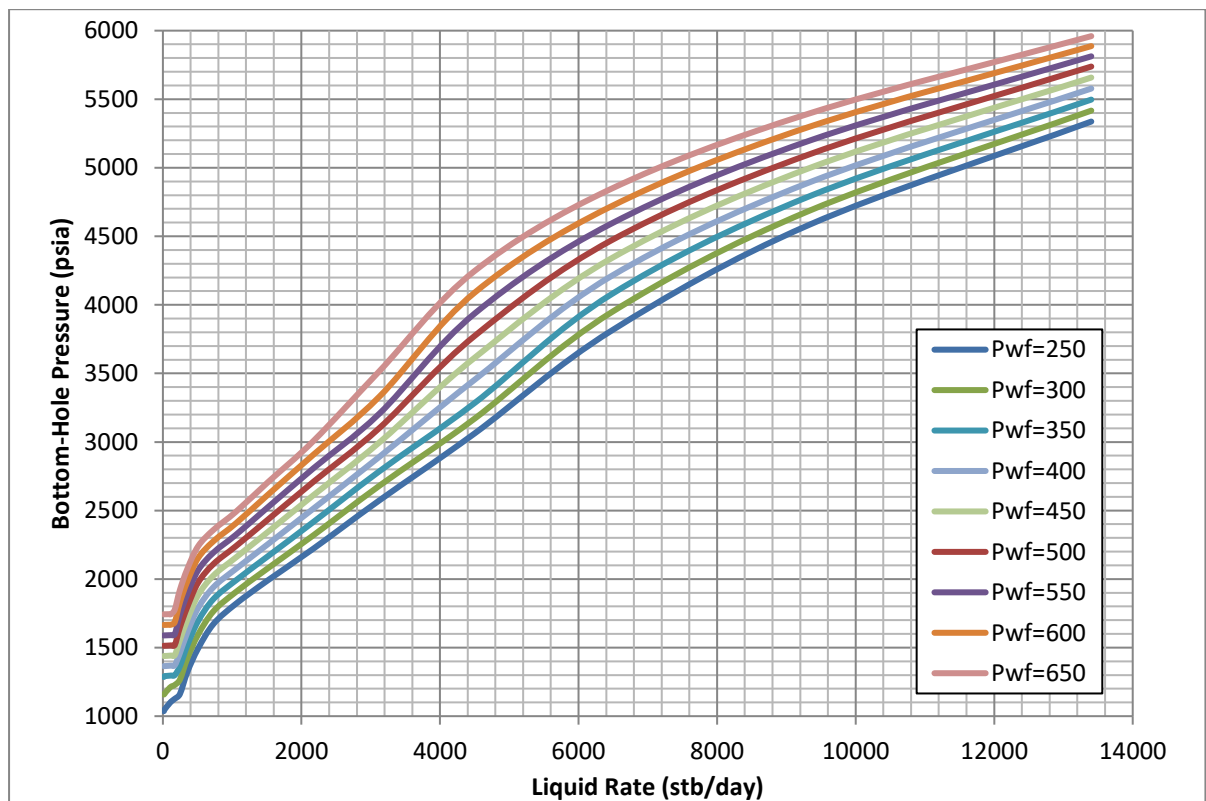


Figure A.36: VLP curves for 4 MMscf/day injection rate and 80% water cut.

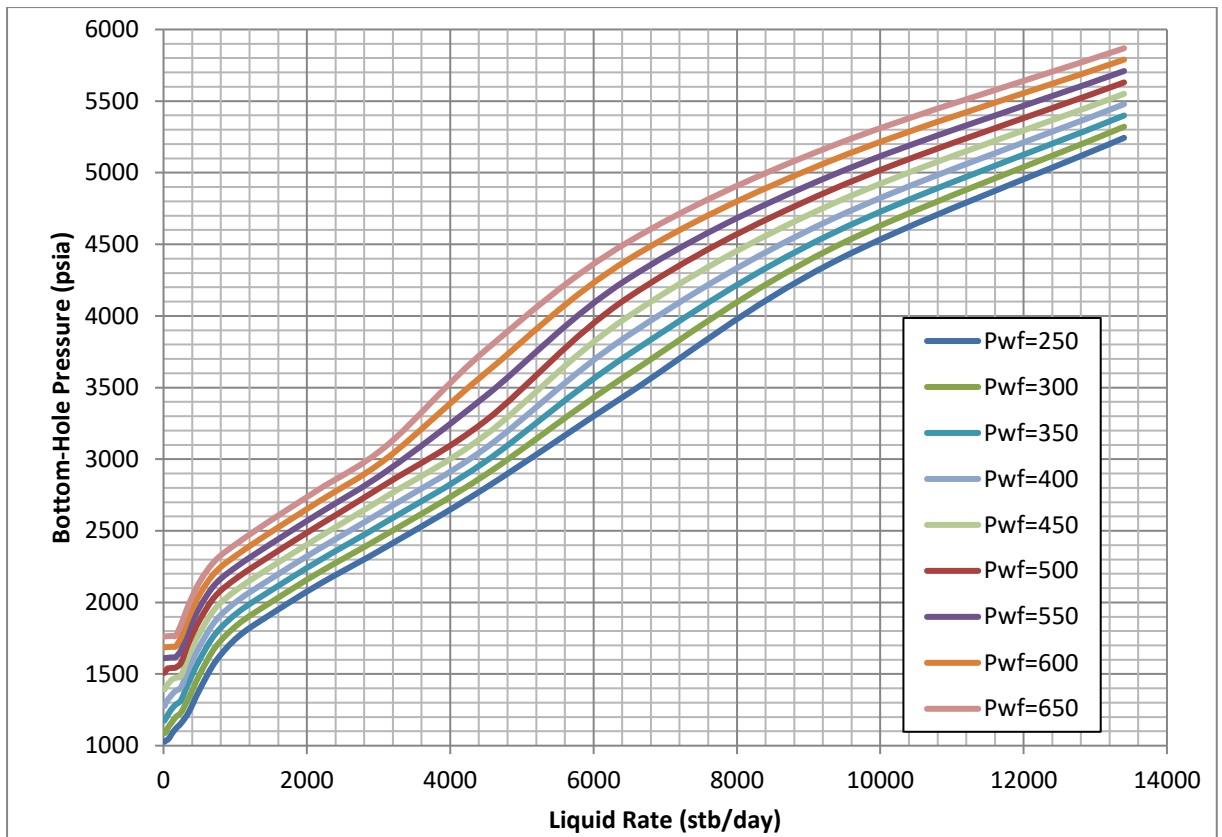


Figure A.37: VLP curves for 6 MMscf/day injection rate and 80% water cut.

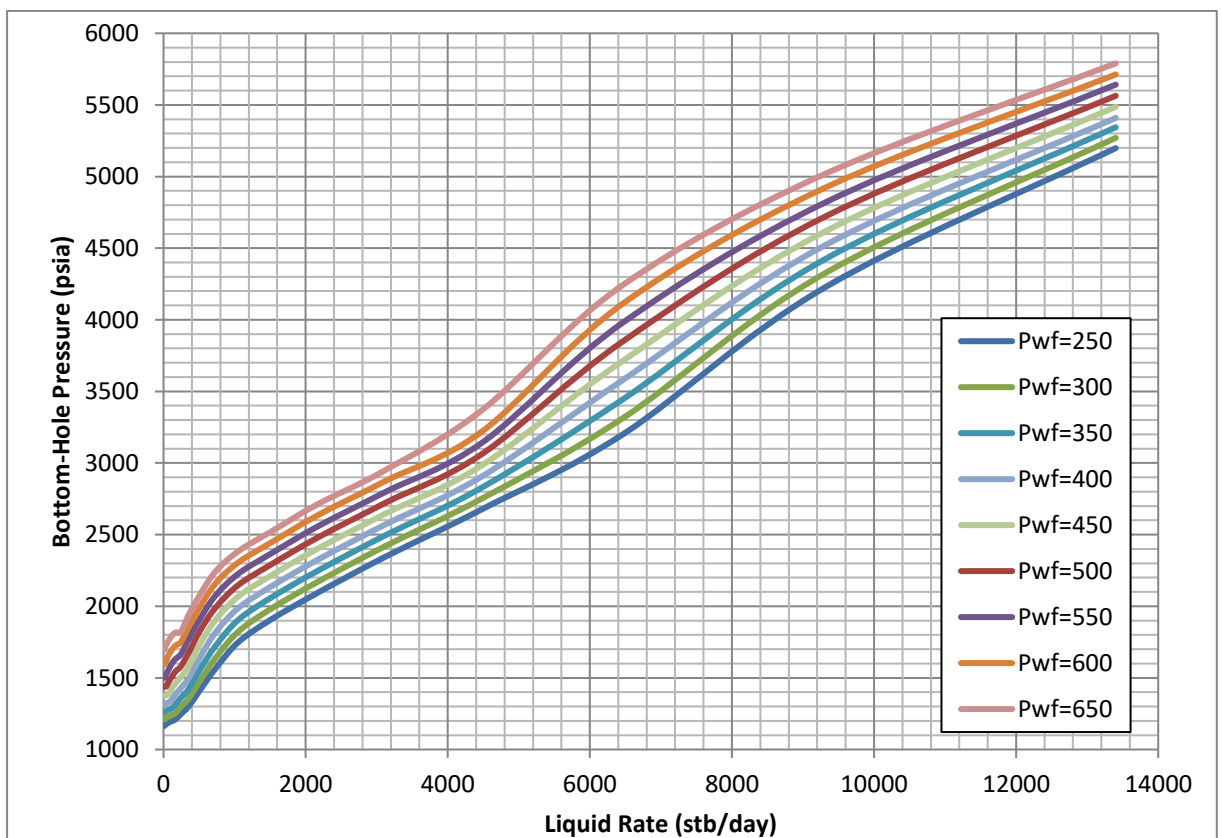


Figure A.38: VLP curves for 9 MMscf/day injection rate and 80% water cut.

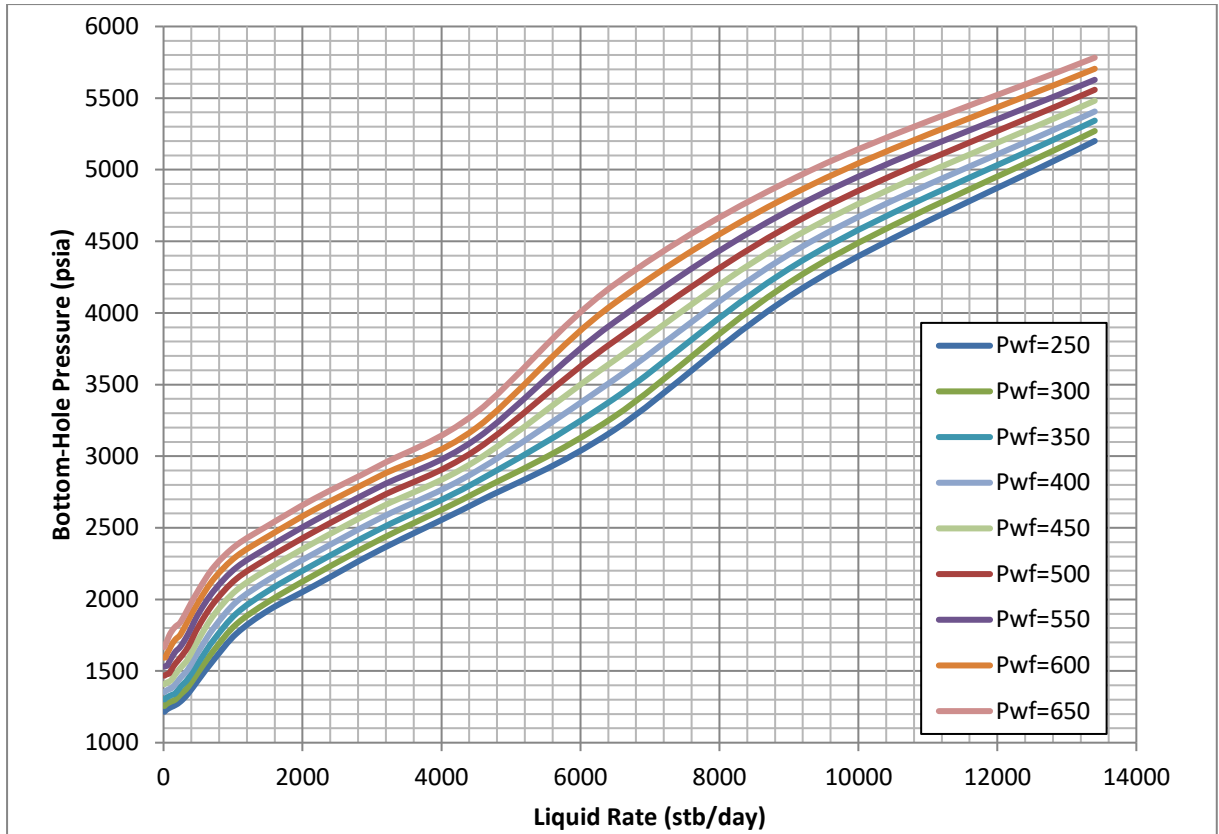


Figure A.39: VLP curves for 10 MMscf/day injection rate and 80% water cut.

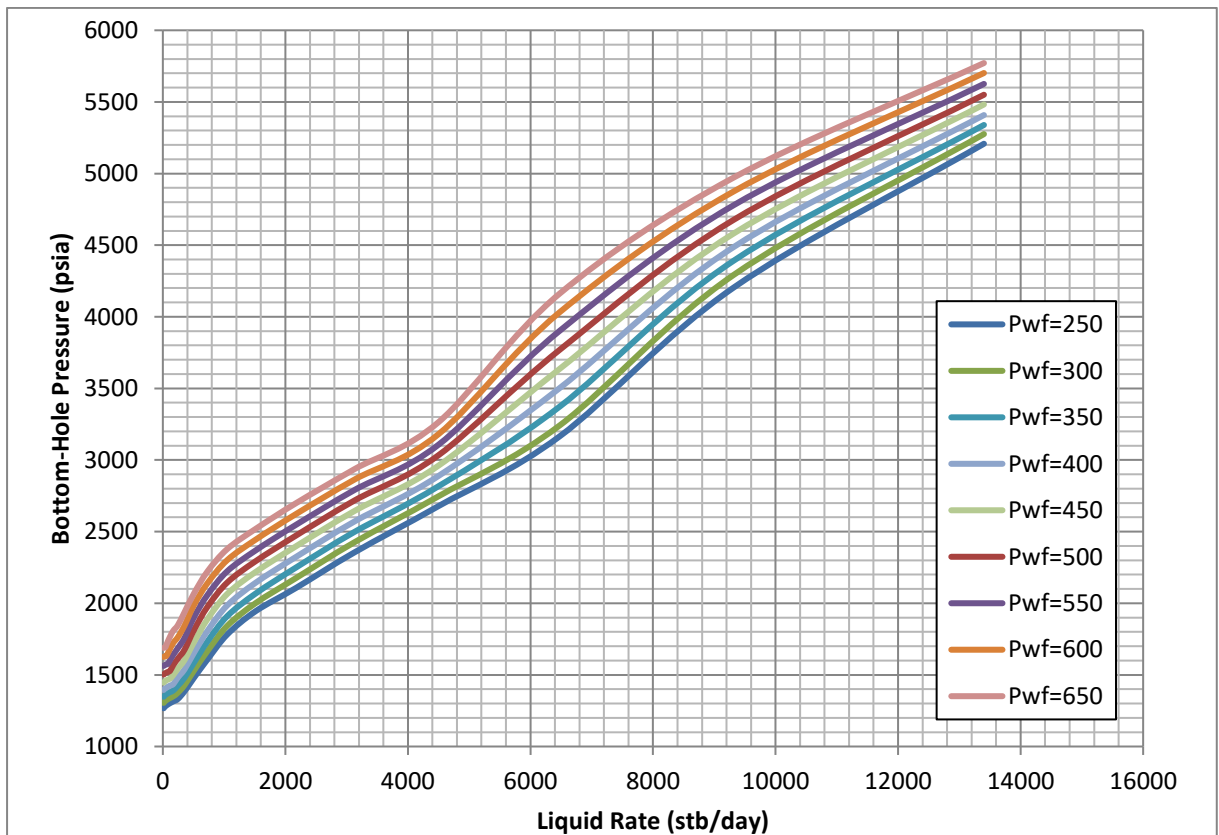


Figure A.40: VLP curves for 11 MMscf/day injection rate and 80% water cut.

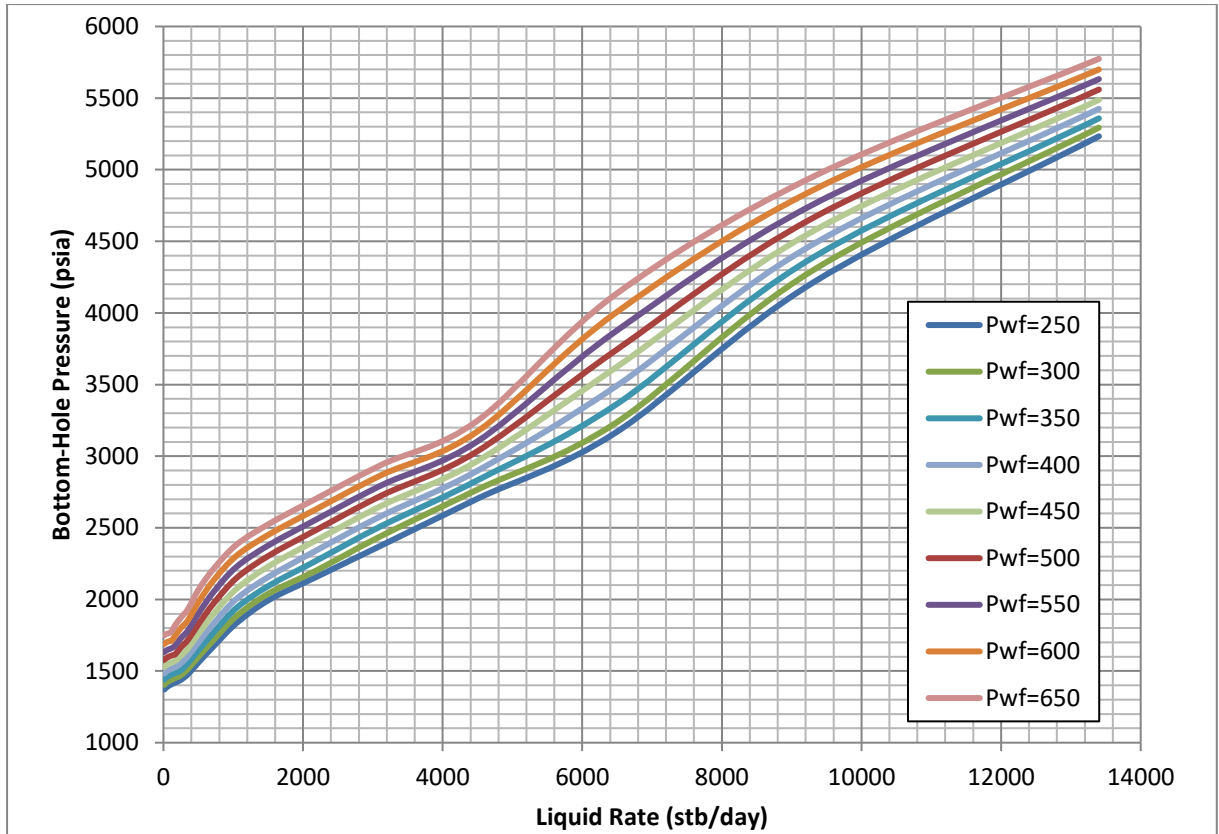


Figure A. 41: VLP curves for 13 MMscf/day injection rate and 80% water cut.

### A.7 Sensitivity for Gas to Liquid Ratio of 4.5" Tubing OD

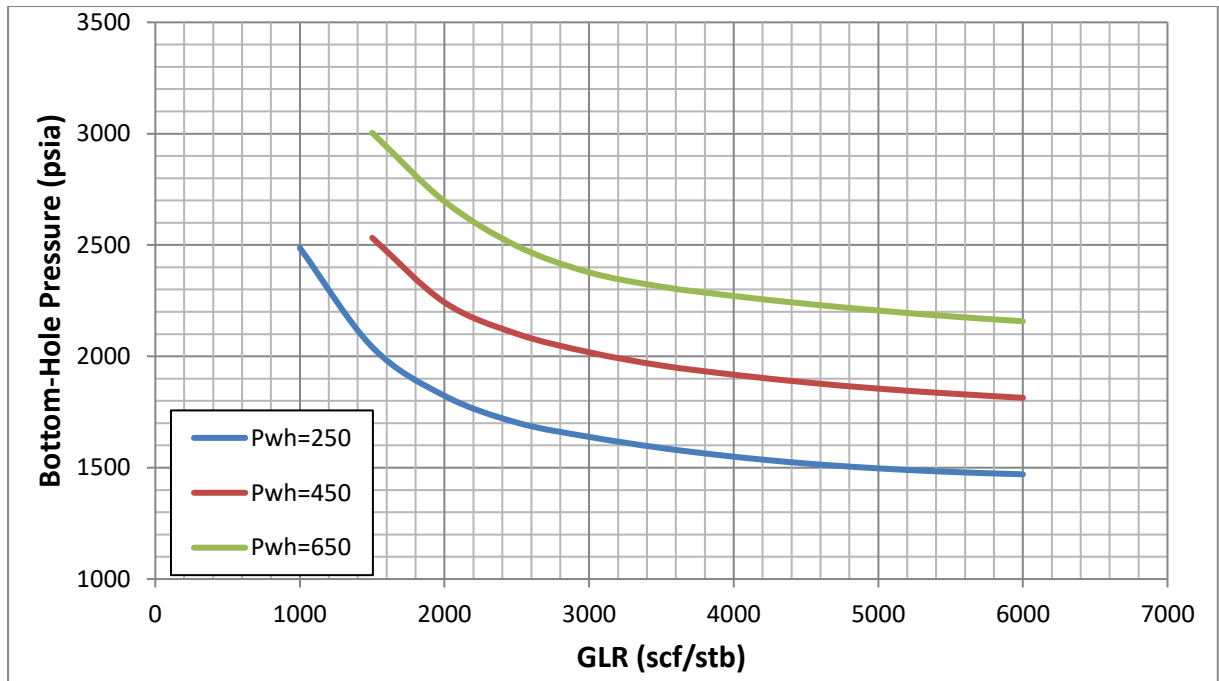


Figure A.42: Effect of GLR for constant liquid rate of 1000 stb/d and 4.5" OD.

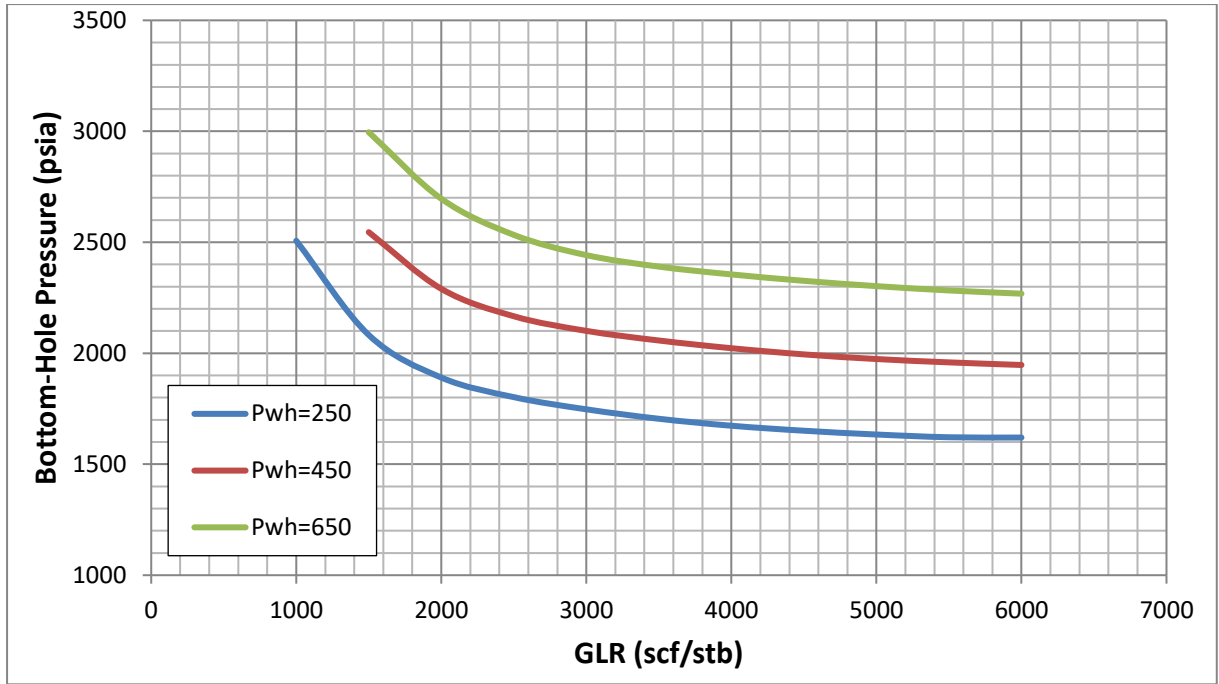


Figure A. 43: Effect of GLR for constant liquid rate of 1500 stb/d and 4.5" OD.

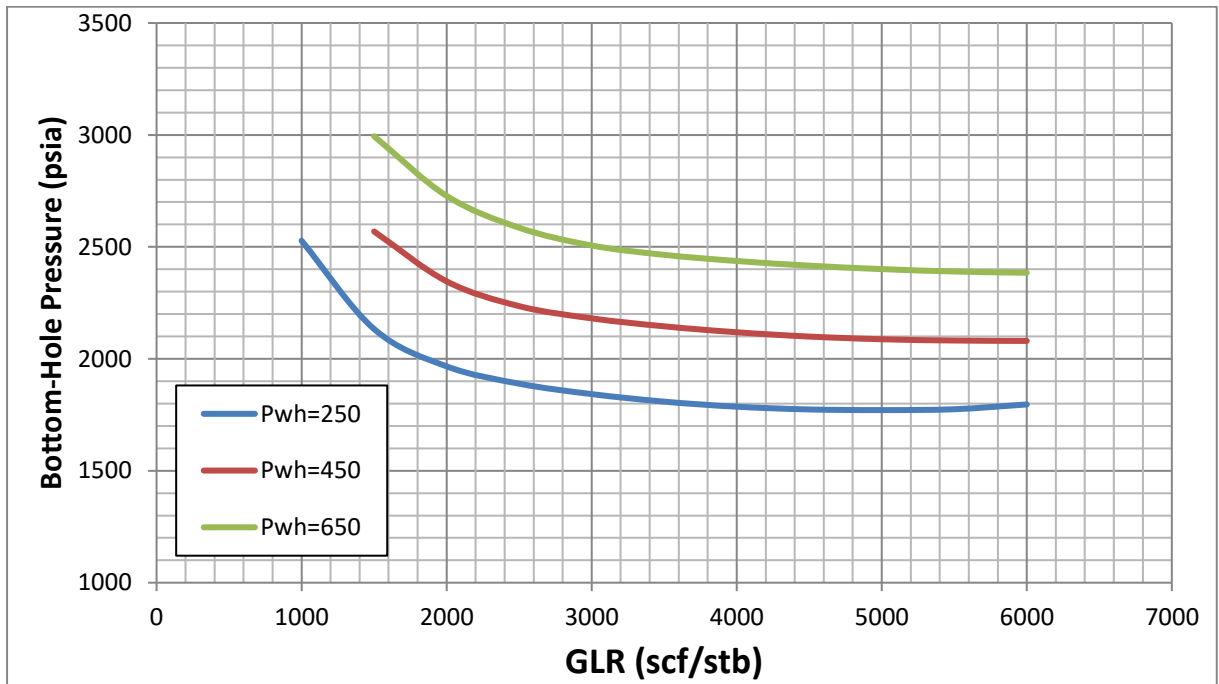


Figure A. 44: Effect of GLR for constant liquid rate of 2000 stb/d and 4.5" OD.

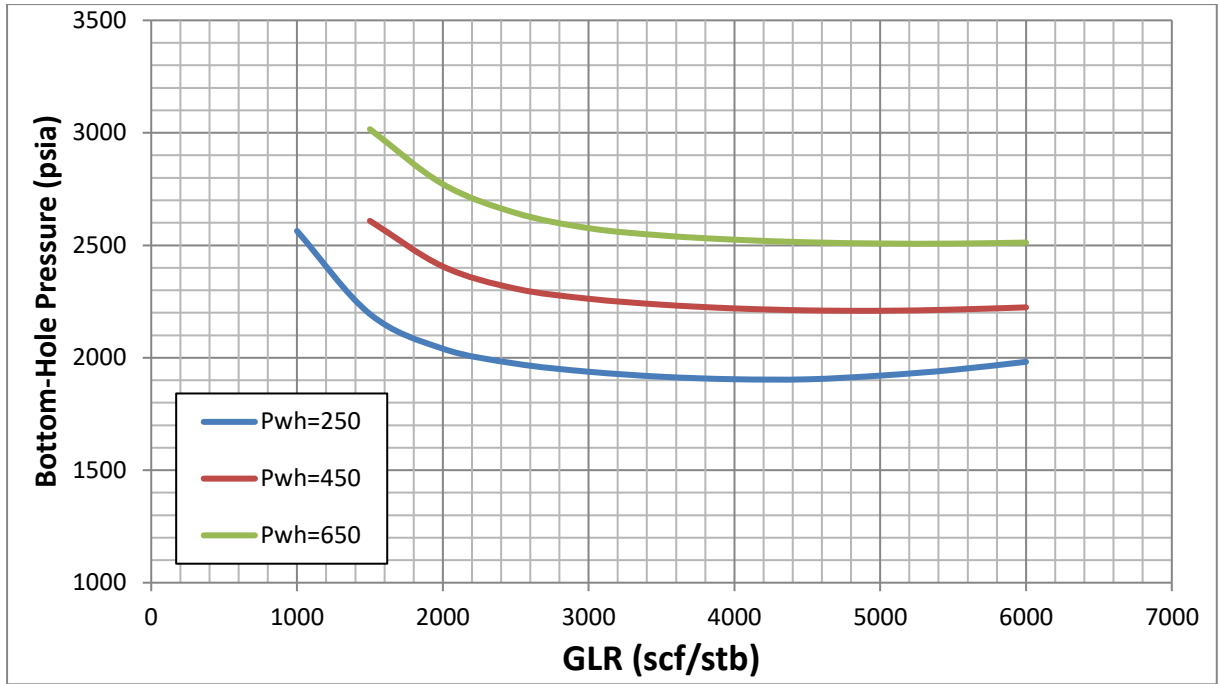


Figure A. 45: Effect of GLR for constant liquid rate of 2500 stb/d and 4.5" OD.

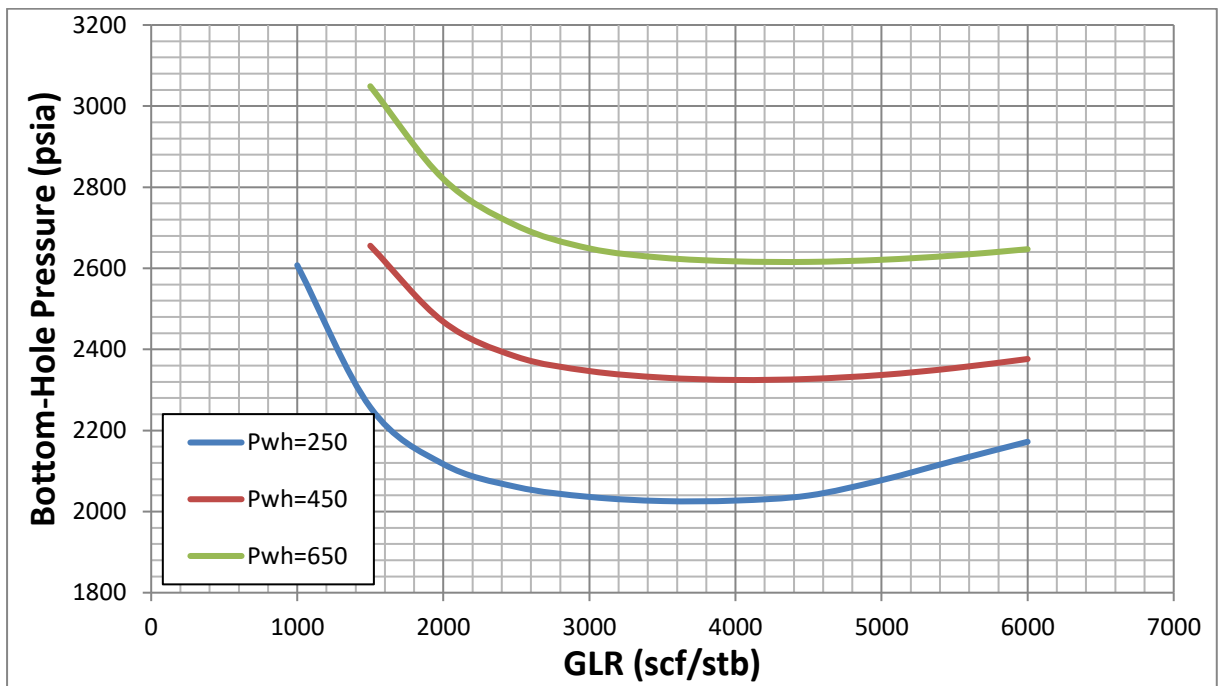


Figure A. 46: Effect of GLR for constant liquid rate of 3000 stb/d and 4.5" OD.

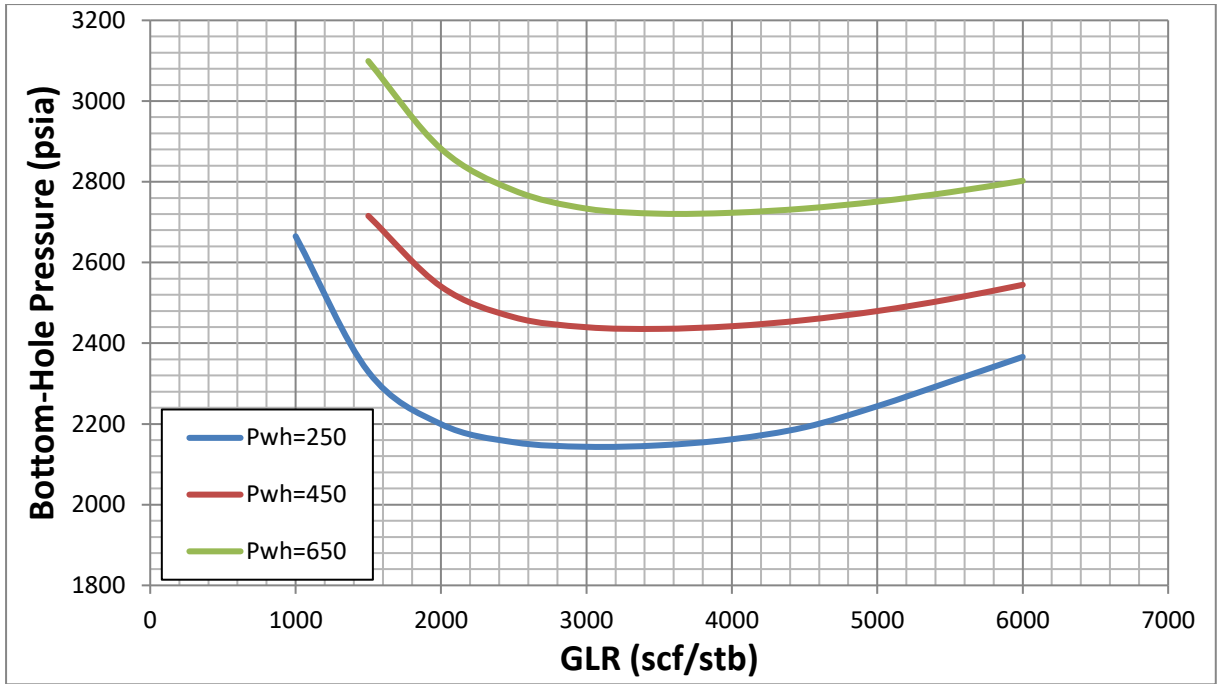


Figure A. 47: Effect of GLR for constant liquid rate of 3500 stb/d and 4.5" OD.

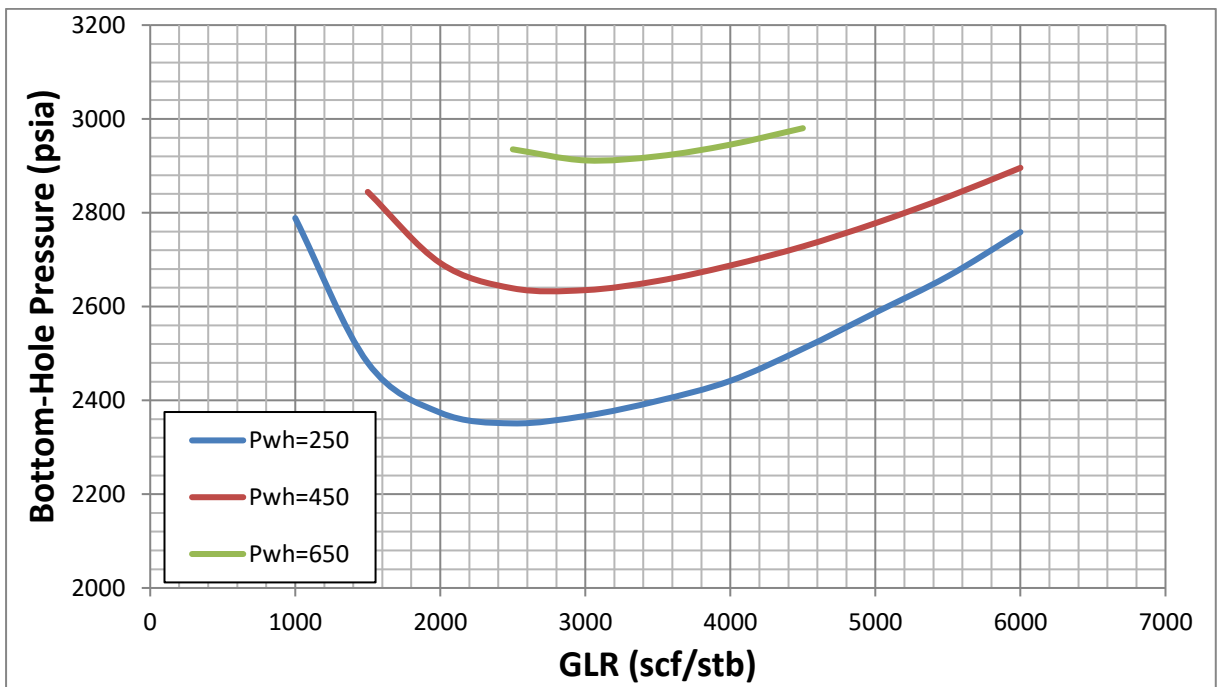


Figure A. 48: Effect of GLR for constant liquid rate of 4500 stb/d and 4.5" OD.

### A-8 Sensitivity of Gas to Liquid Ratio for 3.5" Tubing OD

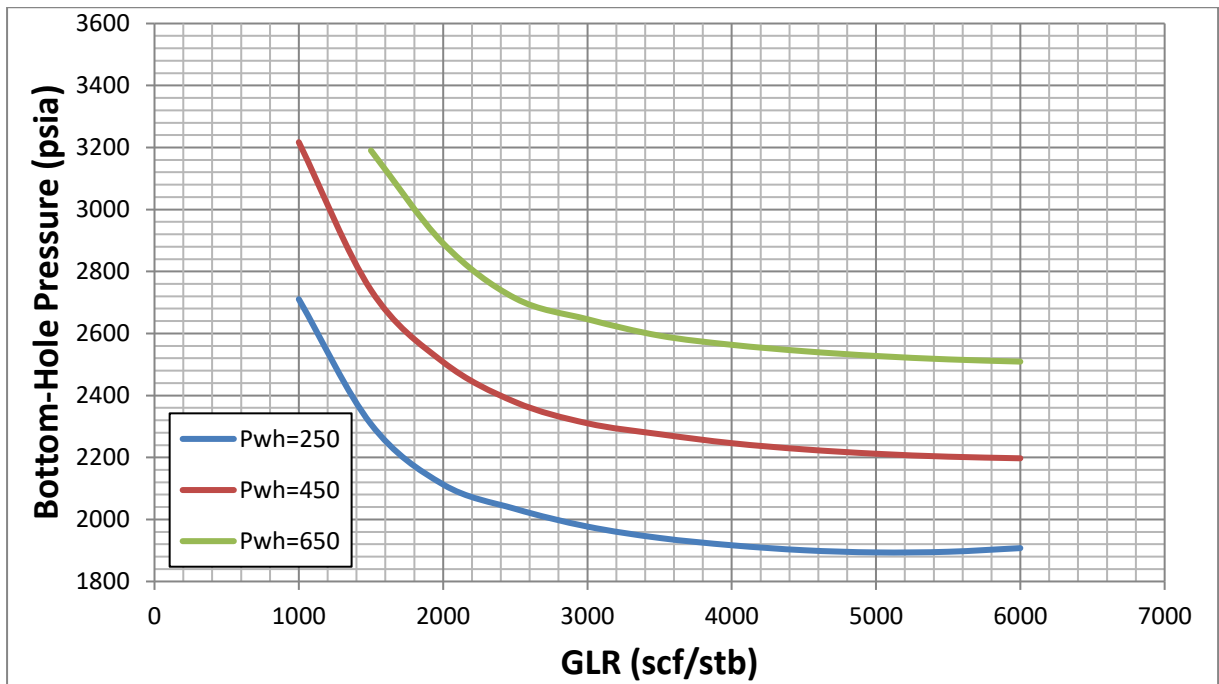


Figure A. 49: Effect of GLR for constant liquid rate of 1000 stb/d and 3.5" OD.

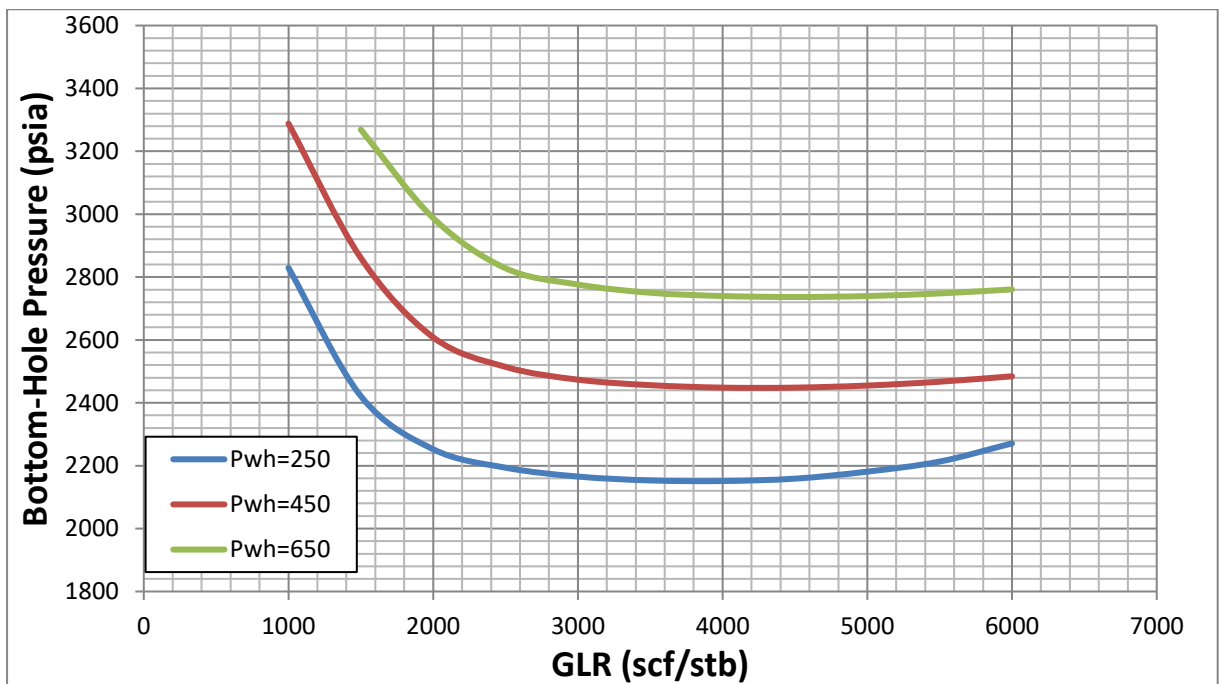


Figure A. 50: Effect of GLR for constant liquid rate of 1500 stb/d and 3.5" OD.

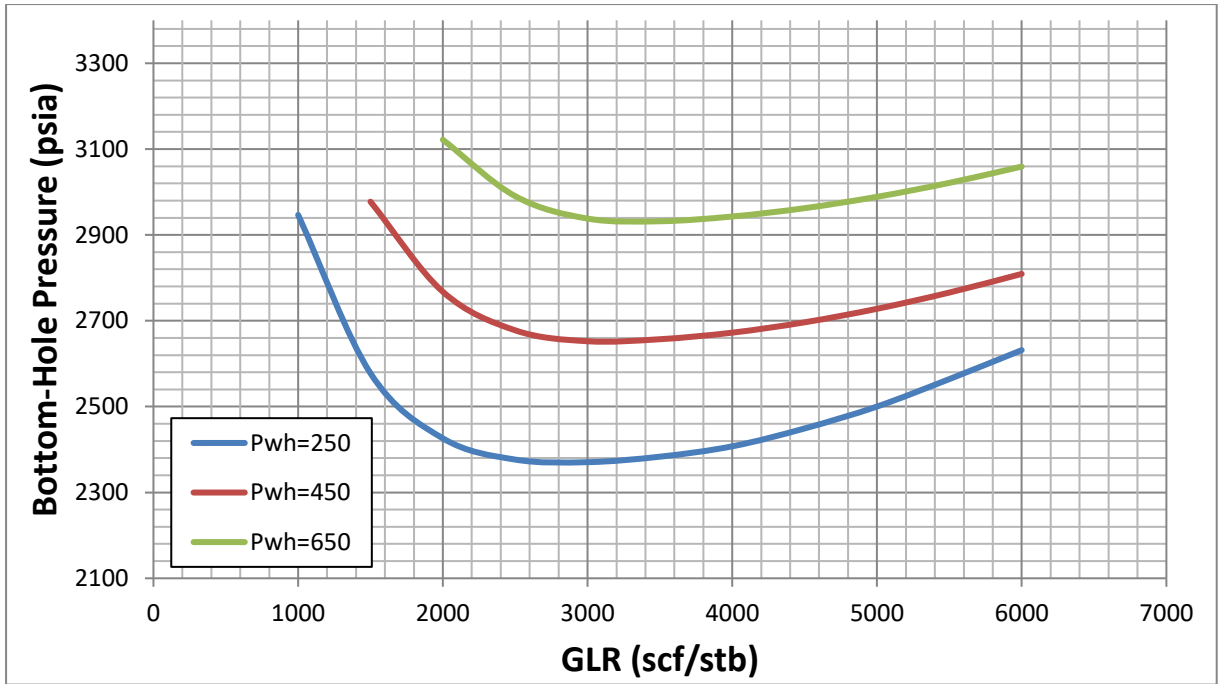


Figure A. 51: Effect of GLR for constant liquid rate of 2000 stb/d and 3.5" OD.

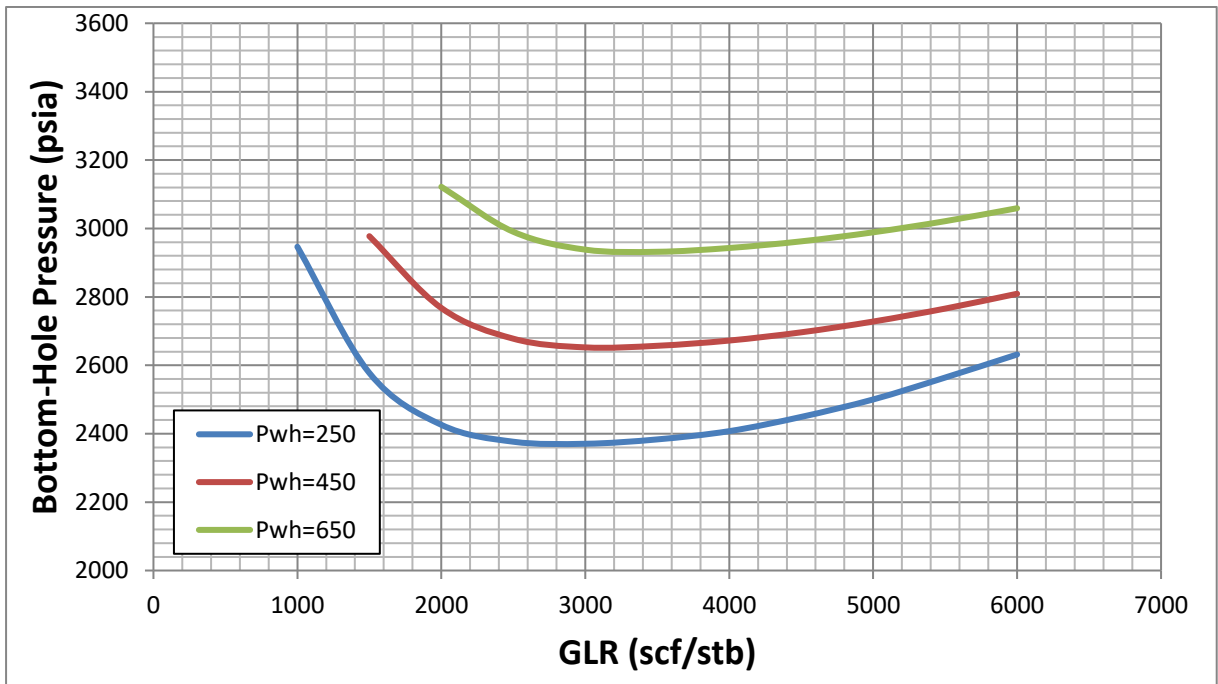


Figure A. 52: Effect of GLR for constant liquid rate of 2500 stb/d and 3.5" OD.